**NATIONAL AND KAPODISTRIAN UNIVERSITY OF ATHENS MEDICAL SCHOOL**
**DEPARTMENT OF ANATOMY**

# INVESTIGATING THE STRUCTURE AND WHITE MATTER FIBER TRACTS OF THE PRECUNEUS: IMPLICATIONS IN APPROACHES TO THE LATERAL VENTRICLE

**PhD DOCTORAL THESIS**

**GEORGIOS SKANDALAKIS, MD, MSc**
**ATHENS, 2020**

**ΕΘΝΙΚΟ ΚΑΙ ΚΑΠΟΔΙΣΤΡΙΑΚΟ ΠΑΝΕΠΙΣΤΗΜΙΟ ΑΘΗΝΩΝ ΙΑΤΡΙΚΗ ΣΧΟΛΗ**
**ΕΡΓΑΣΤΗΡΙΟ ΑΝΑΤΟΜΙΑΣ**

# ΜΕΛΕΤΗ ΤΗΣ ΔΟΜΗΣ ΚΑΙ ΤΩΝ ΔΕΜΑΤΙΩΝ ΤΗΣ ΛΕΥΚΗΣ ΟΥΣΙΑΣ ΤΟΥ ΠΡΟΣΦΗΝΟΕΙΔΟΥΣ ΛΟΒΙΟΥ: Η ΣΧΕΣΗ ΤΟΥΣ ΣΤΙΣ ΠΡΟΣΠΕΛΑΣΕΙΣ ΤΟΥ ΤΡΙΓΩΝΟΥ ΤΗΣ ΠΛΑΓΙΑΣ ΚΟΙΛΙΑΣ

**ΔΙΔΑΚΤΟΡΙΚΗ ΔΙΑΤΡΙΒΗ**

**ΓΕΩΡΓΙΟΣ ΣΚΑΝΔΑΛΑΚΗΣ**

**ΙΑΤΡΟΣ**
**ΑΘΗΝΑ 2020**

The approval of the doctoral dissertation by the Medical School of the National & Kapodistrian University of Athens does not imply approval of the views of the author. (Law 5343/1932, article 202, paragraph 2).

Η έγκριση διδακτορικής διατριβής από Ιατρικής Σχολής του Εθνικού & Καποδιστριακού Πανεπιστημίου Αθηνών, δεν υποδηλώνει την αποδοχή των γνωμών του συγγραφέα (Νόμος 5343/1932, άρθρο 202, παράγραφος 2).

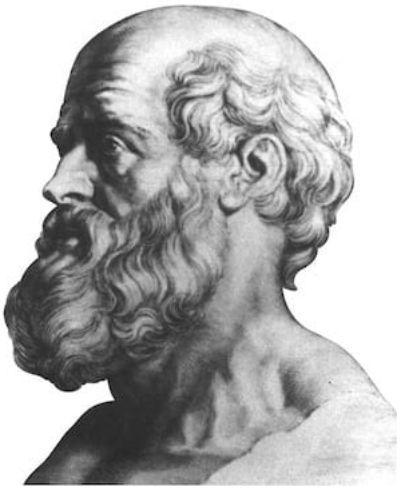

Ουκ ένι ιατρικήν είδέναι, όστις μη οίδεν ότι εστίν άνθρωπος.

It is not possible to know medicine for anyone who does not know what human is.

- Hippocrates

**Advisory Committee**

Theodore Troupis, Professor and Chair, Department of Anatomy, National and Kapodistrian University of Athens, Medical School (Supervisor)

George Stranjalis, Professor, Department of Neurosurgery, National and Kapodistrian University of Athens, Medical School

Vasilios Protogerou, Associate Professor, Department of Anatomy, National and Kapodistrian University of Athens, Medical School

Submission of doctoral thesis title: 20/10/2017
Appointment of advisory committee: 30/11/2017

**Μέλη Τριμελούς Συμβουλευτικής Επιτροπής**

Θεόδωρος Τρουπής, Καθηγητής και Διευθυντής, Εργαστήριο Ανατομίας, Εθνικό και Καποδιστριακό Πανεπιστήμιο Αθηνών, Ιατρική Σχολή (Επιβλέπων)

Γεώργιος Στράντζαλης, Καθηγητής Νευροχειρουργική κλινική, Εθνικό και Καποδιστριακό Πανεπιστήμιο Αθηνών, Ιατρική Σχολή

Βασίλειος Πρωτογέρου, Αναπληρωτής Καθηγητής, Εργαστήριο Ανατομίας, Εθνικό και Καποδιστριακό Πανεπιστήμιο Αθηνών, Ιατρική Σχολή

Κατάθεση Θέματος: 20/10/2017
Σύσταση τριμελούς επιτροπής: 30/11/2017

*To my neurosurgery family*

# Acknowledgments

Growing up I never wanted to become a medical doctor. The sight of blood, the sound of someone in pain or just the smell of a hospital was enough to induce a strong parasympathetic reaction and/or loss of consciousness. Growing up I also had the impression that the world revolves around me, for me. I was blessed to realize that this is not the case. I figured out that I cannot achieve anything by myself. At first my ego became very sensitive about this, but soon I came to realize that the real joy comes when you achieve things with others and the true meaning is achieving things for others. This dissertation is the product of many people inside and outside medicine. People who ignited a fire inside me to want to become a student of the brain, my dad who swore by his everyday actions to get out of his way and provide whatever I would need, my neurosurgery family who fostered me, my spiritual Father who would get me back up and going every time I would fall down, the art of neurosurgery that knows no limits, my advisory committee, the faculty of the Medical School, my teachers and all the everyday fighters of life who inspire me to keep going. I would like to acknowledge Dr. Elizabeth O. Johnson, my first neuroanatomy teacher who had the kindness to have me in her lab before my matriculation into medical school, who believed in me and showed me that to learn the most you have to actively teach someone else, yet always keep the heart and humbleness of a student. Dr. Theodore Troupis who was my first anatomy teacher, had me in his lab even before my matriculation into the medical school and spiked my interest in anatomy. Dr. Nicholas Stefanis who unconditionally mentored me and shared his passion for science with me. Dr. Stranjalis my first mentor in Neurosurgery who entrusted me with his research, training and clinical practice. Dr. Hadjipanayis who was my first mentor overseas, and made my dream come true to study neurosurgery in the US. Dr. Kalyvas who introduced me into the Athens Microneurosurgery laboratory, the lab where all of the dissections of this dissertation took place. Dr. Koutsarnakis, who never lost his patience in mentoring me. Dr. Komaitis for rescuing my RAT. Dr. Lani without whom I would never have completed my Master of Science's dissertation in time. Dr. Piagkou for sharing her passion in neuroanatomy and dissection. Last but not least I have to thank my future wife Mary who fostered the environment in which I was able to complete this dissertation.

# Contents

**CURRICULUM VITAE**


## Georgios Skandalakis

gskandalakis@uoa.gr


---

## EDUCATION

| | |
|---|---|
| | **University of Piraeus**, Piraeus, Greece |
| 2010 - 2014 | **B.B.A.** (Bachelor of Business Administration) |
| | **The American College of Greece-Deree**, Athens, Greece |
| 2012 - 2013 | **Minor** in Psychology<br>GPA 3.87 in a 4.00 scale |
| | **University of Athens School of Medicine**, Athens, Greece |
| 2015 - 2019 | **M.D.**<br>GPA 9.18 in a 10.00 scale |
| 2015 - 2017 | **M.Sc.** in Molecular Physiology<br>Thesis: Molecular mechanisms underlying glioma infiltration through the white matter of the central nervous system.<br>GPA 9.50 in a 10.00 scale |
| 2017 - 2020 | **Ph.D.** in Anatomy<br>Thesis: Investigating the Structure and Whiter Matter Fiber Tracts of the Precuneus. Implications in Approaches to the Atrium of the Lateral Ventricle |

## POSTDOCTORAL TRAINING

09/2019-Present **Postdoctoral Fellowship**, Brain tumor Nanotechnology Laboratory, Department of Neurosurgery, Icahn School of Medicine at Mount Sinai, NY

## HONORS/AWARDS

1. **Gold Medal Award for Pediatric Tumor Research**, AANS/CNS Section of Tumors, June 12th, 2020
2. **2020 Promising Young Investigator Award**, Icahn School of Medicine at Mount Sinai, February 27th, 2020
3. **Barrow Live Aneurysm Surgery Scholarship**, Aesculap Academy, January 9th, 2020
4. **Selected oral presentation,** International Cerebrovascular Symposium CNS Annual meeting, San Francisco, CA October 21st, 2019.
5. **Neurovascular Translational Research Microsurgical Instrumentation Award**, Mizuho, CNS Annual meeting, Houston, TX, October 13th, 2018
6. **Top 5 Submitted Abstract Award**, 32nd Annual Congress of the Hellenic Neurosurgical Society & Joint Meeting with the Society of British Neurological Surgeons and Cyprus Neurosurgical Society, Chania, Greece, May 26th, 2018
7. **Neuroanatomy Laboratory Peer Teacher Leader**, Department of Anatomy and Surgical Anatomy, University of Athens Medical School, Athens, Greece, May 24th, 2016
10. **The Chair's Award**, Department of Physiology, University of Athens Medical School, Athens, Greece, October 2nd, 2015

## CLINICAL EXPERIENCE

| | |
|---|---|
| 10/2015 - 07/2019 | Medical Student Intern<br>Department of Neurosurgery, University of Athens School of Medicine, Athens, Greece |
| 7/2016 - 8/2016 | Visiting Medical Student<br>Department of Neurosurgery, Mount Sinai Health System, New York, NY |
| 8/2016 - 9/2016 | Visiting Medical Student<br>Department of Neurosurgery, Brigham and Women's Hospital, Boston, MA |
| 12/2016 - 1/2017 | Visiting Medical Student<br>Department of Neurosurgery, Mount Sinai Health System, New York, NY |
| 12/2017 - 01/2018 | Visiting Medical Student<br>Department of Neurosurgery, NYU Medical School, New York, NY |
| 10/2018 | Visiting Medical Student<br>Department of Neurosurgery, Lenox Hill Hospital, New York, NY |
| 3/2020 | Visiting Fellow<br>Department of Neurosurgery, Barrow Neurological Institute, Phoenix, AZ, |

## RESEARCH EXPERIENCE

| | |
|---|---|
| 12/2012 - 2/2017 | Laboratory Assistant, Neuroanatomy Laboratory<br>Department of Anatomy & Surgical Anatomy, University of Athens School of Medicine, Athens, Greece |
| 3/2016 - 11/2017 | Laboratory Assistant, Athens Microneurosurgery Laboratory<br>Department of Neurosurgery, University of Athens School of Medicine, Athens, Greece |
| 12/2016 - 1/2017 | Visiting Medical Student, Brain Tumor Nanotechnology Laboratory, Icahn School of Medicine at Mount Sinai Health, New York, NY |
| 11/2017 - present | PhD student, Athens Microneurosurgery Laboratory<br>Department of Neurosurgery, University of Athens School of Medicine, Athens, Greece |
| 12/2017- 01/2018 | Visiting Medical Student, Department of Neurosurgery, NYU Medical School, New York, NY |
| 01/2018 - 02/2018 | Research Intern, Surgical Innovations Laboratory for Skull base and Microneurosurgery<br>Department of Neurological Surgery, Weill Cornell Medical College/ New York-Presbyterian Hospital, New York, NY |
| 06/2018 - 06/2019 | Research fellow, setting up focal cerebral ischemia/reperfusion protocols for the investigation of anti-ischemic and neuroprotective agents utilizing microsurgical transient MCA occlusion models in mice and transgenic mice<br>Department of Pharmacology, University of Athens School of Medicine, Athens, Greece |

## TEACHING EXPERIENCE

| | |
|---|---|
| 2015-2016<br>Fall semester | Peer Teacher, Neuroanatomy Laboratory<br>Department of Anatomy & Surgical Anatomy, University of Athens, Athens, Greece |
| 9/24 -9/26/2015 | Trainer, "Brain and Skull Base Anatomy with Practical Training Workshop",<br>Department of Anatomy / Department of Neurosurgery, University of Athens School of medicine, Athens, Greece |
| 2016-2017<br>Fall semester | Peer Teacher Leader, Neuroanatomy Laboratory<br>Department of Anatomy & Surgical Anatomy, University of Athens School of Medicine, Athens, Greece |
| 4/13/2016 | Trainer, "Trauma Suture Workshop"<br>Anatomy Laboratory, Department of Anatomy & Surgical Anatomy, University of Athens School of Medicine, Athens, Greece |
| 4/21 & 4/22/2016 | Trainer, "White matter Dissection" 2nd International Cadaveric course<br>Athens Microneurosurgery Laboratory, Department of Neurosurgery, University of Athens School of Medicine, Hellenic Neurosurgical Society, Athens, Greece |
| 4/18 – 5/10/2016 | Trainer, "Neuroanatomy Peer Teaching Seminar: Training the Trainers"<br>Department of Anatomy & Surgical Anatomy, University of Athens School of Medicine, Athens, Greece |
| 5/3/2017 | Trainer, "Trauma Suture Workshop"<br>Anatomy Laboratory, Department of Anatomy & Surgical Anatomy, University of Athens School of Medicine, Athens, Greece |

06/01 & 06/02/2017 — Trainer, "White matter Dissection" 3rd International Cadaveric Course
Athens Microneurosurgery Laboratory, Department of Neurosurgery, University of Athens School of Medicine, Hellenic Neurosurgical Society, Athens, Greece

02/06/2018 — Trainer, "Introduction to Neurosurgery" A hands on course for students.
Surgical Innovations Laboratory for Skull base and Microneurosurgery, Department of Neurological Surgery, Weill Cornell Medical College/New York-Presbyterian Hospital, New York, NY

03/03/2018 — Invited lecturer, "Functional neuroanatomy and connectivity of the epithalamus"
Master of Science in Clinical and Experimental Neurosurgery, University of Athens School of Medicine

05/10 & 05/11/2018 — Trainer, "White matter Dissection" 4th International Cadaveric Course
Athens Microneurosurgery Laboratory, Department of Neurosurgery, University of Athens, Hellenic Neurosurgical Society, Athens, Greece

## ORGANIZING COMMITTEE OF SCIENTIFIC MEETINGS AND COURSES

9/24 -9/26/2015 — Assistant, "Brain and Skull Base Anatomy with Practical Training Workshop"
Department of Anatomy & Department of Neurosurgery, University of Athens, School of Medicine, Athens, Greece

4/18 – 4/20/2016 — Assistant, "Neurosurgical Anatomy" 2nd International Course
Athens Microneurosurgery Laboratory, University of Athens School of Medicine, Department of Neurosurgery, Hellenic Neurosurgical Society, Athens, Greece

4/21 & 4/22/2016 — Assistant, "White Matter Dissection" 2nd International Course

| | |
|---|---|
| | Athens Microneurosurgery Laboratory, Department of Neurosurgery University of Athens School of Medicine, Hellenic Neurosurgical Society, Athens, Greece |
| 4/18 – 5/10/2016 | Assistant, "Neuroanatomy Peer Teaching Seminar: Training the Trainers"<br>Department of Anatomy & Surgical Anatomy, University of Athens School of Medicine, Athens, Greece |
| 5/3/2017 | Assistant, **"**Trauma Suture Workshop"<br>Anatomy Laboratory, Department of Anatomy & Surgical Anatomy, University of Athens School of Medicine, Athens, Greece |
| 5/29 – 5/31/2017 | Assistant, "Neurosurgical Anatomy" 3rd International Cadaveric Course<br>Athens Microneurosurgery Laboratory, University of Athens School of Medicine, Department of Neurosurgery, Hellenic Neurosurgical Society, Athens, Greece |
| 06/01 & 06/02/2017 | Assistant, "White Matter Dissection" 3rd International Cadaveric Course<br>Athens Microneurosurgery Laboratory, Department of Neurosurgery University of Athens School of Medicine, Hellenic Neurosurgical Society, Athens, Greece |
| 02/06/2018 | Assistant, "Introduction to Neurosurgery" Course<br>Surgical Innovations Laboratory for Skull base and Microneurosurgery, Department of Neurological Surgery, Weill Cornell Medical College/New York-Presbyterian Hospital, New York, NY |
| 02/10/2018 | Assistant, Spine Cadaveric Course<br>Surgical Innovations Laboratory for Skull base and Microneurosurgery, Department of Neurological Surgery, Weill Cornell Medical College/New York-Presbyterian Hospital, New York, NY |
| 05/07 – 05/09/2017 | Assistant, "Neurosurgical Anatomy" 4th International Cadaveric Course<br>Athens Microneurosurgery Laboratory, University of Athens School of Medicine, Department of Neurosurgery, Hellenic Neurosurgical Society, Athens, Greece |

| | |
|---|---|
| 05/10 & 05/11/2018 | Assistant, "White Matter Dissection" 4th International Cadaveric Course<br>Athens Microneurosurgery Laboratory, Department of Neurosurgery, University of Athens Medical School, Hellenic Neurosurgical Society, Athens, Greece |
| 01/14 - 01/16/2019 | Assistant, "Intraluminal MCA Occlusion/Reperfusion Models in Mice: Methods and Techniques" Course<br>Department of Pharmacology, University of Athens School of Medicine, Athens, Greece |
| 04/14 – 04/16/2019 | Volunteer, Young Neurosurgeons Committee<br>AANS Annual Meeting, San Diego, CA |
| 10/19-10/23/2019 | Sergeant-at-Arms<br>CNS Annual Meeting, San Francisco, CA |

**MANUSCRIPT REVIEWER**

| | |
|---|---|
| 02/2019-Present | Canadian Journal of Psychiatry |
| 03/2019-Present | Therapeutic Advances in Neurological Disorders |
| 09/2020-Present | Scientific Journal of Neurology & Neurosurgery |

**PEER-REVIEWED JOURNAL ARTICLES**

1. Johnson EO, Mytilinaios D, Panagiotopoulos NAI, **Skandalakis GP**, Spinos D, Varthaliti A. Supratentorial Dissection of the Human Brain for Neuroscientists. **Academia Anatomica International**, 2016;2(1):13-2.

2. Koutsarnakis C, Liakos F, Kalyvas AV, **Skandalakis GP**, Komaitis S, Christidi F, Karavasilis E, Liouta E, Stranjalis G: The Superior Frontal Transsulcal Approach to the anterior ventricular system: Exploring the sulcal and subcortical anatomy using anatomic dissections and DTI tractography. **World Neurosurgery**, 2017;106:339-54.

3. **Skandalakis GP**, Korfias S, Kalyvas AV, Anagnostopoulos C, Sakas DE, A Giant Pseudoaneurysm of the Occipital Artery. **Surgical Neurology International**, 2017; 8.

4. Koutsarnakis C, Kalyvas A, Komaitis S., Liakos F, **Skandalakis GP**, Anagnostopoulos C, Stranjalis G; Defining the relationship of the optic radiation to the roof and floor of the

ventricular atrium. A focused microanatomic study. **Journal of Neurosurgery**, 2018; 130(5):1728-39.

5. **Skandalakis GP**, Koutsarnakis C, Kalyvas AV, Skandalakis P, Johnson EO, Stranjalis G: The habenula in neurosurgery for depression: A convergence of functional neuroanatomy, psychiatry and imaging. **Brain Research**, 2018; 1694:13-8.

6. Kostorizos A, Koukakis A, Samolis A, Protogerou V, Margiolis T, Piagkou M, Natsis K, **Skandalakis GP**, Troupis T: Body donation for research and teaching purposes: the contribution of blood donation units in the progress of anatomical science, **Folia Morphologica**, 2019;78(3):575-81.

7. Natsis K, Piagkou M, Chryssanthou I, **Skandalakis GP**, Tsakotos G, Piagkos G, Politis C: A simple method to estimate the linear length of the orbital floor in complex orbital surgery. **Journal of Cranio-Maxillo-Facial Surgery**, 2018; 47(1):185-9.

8. Koutsarnakis C, Kalyvas AV, **Skandalakis GP**, Karavasilis E, Christidi F, Giavri Z, Velonakis G, Kelekis N, Liakos F, Emelifeonwu J, Kalamatianos T, Stranjalis G; Sledge Runner Fasciculus: Anatomic architecture and Tractographic Morphology. **Brain Structure and Function**, 2019;224(3):1051-66.

9. **Skandalakis GP**, Koutsarnakis C, Pantazis N, Kalyvas A, Komaitis S, Lani E, Drosos E, Hadjipanayis CG, Natsis K, Stranjalis G, Piagkou M: The carotico-clinoid bar: A systematic review and Meta-analysis of its prevalence and potential implications in cerebrovascular and skull base surgery. **World Neurosurgery**, 124 (2019): 267-276.

10. Komaitis S, **Skandalakis GP**, Kalyvas A, Drosos E, Lani J, Emelifeonwu J, Liakos F, Piagkou M, Kalamatianos T, Stranjalis G, Koutsarnakis C: The dorsal component of the Superior Longitudinal Fasciculus revisited. New insights from a focused fiber dissection study. **Journal of Neurosurgery**, 2019, Mar 1;1(aop):1-4.

11. Kalamatianos, T, Mavridis I, Karakosta E, Drosos E, **Skandalakis GP**, Kalyvas AV, Piagkou M, Koutsarnakis C, Stranjalis G: The parieto-occipital artery revisited: a microsurgical

anatomic study. **World Neurosurgery**, 2019; 126:e1130-9.

12. Neromyliotis E, Kalyvas A, Drosos E, Komaitis S, Bartziotas D, **Skandalakis GP**, Stranjalis G, Koutsarnakis C: Spinal Atypical rhabdoid teratoid tumor in an adult woman. A rare case report and review of the literature. **World Neurosurgery** 2019; 128:196-9.

13. Drosos E, Kalyvas A, Komaitis S, **Skandalakis GP**, Kalamatianos T, Liouta E, Neromyliotis E, Alexiou G, Stranjalis G, Koutsarnakis C. Angiosarcoma-related cerebral metastases: a systematic review of the literature. **Neurosurgical Review**, 2019, June 4: 1-20.

14. Komaitis S, Kalyvas A, **Skandalakis GP**, Drosos E, Lani E, Liouta E, Liakos F, Kalamatianos T, Piagkou M, Emelifeonwu J, Stranjalis G, Koutsarnakis C: Frontal Longitudinal System as revealed through the fiber micro-dissection technique: Structural evidence underpinning the direct connectivity of the prefrontal-premotor circuitry. **Journal of Neurosurgery**, 1 (aop), 1-13.

15. Koutsarnakis C, Komaitis S, Drosos E, Kalyvas AV, **Skandalakis GP**, Liakos F, Neromyliotis E, Lani E, Kalamatianos T, Stranjalis G. Mapping the superficial morphology of the occipital lobe: proposal of a universal nomenclature for clinical and anatomical use. **Neurosurgical review**. 2019 Nov 22:1-6.

16. Kalyvas A, Koutsarnakis C, Komaitis S, Karavasilis E, Christidi F, **Skandalakis GP**, Liouta E, Papakonstantinou O, Kelekis N, Duffau H, Stranjalis G. Mapping the human middle longitudinal fasciculus through a focused anatomo-imaging study: shifting the paradigm of its segmentation and connectivity pattern. **Brain Structure and Function**. 2020; 225(1):85-119.

17. **Skandalakis GP**, Komaitis S, Kalyvas A, Lani E, Kontrafouri C, Drosos E, Liakos F, Piagkou M, Placantonakis DG, Golfinos JG, Fountas KN, Kapsalaki EZ, Hadjipanayis CG, Stranjalis G, Koutsarnakis C. Dissecting the default mode network: direct structural evidence on the morphology and axonal connectivity of the fifth component of the cingulum bundle. **Journal of Neurosurgery**. 2020 Apr 24;1(aop):1-2.

18. Kalyvas A, Neromyliotis E, Koutsarnakis C, Komaitis S, Drosos E, **Skandalakis GP**, Pantazi M, Gobin YP, Stranjalis G, Patsalides A. A systematic review of surgical treatments of idiopathic intracranial hypertension (IIH). **Neurosurgical review**. 2020 Apr 25.

19. **Skandalakis GP**, Rivera D, Rizea CD, Bouras A, Jesu Raj JG, Bozec D, Hadjipanayis CG. Hyperthermia treatment advances for brain tumors. **International Journal of Hyperthermia**, 37(2), pp.1-2.

20. Salmas M, Chytas D, Paraskevas G, Noussios G, **Skandalakis GP**, Troupis T. Letter to the Editor Regarding: "Three-Dimensional Virtual Intraoperative Reconstruction: A Novel Method to Explore a Virtual Neurosurgical Field", **World Neurosurgery**. 2020 Oct; 142:543.

21. Salmas M, Chronopoulos E, Nikolaou VS, Babis GC, Kaseta M, **Skandalakis GP**, Chytas D. Letter to the Editor Regarding: Usefulness of 3D Printed Models in the Management of Complex Craniovertebral Junction Anomalies: Choice of Treatment Strategy, Design of Screw Trajectory, and Protection of Vertebral Artery. **World Neurosurgery**. 2020 Oct; 142:558.

22. Natsis K, Antonopoulos I, Politis C, Nikolopoulou E, Lazaridis N, **Skandalakis GP**, Chytas D, Piagkou M: Pterional variable topography and morphology: An anatomical study and its clinical significance. **Folia Morphologica** 2020 Sep 3.

23. Salmas M, Chytas D, Protogerou V, Demesticha T, **Skandalakis GP**, Troupis T: Letter to the Editor Regarding: "Tactile Skill-Based Neurosurgical Simulators Are Effective and Inexpensive". **World Neurosurgery**. Accepted – In press.

24. Komaitis S, Koutsarnakis C, Lani E, Kalamatianos T, Drosos E, **Skandalakis GP**, Liakos F, Liouta E, Kalyvas AV, Stranjalis G: Deciphering the Fronto-striatal circuitry through the fiber dissection technique: Direct structural evidence on the morphology and axonal connectivity of the Fronto-caudate Tract. **Journal of Neurosurgery.** Accepted – Under production

## PEER-REVIEWED BOOK CHAPTERS

1. **Skandalakis GP**, Ladner TR, Sarkiss C, Hadjipanayis CG: Planum/Tuberculum Sellae Meningiomas: Supraorbital Keyhole Approach. In, Evans J, Kenning T, Farrell C, and Kshettry V (Eds.): Endoscopic and Keyhole Cranial Surgery, **Springer Nature**, 2018.

## POSTER PRESENTATIONS

1. Surgical resection of a traumatic pseudoaneurysm of the occipital artery. A case report Kalyvas AV, Korfias C, Anagnostopoulos C, **Skandalakis G**, Themistocleous M, Sakas DE, University of Athens, Evangelismos Hospital, Neurosurgery Department, Athens, Greece, **EANS congress**, Athens, Greece, September 4-8, 2016.

2. Insights on the Connectivity of the Precuneus: Introducing the Retrosplenial Aslant Tract (RAT). **Skandalakis GP**, Koutsarnakis C, Kalyvas A, Placantonakis DG, Golfinos JG, Hadjipanayis CG, Kostas N. Fountas KN, Kapsalaki EZ and George Stranjalis G, **CNS Annual meeting**, Houston, TX, October 6-8, 2018.

3. Comparative Effectiveness of Preventive and Treatment Interventions for Cerebral Hyperperfusion Syndrome Following Bypass Surgery.": **Skandalakis GP**, Kalyvas A, Lani E, Komaitis S, Chatzopoulou D, Manolakou D, Pantazis N, Zenonos GA, Hadjipanayis CG, Stranjalis GS, Koutsarnakis C., **CNS Annual meeting**, San Francisco, CA October 19-23, 2019.

4. A Systematic Review of Surgical Treatments of Idiopathic Intracranial Hypertension (IIH): Should Venous Sinus Stenting (VSS) Be Regarded As The First Line Surgical Modality? Kalyvas A, Neromyliotis E, **Skandalakis GP**, Koutsarnakis C, Komaitis S, Zadeh G, Gentili F, Duffau H, Stranjalis G, Gobin P, Patsalides A. **AANS Annual Scientific Meeting**, (e-poster) 2020.

5. Mapping the Human Middle Longitudinal Fasciculus Through a Focused Anatomo-Imaging Study: Shifting The Paradigm Of Its Segmentation And Connectivity Pattern. Kalyvas A, Koutsarnakis C, Komaitis S, **Skandalakis GP**, Drosos E, Karavasilis E,

Christidi F, Zadeh G, Gentili F, Duffau H, Stranjalis G. **AANS Annual Scientific Meeting**, (e-poster) 2020.

6. The Cingulum Bundle-V as Revealed Through the Fiber Microdissection Technique: Structural Data Demonstrating the Direct Connectivity of the medial Temporo-Parietal Circuitry. **Skandalakis GP**, Komaitis S, Kalyvas A, Lani E, Kontrafouri C, Drosos E, Liakos F, Piagkou M, Placantonakis DG, Golfinos JG, Fountas KN, Kapsalaki EZ, Stranjalis G, **AANS Annual Scientific Meeting**, (e-poster) 2020.

## ORAL PRESENTATIONS

1. "Cognitive Dysfunction on Bipolar Disorder", **Skandalakis GP**. *Round Table on Cognitive Dysfunctions in Psychiatric Disorders* on the 21st Scientific Congress of Hellenic Medical Students, Megaron International Conference Centre, Athens, Greece, May 17, 2015.

2. "Epithalamus; Habenula & Pineal Gland", **Skandalakis GP**, Johnson EO, Stranjalis G. *Neurosurgery Grand Rounds*, Department of Neurosurgery, University of Athens, Evangelismos General Hospital, Athens, Greece, January 27, 2016.

3. "Roles and Duties of a Peer Teacher", **Skandalakis GP**, Johnson EO *"Neuroanatomy Peer Teaching Seminar: Training the Trainers"*, University of Athens School of Medicine, April 18, 2016.

4. "Glioma Infiltration through the White Matter: Data of a Systematic Review" **Skandalakis GP**, Kalyvas A, Lani E, Koutsarnakis C, Komaitis S, Stranjalis G, Hadjipanayis CG, *Tumor Board*, The Hellenic Center for neurosurgery research (H.C.N.R.), Athens, Greece, November 7, 2017.

5. "Cranioplasty in Trauma Neurosurgery" **Skandalakis GP**. *Round Table on the role of the Neurosurgeon in Neurotrauma* on the 24th Scientific Congress of Hellenic Medical Students & 12th International Forum for Medical Students and Young Doctors, Divani Caravel Hotel, Athens, Greece, April 29, 2018.

6. "Sledge Runner Fasciculus: Microanatomic architecture and Tractographic Morphology of a fiber tract subserving Spatial Navigation and Visuospatial imagery." Kalyvas A, Koutsarnakis C, **Skandalakis GP**, Komaitis S, Stranjalis G; 32nd Annual Congress of the Hellenic Neurosurgical Society & Joint Meeting with the Society of British Neurological Surgeons and Cyprus Neurosurgical Society, Chania, Greece, May 26, 2018.

7. "White matter dissection data indicating the existence of a previously unknown tract: Introducing the Retrosplenial Aslant Tract (RAT)". **Skandalakis GP**, Koutsarnakis C, Kalyvas A, Lani E, Kontrafouri C, Komaitis S, Piagkou M, Placantonakis DG, Golfinos JG, Hadjipanayis CG, and Stranjalis G, Department of Radiology Metropolitan Hospital, Athens Greece, July 23, 2018.

8. "Misadventures in mouse-cerebrovascular surgery: How to avoid them, how to manage them." **Skandalakis GP**, "Intraluminal MCA occlusion/reperfusion models in mice: methods and techniques hands on course" Department of Pharmacology, University of Athens School of Medicine, Athens, Greece, January 15, 2019.

9. "The Retrosplenial Aslant Tract: Previously unknown tract connecting high-order brain regions" **Skandalakis GP**, Koutsarnakis C, Kalyvas A, Lani E, Kontrafouri C, Komaitis S, Piagkou M, Placantonakis DG, Golfinos JG, Hadjipanayis CG, Fountas KN, Kapsalaki EZ, Stranjalis G. Department of Neuroradiology, University of Athens School of Medicine, Athens, Greece, January 23, 2019.

10. "Comparative Effectiveness of Preventive and Treatment Interventions for Cerebral Hyperperfusion Syndrome Following Bypass Surgery.": **Skandalakis GP**, Kalyvas A, Lani E, Komaitis S, Chatzopoulou D, Manolakou D, Pantazis N, Zenonos GA, Hadjipanayis CG, Stranjalis GS, Koutsarnakis C **International Cerebrovascular Symposium, CNS Annual meeting**, San Francisco, CA October 21, 2019.

11. "Photodynamic therapy of diffuse intrinsic pontine glioma in combination with radiation.": **Skandalakis GP**, Rivera D, Bouras A, Rizea CD, Jesu Raj JG, Bozec D, Hadjipanayis, CG: Tumor Talk, The Journal of Neuro-oncology, June 2020

12. "Combination Photodynamic Therapy and Fractionated Radiation for Diffuse Intrinsic Pontine Glioma" **Skandalakis GP**, Rivera D, Bouras A, Rizea CD, Jesu Raj JG, Bozec D, Hadjipanayis, C.G, Photodynamic Therapy and Photodiagnosis Update 2020 e-congress, Nancy, France, November 7, 2020

## SCIENTIFIC CONGRESSES, MEETINGS, AND COURSE PARTICIPATION

1. 29th Panhellenic Congress of Neurosurgery, Athens, Greece, May 28-30, 2015.

2. Larissa International Neurovascular Course "Cerebral Aneurysms", Department of Neurosurgery, University of Thessaly, School Health Sciences, Larisa, Greece, May 18-19, 2016.

3. "MEN Seminar for patients and their support networks", Department of Surgery, Endocrine Surgery Program, Mount Sinai Hospital, New York, NY, July 22, 2016.

4. "Intracranial Glioma Workshop from A to Z" Department of Neurosurgery, University of Thessaly, School Health Sciences, Larisa, Greece, April 6-8, 2017.

5. ENLS (Emergency Neurological Life Support) course, Neurocritical Care Society, 251 Airforce General Hospital, Athens, Greece, September 14-15, 2018.

6. CNS Annual Meeting, Houston, Texas, October 5-11, 2018.

7. International Neurovascular Course "Mulitmodality Management of Intracranial and Spinal AVMs", Royal Olympic Hotel, Athens, Greece, March 29-30, 2019 Evandro De Oliveira Symposium, AANS, San Diego, CA, USA, April 11-12, 2019.

8. AANS Annual Scientific Meeting, San Diego, CA, USA, April 13-18, 2019.

9. Evandro De Oliveira Symposium, AANS, San Diego, CA, USA, April 11-12, 2019.

10. "Intracranial Glioma Workshop from A to Z" Department of Neurosurgery, University of Thessaly, School Health Sciences, Royal Olympic Hotel, Athens, Greece, May 9-11, 2019.

11. CNS Annual Meeting, San Francisco, CA, October 19-23, 2019.

12. Second Annual Fluorescence-Guided Surgery Brain Tumor Symposium, Leon & Norma Hess Center for Science and Medicine, New York, NY, Dec 6, 2019.

13. New York Neurosurgery Update: A One Day Symposium, NYU Langone Health, New York, NY, Dec 6, 2019.

14. Mastering the basics of Neurosurgery: Common Approaches, Surgical Innovations Laboratory for Skull base and Microneurosurgery, Department of Neurological Surgery, Weill Cornell Medical College/New York-Presbyterian Hospital, New York, NY.

15. Barrow Live Aneurysm Surgery Course, Barrow Neurological Institute, Phoenix, AZ, March 8-11, 2020.

16. Last Samurai 1st Annual Lawton-Tanikawa Vascular Neurosurgery Course, The Loyal & Edith Davis Neurosurgical Research Laboratory, Barrow Neurological Institute Phoenix, AZ, March 12-13, 2020.

## PROFESSIONAL MEMBERSHIPS

1. Congress of Neurological Surgeons
2. American College of Surgeons
3. American Heart Association/ American Stroke Association
4. Hellenic Society for Neurosciences
5. Federation of European Neuroscience Societies
6. Hellenic Medical Society of New York
7. Greek American Neurosurgical Society

## OTHER EMPLOYMENT EXPERIENCE

| | |
|---|---|
| 2008-2012 | Managing Director, Stefanakis Hotel, Varkiza, Greece.<br>Audit Consultant, G. Stefanakis S.A., Athens, Greece. |
| 2005-2008 | Front Desk Receptionist, Stefanakis Hotel, Varkiza, Greece. |

## ATHLETIC AWARDS

1. Shot Put: 2nd Place, Athens College Track and Field, 1998
2. Swimming: 1st Place, Athens College 50m & 100m Butterfly & Free style, 1999 – 2002
3. Hammer Throw: 1st Place, Athens College, Track and Field, 2001
4. Tennis: Various Awards, 1999 - 2004

## CERTIFICATIONS

2nd stage Freediver, 2012

## INTERESTS

Spending time with family and friends, running, hiking, swimming, literature, history, reading about lives of neurosurgeons and how they improved patient care.

# Publications

## PEER-REVIEWED JOURNAL ARTICLES

1. Koutsarnakis C, Kalyvas AV, **Skandalakis GP**, Karavasilis E, Christidi F, Giavri Z, Velonakis G, Kelekis N, Liakos F, Emelifeonwu J, Kalamatianos T, Stranjalis G; Sledge Runner Fasciculus: Anatomic architecture and Tractographic Morphology. **Brain Structure and Function**, 2019;224(3):1051-66.

2. Komaitis S, **Skandalakis GP**, Kalyvas A, Drosos E, Lani J, Emelifeonwu J, Liakos F, Piagkou M, Kalamatianos T, Stranjalis G, Koutsarnakis C: The dorsal component of the Superior Longitudinal Fasciculus revisited. New insights from a focused fiber dissection study. **Journal of Neurosurgery**, 2019, Mar 1;1(aop):1-4.

3. Kalyvas A, Koutsarnakis C, Komaitis S, Karavasilis E, Christidi F, **Skandalakis GP**, Liouta E, Papakonstantinou O, Kelekis N, Duffau H, Stranjalis G. Mapping the human middle longitudinal fasciculus through a focused anatomo-imaging study: shifting the paradigm of its segmentation and connectivity pattern. **Brain Structure and Function**. 2020; 225(1):85-119.

4. **Skandalakis GP**, Komaitis S, Kalyvas A, Lani E, Kontrafouri C, Drosos E, Liakos F, Piagkou M, Placantonakis DG, Golfinos JG, Fountas KN, Kapsalaki EZ, Hadjipanayis CG, Stranjalis G, Koutsarnakis C. Dissecting the default mode network: direct structural evidence on the morphology and axonal connectivity of the fifth component of the cingulum bundle. **Journal of Neurosurgery**. 2020 Apr 24;1(aop):1-2.

## POSTER PRESENTATIONS

1. Insights on the Connectivity of the Precuneus: Introducing the Retrosplenial Aslant Tract (RAT). **Skandalakis GP**, Koutsarnakis C, Kalyvas A, Placantonakis DG, Golfinos JG, Hadjipanayis CG, Kostas N. Fountas KN, Kapsalaki EZ and George Stranjalis G, **CNS Annual meeting**, Houston, TX, October 6-8, 2018.

2. Mapping The Human Middle Longitudinal Fasciculus Through a Focused Anatomo-Imaging Study: Shifting The Paradigm Of Its Segmentation And Connectivity Pattern. Kalyvas A, Koutsarnakis C, Komaitis S, **Skandalakis GP**, Drosos E, Karavasilis E, Christidi F, Zadeh G, Gentili F, Duffau H, Stranjalis G. **AANS Annual Scientific Meeting**, (e-poster) 2020.

3. The Cingulum Bundle-V as Revealed Through the Fiber Microdissection Technique: Structural Data Demonstrating the Direct Connectivity of the medial Temporo-Parietal Circuitry. **Skandalakis GP**, Komaitis S, Kalyvas A, Lani E, Kontrafouri C, Drosos E, Liakos F, Piagkou M, Placantonakis DG, Golfinos JG, Fountas KN, Kapsalaki EZ, Stranjalis G, **AANS Annual Scientific Meeting**, (e-poster) 2020.

## ORAL PRESENTATIONS

1. "Sledge Runner Fasciculus: Microanatomic architecture and Tractographic Morphology of a fiber tract subserving Spatial Navigation and Visuospatial imagery." Kalyvas A, Koutsarnakis C, **Skandalakis GP**, Komaitis S, Stranjalis G; 32nd Annual Congress of the Hellenic Neurosurgical Society & Joint Meeting with the Society of British Neurological Surgeons and Cyprus Neurosurgical Society, Chania, Greece, May 26, 2018.

2. "The Retrosplenial Aslant Tract: Previously unknown tract connecting high-order brain regions" **Skandalakis GP**, Koutsarnakis C, Kalyvas A, Lani E, Kontrafouri C, Komaitis S, Piagkou M, Placantonakis DG, Golfinos JG, Hadjipanayis CG, Fountas KN, Kapsalaki EZ, Stranjalis G. Department of Neuroradiology, University of Athens School of Medicine, Athens, Greece, January 23, 2019.

# Honors/Awards

**1. 2020 Promising Young Investigator Award**, Icahn School of Medicine at Mount Sinai, February 27th, 2020

**2. Top 5 Submitted Abstract Award**, 32nd Annual Congress of the Hellenic Neurosurgical Society & Joint Meeting with the Society of British Neurological Surgeons and Cyprus Neurosurgical Society, Chania, Greece, May 26th, 2018

# Preface

Endeavors to understand and describe the architecture of the human brain date back more than twenty centuries years ago. The first significant contributions to neuroanatomy were made by Herophilus and Erasistratus during the third century BC.[53] The recent revival of the white matter fiber dissection technique first described by Klingler- and its incorporation to neurocognitive research, in combination with the advent of sophisticated neuroimaging methods such as functional magnetic resonance imaging (fMRI) and diffusion tensor imaging (DTI) have led to a more profound understanding of the brain connectivity and anatomo-functional organization.[88] The concept of brain hodotopy (deriving from the Greek words hodos meaning road, pathway and topos meaning place) introduces a new model of perceiving cerebral function not merely as a localized cortical phenomenon but as an integrative network epiphenomenon; thus, emphasizing the role of the white matter connectivity in brain function.[43] Since brain anatomy and function are reciprocal, a special interest has aroused over the past few years regarding the intricate architecture of white matter pathways previously described in core neuroanatomical texts, aiming not only to refine anatomical knowledge but mainly to improve our understanding of cerebral connectivity and function.[49] Recent functional findings in healthy individuals suggest that the precuneus is the core structure of the default mode network[56,200] and is involved in a broad range of high-order functions including navigation, memory retrieval, attention and reasoning.[2,121,139,165,215] Nonetheless, the anatomy of the human precuneus exhibits significant variability and has remained one of the less accurately mapped areas of the human.[31] Moreover, although the functional connectivity of the precuneus and its significance have been repeatedly reported, the underlying structural circuit has not been characterized. This dissertation aims to gather insights on the anatomy of the precuneus and pass them on allowing the study of high-level functioning circuits residing in the posteromedial cortex in greater detail; thus, setting the ground for a more thorough understanding of these networks in normal brain function and medical conditions of the brain. Hopefully, whatever insight is contained on the following pages will inform researchers and medical practitioners while also benefiting patients with lesions planned to be treated through an approach involving the precuneus

# Abbreviations

AAR = anterior ascending ramus of the sylvian fissure

AG = angular gyrus

Ant and PostOlfS = anterior and posterior paraolfactory sulcus

AntCom = anterior commissure

AntLimb = anterior limb of the internal capsule

AntLimS = anterior limiting sulcus of the insula

AntOrbG = anterior orbital gyrus

AntPerfSubst = anterior perforated substance

Ap = insular apex

ARSyF = anterior ramus of sylvian fissure

ASCR = anterior subcentral ramus of sylvian fissure

Atr = atrium of lateral ventricle

BC = Before Christ

BodCaN = body of the caudate nucleus

BoFo = body of fornix

BrSt = brainstem

CaF = calcarine fissure

CaN = caudate nucleus

CaS = callosal sulcus

CB-V = Fifth component of the cingulum bundle

CC= Corpus Callosum

CdN= Caudate Nucleus (body)

CgG= Cingulate Gyrus

Cgra= Radiations of the cingulum towards the precuneus

Cgs= Cingulate Sulcus

Cgsa = Cingulum Superior Arm

ChPl = choroid plexus

CInsS = central insular sulcus

CiPo = cingulate pole

CITP = Contralateral interhemispheric transfalcine transprecuneus approach

ColS = collateral sulcus

CoR = Corona Radiata

CoS= Collateral sulcus

CR= Callosal Radiations

CS = central sulcus

Cu = cuneus

ExtPerpF = external perpendicular fissure

FMaS = frontomarginal sulcus

Fo = fornix

Fpo= Frontoparietal Operculum

FuG = fusiform gyrus

GRe = gyrus rectus

HeG = Heschl gyrus

HG Heschl's gyrus

HR = horizontal ramus of sylvian fissure

HySta = hypophyseal stalk

IFG = inferior frontal gyrus

IFOF = Inferior fronto-occipital fasciculus

IFS = inferior frontal sulcus

IFS/PreCS = IFS and precentral sulcus

IHF = interhemispheric fissure

IIIn = oculomotor nerve

IIIV = third ventricle

IIIV = third ventricle

IIn = optical nerve

InfLimS = inferior limiting sulcus

InfRosS = inferior rostral sulcus

Ins = insula

IntCap = internal capsule

IntCps= Internal Capusle

IOS = inferior occipital sulcus

IPaLob = inferior parietal lobule

IPS = intraparietal sulcus

IPS intraparietal sulcus

IRP = inferior rolandic point, projection of the central sulcus in the sylvan fissure

IsCiG= Isthmus of the Cingulate gyrus

ISJ = intermediary sulcus of Jensen

Ist = isthmus of cingulate gyrus

Ist = isthmus of cingulate gyrus

ITG = inferior temporal gyrus

ITG = inferior temporal gyrus

ITS = inferior temporal sulcus

IVeFo = interventricular foramen of Monro

IVn = trochlear nerve

IVV = fourth ventricle.

LatGeBo = lateral geniculate body

LatMeS = lateral mesencephalic sulcus

LatOlfStr = lateral olfactory striae

LatOrbG = lateral orbital gyrus

LatV = lateral ventricle

LatV = lateral ventricle

LiG = lingual gyrus

MaBo = mamillary body

MaCiS = marginal ramus of the cingulate sulcus

MedFG = medial frontal gyrus

MedOlfStr = medial olfactory striae

MedOrbG = medial orbital gyrus

MeFS = medial frontal sulcus

MeGeBod = medial geniculate body

MFG = middle frontal gyrus

MFS = middle frontal sulcus

MOG = middle occipital gyrus

Mrg= Marginal ramus of the cingulate sulcus

MTG = middle temporal gyrus

OcPo = occipital pole

OL = occipital lobe

OlfBu = olfactory bulb

OlfS = olfactory sulcus

OlfTr = olfactory tract

Op = opercular part of inferior frontal gyrus

OpIFG = opercular part of the inferior frontal gyrus

OptTr = optic tract

Orb = orbital part of inferior frontal gyrus

OrbGi = orbital gyri

OrbS = orbital sulcus

OTS = occipitotemporal sulcus

PaCLob = paracentral lobule

PaCS = paracentral sulcus

PaOccCo = parietooccipital arch

PaOlfG = paraolfactory gyri

PAR = posterior ascending ramus of sylvian fissure

PARSyF = posterior ramus of sylvian fissure

PaTeG = paraterminal gyrus

PCG = postcentral gyrus,

PcgG = Paracingulate gyrus

PcgS= Paracingulate sulcus

PCS = postcentral sulcus

PHG = parahippocampal gyrus

Pi = pineal gland

PoPl = polar plane of the opercular temporal surface

POS = parietooccipital sulcus

PostCG = postcentral gyrus

PostCS = postcentral sulcus

PostDescR = posterior descending ramus of sylvian fissure

PostMedOrbLob = posteromedial orbital lobule

PostOrbG = posterior orbital gyrus

PostPerfSubst = posterior perforated substance

PrCn(a)= Anterior Precuneus

Prcn= Precuneus

PrCS = precentral sulcus

Pre-SMA= Pre-Supplementary Motor Area

PreCG = precentral gyrus

PreCS = precentral sulcus

PreCu = precuneus

PreOccNo = preoccipital notch

PrG precentral gyrus

PrG= Precentral Gyrus

PrS= Precentral Sulcus

PRSyF = posterior ramus of sylvian fissure

PSCR = posterior subcentral ramus of sylvian fissure

PSyP = posterior sylvian point.

PTA posterior transverse area

PtG= Postcentral Gyrus

Pulv = pulvinar of thalamus

RhiS = rhinal sulcus

RhiS = rhinal sulcus

RoCC = rostrum of the corpus callosum

SFG = superior frontal gyrus

SFS = superior frontal sulcus

ShIG = short insular gyri

SLF-1 = Dorsal Component of the Superior Longitudinal Fasciculus

SLF-Ia= Superior Longitudinal Fasciculus I – anterior segment

SLF-Ip= Superior Longitudinal Fasciculus I – posterior segment

SLF/AF Superior Longitudinal Fasciculus/Arcuate Fasciculus Complex,

SMA= Supplementary Motor Area

SMG = supramarginal gyrus

SOG = superior occipital gyrus

SoJ = sulcus of jensen

SOS = superior occipital sulcus

SPaLob = superior parietal lobe

Spl = splenium of corpus callosum

Spl = splenium of corpus callosum

SPL superior parietal lobule

SPLob = superior parietal lobe

SpS= Subparietal sulcus

SRF= Sledge Runner fasciculus

STG superior temporal gyrus,

StrTe = stria terminalis

STS = superior temporal sulcus

SubCG = subcentral gyrus

SubPS = subparietal sulcus

SupLimS = superior limiting sulcus of insula

SupRosS = superior rostral sulcus

SyF = sylvian fissure

TePl = temporal plane.

TePo = temporal pole

Tha = thalamus

TP temporal pole

Tr = triangular part of inferior frontal gyrus

TrInsG = transverse insular gyrus

TTS = transverse temporal sulcus

Un = uncus

# Abstract

The anatomy of the human precuneus exhibits significant variability and has remained one of the less accurately mapped areas of the human brain. Although the functional connectivity of the precuneus and its significance have been repeatedly reported, the underlying structural circuit has not been characterized. Understanding the underlying structural connectivity of these networks is critical for refining their circuitry, clarifying their function and implementing safe neurosurgical approaches. The aim of this dissertation was to investigate the surface anatomy and fiber tracts of the precuneal region in cadaveric specimens. By mapping the sulcal anatomy of the precuneus and employing the fiber microdissection technique, we demonstrate the variations of the Subparietal sulcus (SpS) and the parietooccipital sulcus (POS) and the anatomy and connectivity of the Sledge Runner Fasciculus (SRF), dorsal component of the superior longitudinal fasciculus (SLF- 1), middle longitudinal fasciculus (Mdlf), inferior fronto-occipital fasciculus (IFOF), claustrocortical fibers and fifth component of the cingulum bundle (CB-V). We found the Precuneus surface anatomy to be considerably variable. We also found The MdLF-I, connecting the dorsolateral Temporal Pole and STG to the precuneus; SRF not to participate in the connectivity of the precuneus but connecting the cortical areas of the anterior cuneus, anterior lingula, isthmus of the cingulum and posterior parahippocampal gyrus; SLF- 1 connecting the precuneus with areas of the medial frontal lobe ; the IFOF connecting the precuneus with the frontal lobe; claustrocortical fibers connecting the precuneus with the claustrum and The CB-V connecting the precuneus with the regions of the temporal lobe

# Greek Abstract/Περίληψη

Η ανατομία του ανθρώπινου προσφηνοειδούς λοβίου παρουσιάζει αρκετές παραλλαγές και παραμένει μία από τις λιγότερο χαρτογραφημένες περιοχές του ανθρώπινου εγκεφάλου. Αν και έχει αναφερθεί επανειλημμένα η λειτουργική συνδεσιμότητα του προσφηνοειδούς λοβίου καθώς και η σημασία της, το υποκείμενο κύκλωμα των δεματίων της λευκής ουσίας δεν έχει χαρακτηριστεί ακόμα. Η κατανόηση της υποκείμενης δομικής συνδεσιμότητας αυτών των δικτύων της λευκής ουσίας έχει μεγάλη σημασία για τον ακριβή χαρακτηρισμό των δεματίων, την αποσαφήνιση της λειτουργίας τους και την σχέση τους σε νευροχειρουργικές προσπελάσεις. Ο σκοπός αυτής της διατριβής ήταν η μελέτη της φλοιώδης επιφανειακής ανατομίας και των δεματίων της περιοχής του προσφεινοειδούς λοβίου σε ανατομικά παρασκευάσματα. Χαρτογραφώντας την επιφανειακή ανατομία του προσφηνοειδούς λοβίου και χρησιμοποιώντας την τεχνική διατομής λευκής ουσίας, αναδεικνύουμε τις παραλλαγές της υποβρεγμάτιας αύλακας και της βρεγματοϊνιακής σχισμής καθώς και την ανατομία και συνδεσιμότητα του Sledge Runner Fasciculus (SRF), ραχιαίου τμήματος του άνω επιμήκους δεματίου (SLF-1), του μέσου επιμήκους δεματίου (Mdlf), της κάτω μετωπιαία-ινιακής δεσμίδας, έξω κάψας και του πέμπτου τμήματος του προσαγωγείου (CB-V). Βρήκαμε ότι η επιφανειακή ανατομία του Precuneus εμφανίζει πολλές παραλλαγές. Επίσης καταγράψαμε  ότι το MdLF-I συνδέει τον πόλο του κροταφικού λοβού και την άνω κροταφική έλικα με το προσφηνοειδές λοβίο, το SRF να μην συμμετάσχει στη συνδεσιμότητα του προσφηνοειδούς λοβίου αλλά να συνδέει τις φλοιώδεις περιοχές του πρόσθιου σφηνοειδούς λοβίου, του ισθμού του προσαγωγείου και του οπίσθιου τμήματος της παραϊοππόκαμπιας έλικας; το SLF- 1 να συνδέει το προσφηνοειδές λοβίο με περιοχές της έσω επιφάνειας του μετωπιαίου λοβού; το IFOF να συνδέει τον προσφηνοειδές λοβίο με τον μετωπιαίο λοβό και το CB-V να συνδέει το προσφηνοειδές λοβίο με τον έσω κροταφικό λοβό και την ατρακτοειδή έλικα.

# Introduction

## 1.1 The Sulci, Gyri, and Cerebral Lobes

Given the visual evidence of the lateral cerebral sulcus, or sylvian fissure, together with the distinct, slightly oblique arrangement of the precentral and postcentral gyri as well as of the sulci that delineate them at approximately the center of the external brain surface, the character of the remaining gyri of the superolateral surface of each cerebral hemisphere can be more easily understood if we take as our starting point and basis those sulcal spaces and cerebral gyri. The macroscopic study of the sulci and gyri of each cerebral hemisphere should therefore begin with the identification of the sylvian fissure, which clearly separates the superolateral surfaces of the frontal, central, and parietal lobes from the temporal lobe, and should be followed by the identification of the precentral and post- central gyri, which divide the portion of this surface that is superior and posterior to the sylvian fissure into its anterior and posterior halves. Adopting this approach, we will describe the 7 lobes of each cerebral hemisphere as follows: frontal, central, parietal, occipital, temporal, insular, and limbic.[221] Since the connections of the limbic lobe are particularly complex, the text related to that lobe also addresses the adjacent and correlated areas.

The Frontal Lobe

The frontal lobe constitutes the largest, most anterior part of each hemisphere. Within the scheme adopted in this article, the frontal lobe is delineated posteriorly by the oblique precentral sulcus and is composed of the superior, middle, and inferior frontal gyri, which are oriented longitudinally and separated by the superior and inferior frontal sulci, also longitudinally oriented (Fig. 1.1). These gyri are often referred to as F1, F2, and F3, respectively. [1]

Portion of this section has been previously published in Ribas GC. The cerebral sulci and gyri. Neurosurgical focus. 2010 and has been reproduced with permission from JNS Publishing group

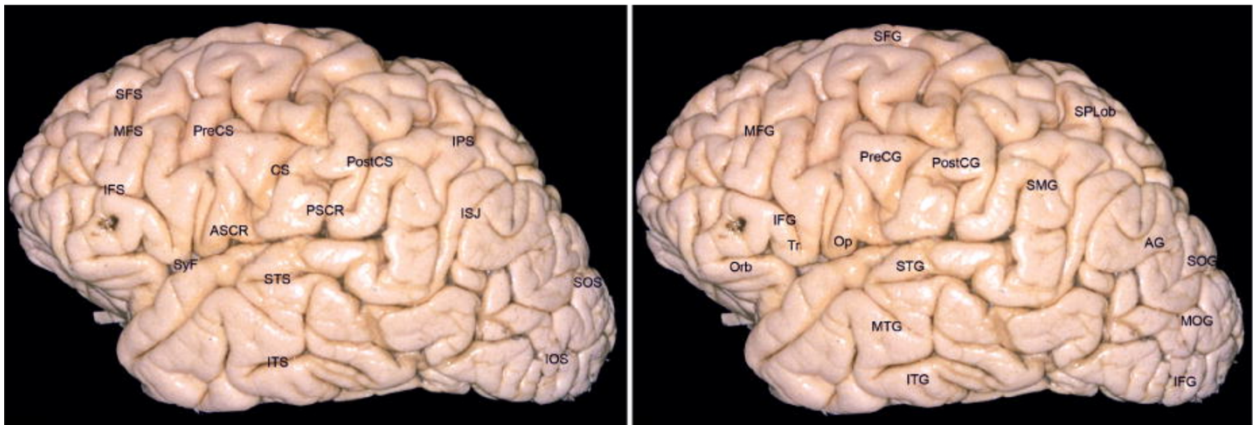


**Figure 1.1** The main sulci (left) and gyri (right) of the superolateral surface of the brain. AG = angular gyrus; ASCR = anterior subcentral ramus of sylvian fissure; CS = central sulcus; IFG = inferior frontal gyrus; IFS = inferior frontal sulcus; IOS = inferior occipital sulcus; IPS = intraparietal sulcus; ISJ = intermediary sulcus of Jensen; ITG = inferior temporal gyrus; ITS = inferior temporal sulcus; MFG = middle frontal gyrus; MFS = middle frontal sulcus; MOG = middle occipital gyrus; MTG = middle temporal gyrus; Op = opercular part of inferior frontal gyrus; Orb = orbital part of inferior frontal gyrus; PostCG = postcentral gyrus; PostCS = postcentral sulcus; PreCG = precentral gyrus; PreCS = precentral sulcus; PSCR = posterior subcentral ramus of sylvian fissure; SFG = superior frontal gyrus; SFS = superior frontal sulcus; SMG = supramarginal gyrus; SOG = superior occipital gyrus; SOS = superior occipital sulcus; SPLob = superior parietal lobe; STG = superior temporal gyrus; STS = superior temporal sulcus; SyF = sylvian fissure; Tr = triangular part of inferior frontal gyrus. By permission of JNS Publishing group

On the cerebral surface posteriorly, the superior frontal gyrus is connected to the precentral gyrus by at least 1-fold, which more commonly lies medially along the inter- hemispheric fissure. Anteriorly, the superior frontal gyrus might be connected to the middle frontal gyrus, with the orbital gyri and the gyrus rectus. In general terms, the superior frontal gyrus is subdivided into 2 longitudinal portions by the so-called medial frontal sulcus, and its medial portion is at times designated the medial frontal gyrus.[137] Along the most medial portion of the superior frontal gyrus and immediately facing the precentral gyrus is the important region known as the supplementary motor area, which varies from person to person and has poorly defined borders.[17,216]

The middle frontal gyrus is typically the largest of the frontal gyri and often has a sulcus that is shallower than that of the other frontal gyri, usually running along its anterior two-thirds and known as the middle or intermediate frontal sulcus.[137] In most human brains, the middle frontal gyrus is superficially connected to the precentral gyrus by a prominent root that lies between the extremities of a marked interruption in the precentral sulcus. The frequent

interruptions in the inferior frontal sulcus are attributable to connections between the middle and inferior frontal gyri.

The inferior frontal gyrus is irregular, crisscrossed by various small branches of the inferior frontal sulcus, which typically superiorly delineate the gyrus in an interrupted manner. Inferiorly, this gyrus is delineated and crisscrossed by rami of the sylvian fissure. Anteriorly, the inferior frontal gyrus terminates, merging with the anterior portion of the middle frontal gyrus. Posteriorly, it is connected to the precentral gyrus. The inferior frontal gyrus is composed of, from anterior to posterior, its orbital, triangular, and opercular parts.

The emergence of the horizontal and ascending anterior rami from the same point in the sylvian fissure characterizes the triangular part of the inferior frontal gyrus, which is typically more retracted than the other 2 parts (Figs. 1.2 and 1.3).

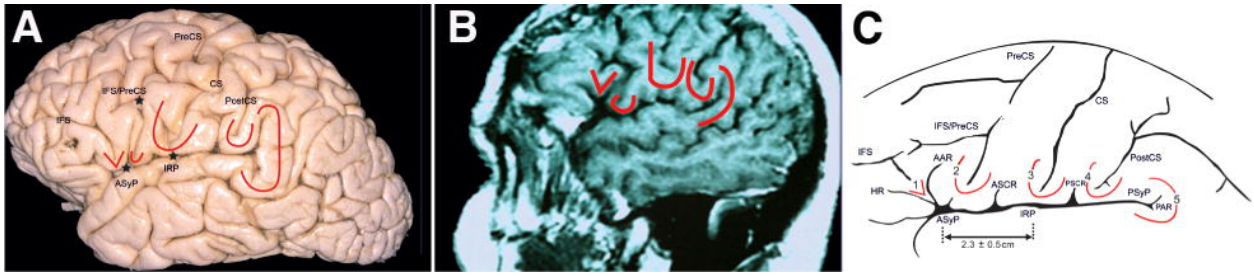


**Figure 1.2** The frontoparietal operculum: cadaveric specimen (A), MR image (B), and sketch of sulcal and gyri morphology (C). The frontoparietal operculum is characterized by a V-shaped convolution consisting of the triangular part of the inferior frontal gyrus (IFG) (1), located just superiorly to the anterior sylvian point (ASyP), and usually containing a descending branch of the inferior frontal sulcus (IFS); the 3 following U-shaped convolutions respectively composed by the opercular part of the IFG (2), which is always intersected by the inferior part of the precentral sulcus; the subcentral gyrus or rolandic operculum (3), composed of the inferior connection of the pre- and postcentral gyri enclosing the inferior part of the central sulcus (CS); the connection arm between the postcentral and supramarginal gyri (4) that contains the inferior part of the postcentral sulcus; and finally the C- shaped convolution (5) constituted by the connection of the supramarginal and superior temporal gyri that encircles the posterior end of the sylvian fissure. The bottoms of the U-shaped convolutions and their related sulcal extremities can be situated either superior to the fissure or inside its cleft. Stars designate the areas labeled. AAR = anterior ascending ramus of the sylvian fissure; ASCR = anterior subcentral ramus of sylvian fissure; HR = horizontal ramus of sylvian fissure; IFS/PreCS = IFS and precentral sulcus; IRP = inferior rolandic point, projection of the central sulcus in the sylvan fissure; PAR = posterior ascending ramus of sylvian fissure; PostCS = postcentral sulcus; PreCS = precentral sulcus; PSCR = posterior subcentral ramus of sylvian fissure; PSyP = posterior sylvian point. By permission of JNS Publishing group

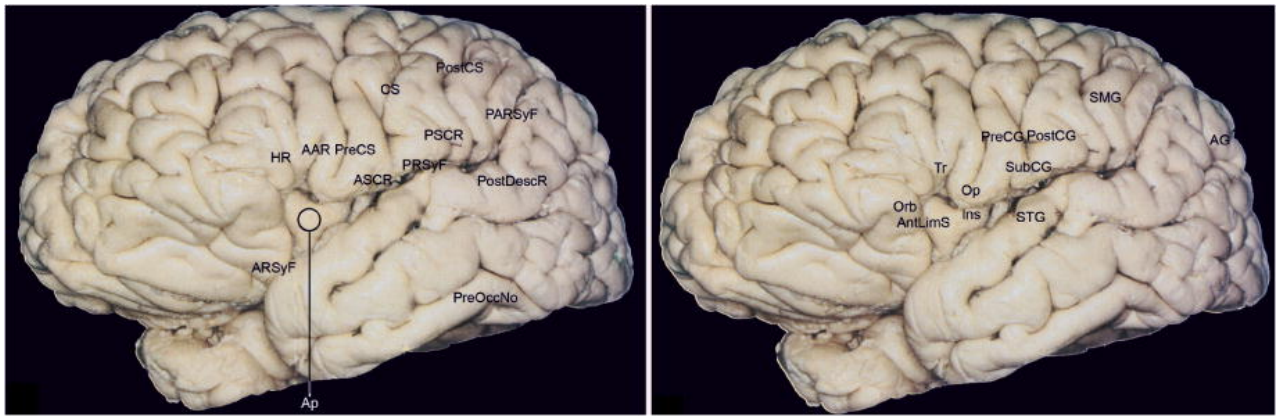


**Figure 1.3** Sulci (left) and gyri (right) of the frontoorbital, frontoparietal, and temporal operculi. AAR = anterior ascending ramus of the sylvian fissure; AG = angular gyrus; AntLimS = anterior limiting sulcus of the insula; Ap = insular apex; ARSyF = anterior ramus of sylvian fissure; ASCR = anterior subcentral ramus of sylvian fissure; CS = central sulcus; HR = horizontal ramus of sylvian fissure; Ins = insula; Op = opercular part of inferior frontal gyrus; Orb = orbital part of inferior frontal gyrus; PARSyF = posterior ramus of sylvian fissure; PostCG = postcentral gyrus; PostCS = postcentral sulcus; PostDescR = posterior descending ramus of sylvian fissure; PreCG = precentral gyrus; PreCS = precentral sulcus; PreOccNo = preoccipital notch; PRSyF = posterior ramus of sylvian fissure; PSCR = posterior subcentral ramus of sylvian fissure; SMG = supramarginal gyrus; STG = superior temporal gyrus; SubCG = subcentral gyrus; Tr = triangular part of inferior frontal gyrus. By permission of JNS Publishing group

The orbital part is the most prominent of the 3, and the opercular part is consistently U-shaped. Given the usual retraction of the triangular part, the horizontal and ascending anterior branches of the sylvian fissure typically emerge from a small widening of the subarachnoid space, designated the anterior sylvian point.[161,224] Therefore, the anterior sylvian point is situated inferior to the triangular part and anterior to the base of the opercular portion. The point, which is typically visible to the naked eye, divides the sylvian fissure into its anterior and posterior branches. [161,224]

The triangular part is quite often divided superiorly by a small descending branch of the inferior frontal sulcus, and the inferior most portion of the precentral sulcus is always harbored within the U of the opercular part.[161] Inferiorly and anteriorly delineated by the anterior sylvian point and posteriorly delineated by the anterior sub-central branch of the sylvian fissure, the posterior half of the U that characterizes the opercular part corresponds to the important connective fold that is always situated between this portion of the inferior

frontal gyrus and the precentral gyrus. In some cases, the anterior basal portion of the opercular part is more developed and is divided by another branch of the sylvian fissure. That branch runs from front to back and is called the diagonal sulcus of Eberstaller. When the diagonal sulcus of Eberstaller is present, it divides the anterior portion of the opercular part into 2 triangular portions that are positioned inversely to each other.

In the dominant hemisphere, the opercular and triangular parts of the inferior gyrus correspond to the Broca area, which is responsible for the production of spoken language.[16,17,70,150,216]

Inferiorly, although the orbital part continues with the lateral orbital gyrus, at times passing under a shallow sulcus known as the frontoorbital sulcus, the triangular part is always superior to the sylvian fissure, and the base of the opercular part can be located either superiorly or within that same fissure.[137,159]

The triangular and opercular parts together with the subcentral gyrus, which connects the precentral and postcentral gyri, and the anteroinferior portion of the supramarginal gyrus cover the superior aspect of the insular surface and constitute the frontoparietal operculum (Figs. 1.2 and 1.3). Therefore, the frontoparietal operculum is situated between the horizontal and posterior ascending branches of the sylvian fissure.[161,216]

Anteriorly, the frontal gyri are delineated by the appropriately named fronto marginal sulcus, which lies superior and parallel to the supraciliary margin, separating the superolateral and orbital frontal surfaces.[137,221]

On the frontobasal, or orbital, surface of each frontal lobe, the deep olfactory sulcus, which harbors the olfactory bulb and olfactory tract, is very deep and lies longitudinally in a paramedian position (Fig. 1.4). Posteriorly, the olfactory tract is divided into the medial and lateral striae, which delineate the anteriormost aspect of the anterior perforated substance.

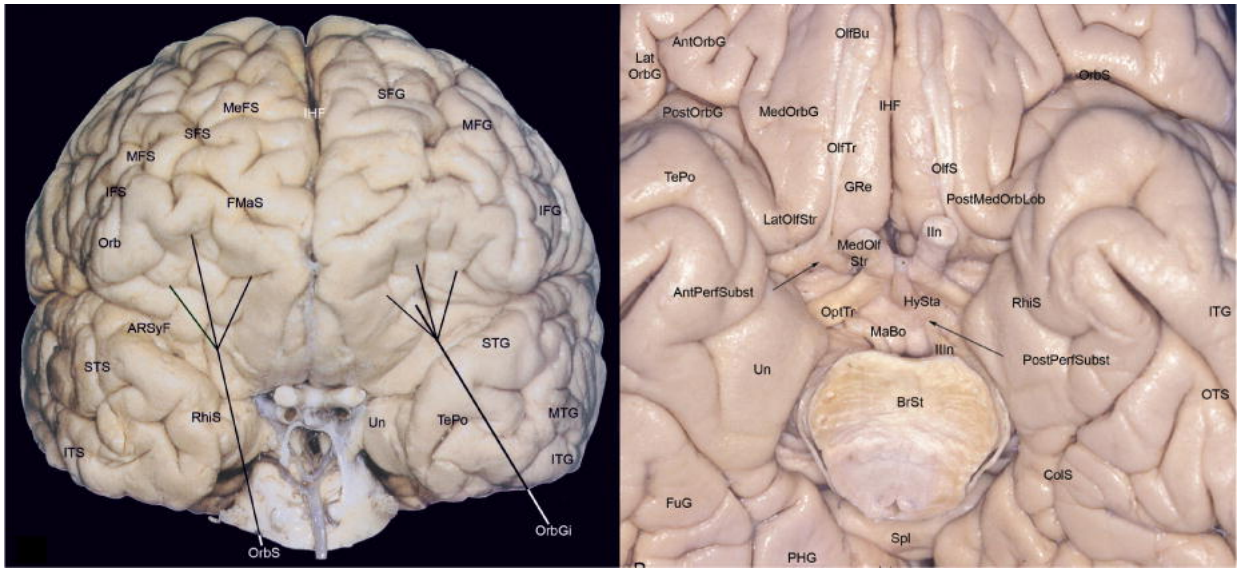


**Figure 1.4** Anterior view of cerebral hemispheres (left) and view of the basal frontotemporal surface (right). AntOrbG = anterior orbital gyrus; AntPerfSubst = anterior perforated substance; ARSyF = anterior ramus of sylvian fissure; BrSt = brainstem (pons); ColS = collateral sulcus; FMaS = frontomarginal sulcus; FuG = fusiform gyrus; GRe = gyrus rectus; HySta = hypophyseal stalk; IFG = inferior frontal gyrus; IFS = inferior frontal sulcus; IHF = interhemispheric fissure; Ist = isthmus of cingulate gyrus; ITG = inferior temporal gyrus; ITS = inferior temporal sulcus; LatOlfStr = lateral olfactory striae; LatOrbG = lateral orbital gyrus; MaBo = mamillary body; MedOlfStr = medial olfactory striae; MedOrbG = medial orbital gyrus; MeFS = medial frontal sulcus; MFG = middle frontal gyrus; MFS = middle frontal sulcus; MTG = middle temporal gyrus; OlfBu = olfactory bulb; OlfS = olfactory sulcus; OlfTr = olfactory tract; OptTr = optic tract; Orb = orbital part of inferior frontal gyrus; OrbGi = orbital gyri; OrbS = orbital sulcus; OTS = occipitotemporal sulcus; PHG = parahippocampal gyri; PostMedOrbLob = posteromedial orbital lobule; PostOrbG = posterior orbital gyrus; PostPerfSubst = posterior perforated substance; RhiS = rhinal sulcus; SFG = superior frontal gyrus; SFS = superior frontal sulcus; Spl = splenium of corpus callosum; STG = superior temporal gyrus; STS = superior temporal sulcus; TePo = temporal pole; Un = uncus; IIn = optical nerve; IIIn = oculomotor nerve. By permission of JNS Publishing group

Medial to the olfactory sulcus is the long and narrow gyrus rectus, considered the most anatomically constant of the cerebral gyri, which is continuous with the superior frontal gyrus along the medial surface of the hemisphere (Fig. 1.5).

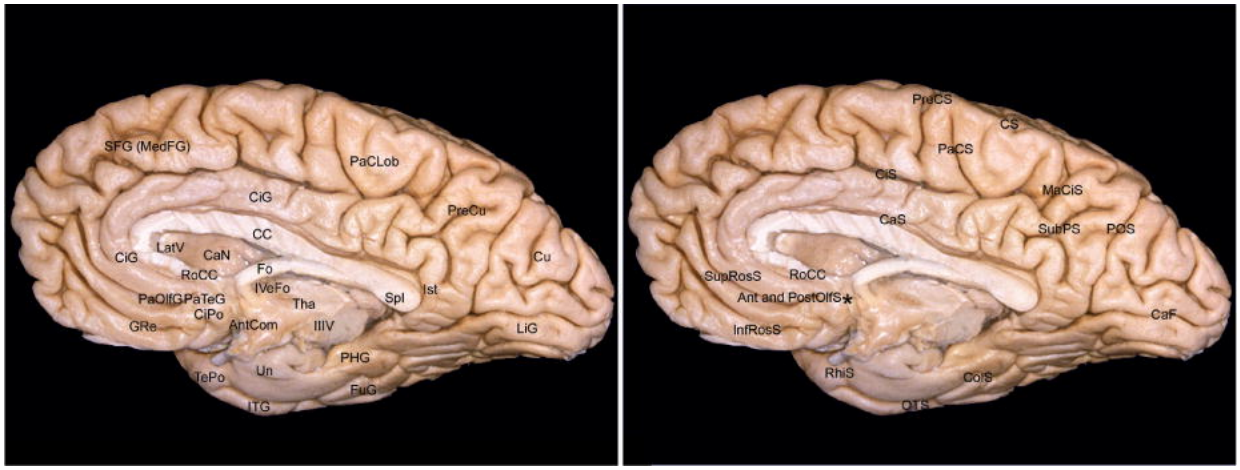


**Figure 1.5** The main sulci (left) and gyri (right) of the medial and basal temporooccipital surfaces. AntCom = anterior commissure; Ant and PostOlfS = anterior and posterior paraolfactory sulcus; CaF = calcarine fissure; CaN = caudate nucleus; CaS = callosal sulcus; CC = corpus callosum; CiG = cingulate gyrus; CiPo = cingulate pole; CiS = cingulate sulcus; ColS = collateral sulcus; CS = central sulcus; Cu = cuneus; Fo = fornix; FuG = fusiform gyrus; GRe = gyrus rectus; IIIV = third ventricle; InfRosS = inferior rostral sulcus; Ist = isthmus of cingulate gyrus; ITG = inferior temporal gyrus; IVeFo = interventricular foramen of Monro; LatV = lateral ventricle; LiG = lingual gyrus; MaCiS = marginal ramus of the cingulate sulcus; MedFG = medial frontal gyrus; OTS = occipitotemporal sulcus; PaCLob = paracentral lobule; PaCS = paracentral sulcus; PaOlfG = paraolfactory gyri; PaTeG = paraterminal gyrus; PHG = parahippocampal gyri; POS = parietooccipital sulcus; PreCS = precentral sulcus; PreCu = precuneus; RhiS = rhinal sulcus; RoCC = rostrum of the corpus callosum; SFG = superior frontal gyrus; Spl = splenium of corpus callosum; SubPS = subparietal sulcus; SupRosS = superior rostral sulcus; TePo = temporal pole; Tha = thalamus; Un = uncus. By permission of JNS Publishing group

Lateral to the olfactory sulcus are the orbital gyri, which account for the greatest proportion of the frontobasal surface (Fig. 1.4). The H-shaped orbital sulcus (cruciform sulcus of Rolando) delineates the anterior, posterior, medial, and lateral orbital gyri. The posterior orbital gyrus is situated anterior to the anterior perforated sub- stance and typically presents a configuration similar to a tricorner or “Napoleon” hat, which can facilitate its identification in anatomical specimens in which the H-shaped orbital sulcus presents variations.

The posterior orbital gyrus is connected medially to the medial orbital gyrus, characterizing the postero-medial orbital lobule situated posterior and along the olfactory tract and the lateral olfactory striae, which is in turn connected to the anterior portion of the insula via the

transverse insular gyrus. The remaining orbital gyri are connected to the superior, middle, and inferior frontal gyri, along the frontal pole.

The Central Lobe

The central lobe consists of the precentral (motor gyrus) and postcentral gyri (sensitive gyrus; Fig. 1.6), which are oriented obliquely on the superolateral surface and are separated by the central sulcus, by their inferior (subcentral gyrus) and superior connections (paracentral gyrus, or lobule, located on the medial surface) and by the other related sulci.[221] Morphologically, the central lobe is situated obliquely over the sylvian fissure corresponding approximately to the median portion of the cerebral hemisphere.

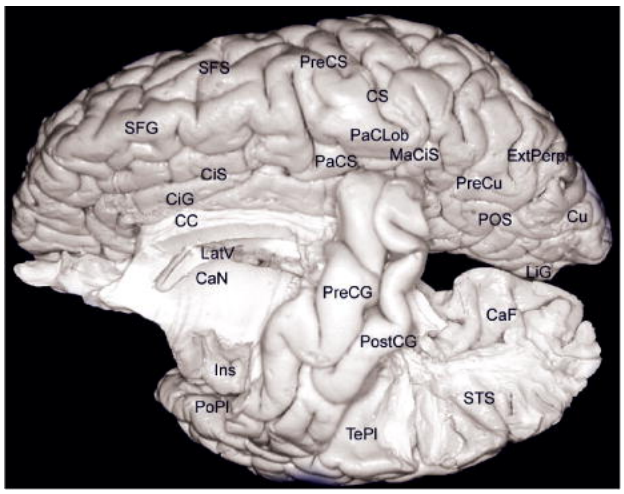


**Figure 1.6** The central lobe and medial contralateral surface. CaF = calcarine fissure; CaN = caudate nucleus; CC = corpus callosum; CiG = cingulate gyrus; CiS = cingulate sulcus; CS = central sulcus; Cu = cuneus; ExtPerpF = external perpendicular fissure; Ins = insula; LatV = lateral ventricle; LiG = lingual gyrus; MaCiS = marginal ramus of the cingulate sulcus; PaCLob = paracentral lobule; PaCS = paracentral sulcus; PoPl = polar plane of the opercular temporal surface; POS = parietooccipital sulcus; PostCG = postcentral gyrus; PreCG = precentral gyrus; PreCS = precentral sulcus; PreCu = precuneus; SFG = superior frontal gyrus; SFS = superior frontal sulcus; STS = superior temporal sulcus; TePl = temporal plane. By permission of JNS Publishing group

On the superolateral surface, the central lobe is de- lineated anteriorly by the precentral and anterior subcentral sulci, and posteriorly by the postcentral and posterior subcentral sulci (Figs. 1.1, 1.2 and 1.3). On the medial surface of the cerebral hemisphere (Fig. 1.5), the paracentral lobule is delineated anteriorly by the paracentral sulcus, and inferiorly and

posteriorly by the ascending and distal part of the cingulate sulcus, which is known as the marginal ramus of the cingulate sulcus.[137]

The precentral and postcentral gyri are situated obliquely in relation to the interhemispheric fissure, being less serpiginous than the other gyri of the cerebral convexity, and are connected to adjacent gyri via the usual interruptions in the precentral and postcentral sulci. The precentral and postcentral gyri are consistently united inferiorly by the subcentral gyrus (Broca's inferior frontoparietal pli de passage, or rolandic operculum) and superiorly by the paracentral lobule (Broca's superior frontoparietal pli de passage), which is located on the medial surface of each hemisphere. The precentral and postcentral gyri together resemble an elongated ellipse that is furrowed by the central sulcus, which is usually continuous, and are respectively delineated anteriorly and posteriorly by the precentral and postcentral sulci, which are typically discontinuous. This morphological unit, together with the functional interaction between motricity and sensitivity, justifies the characterization of these gyri as constituting a single lobe.

Inferiorly, the subcentral gyrus is delineated anteriorly and posteriorly by the anterior and posterior subcentral rami of the sylvian fissure, respectively. It can be situated either completely over the sylvian fissure or in part internal to the fissure, giving the false impression that the central sulcus is a branch of the sylvian fissure.[159,161] The portion of the subcentral gyrus that corresponds to the base of the postcentral gyrus consistently lies over the transverse gyrus of Heschl, which is situated on the opercular surface of the temporal lobe.[214]

Superiorly, and situated in the interhemispheric fissure, the paracentral lobule is delineated anteriorly by the paracentral sulcus and posteriorly by distal part of the cingulate sulcus, that is, the ascending marginal ramus of the cingulate sulcus.

The precentral gyrus typically presents 3 prominences known as knees: the superior and inferior knees are characterized by anterior convexities, and the middle knee is characterized by a posterior convexity. The precentral gyrus, in addition to its superior and

inferior connections with the postcentral gyrus via the superior (paracentral lobule) and inferior frontoparietal fold (subcentral gyrus, or rolandic operculum), is usually also connected to the postcentral gyrus via a transverse gyrus that lies along the bottom of the central sulcus and constitutes the so-called Broca's medial frontoparietal pli de passage.[13,188] This fold is situated at the level of the middle knee of the precentral gyrus, which is itself normally situated at the level of the superior frontal sulcus, corresponding to the portion of the gyrus that functionally harbors the motor representation of the contralateral hand. Therefore, the superior frontal sulcus tends to point the way to the me- dial frontoparietal pli de passage, as well as to the middle knee of the precentral gyrus, with its respective motor representation of the hand.[13] On axial MR images, this part of the precentral gyrus frequently presents a configuration that resembles the Greek letter Ω.[13]

Since they are disposed obliquely, the superior portions of the precentral and postcentral gyri that constitute the paracentral lobule on the medial surface of the cerebral hemisphere are topographically related to the ventricular atrium, which is situated posteriorly to the thalamus (Fig. 1.6). In contrast, the inferior portions cover the posterior half of the insula and are topographically related to the body of the lateral ventricle, which is situated superior to the thalamus.

The Parietal Lobe

The parietal lobe anatomy is more complex in the sense that it is composed of gyri structurally less well defined and particularly serpiginous and curved. These gyri are also referred to as lobules. On the superolateral surface, the parietal lobe is de lineated anteriorly by the postcentral sulcus and posteriorly by the imaginary line running from the point from which the parietooccipital sulcus emerges (on the supero-medial border) to the preoccipital notch, which is situated on the inferolateral border, ~ 5 cm anterior to the occipital pole.[214] The intraparietal sulcus, which originates from around the midpoint of the postcentral sulcus, is prominent along the parietal superolateral surface, in general runs almost parallel to the interhemispheric fissure, and posteriorly penetrates into the occipital lobe. The

intraparietal sulcus divides the superolateral parietal surface into the superior and inferior parietal lobules (Fig. 1.7).

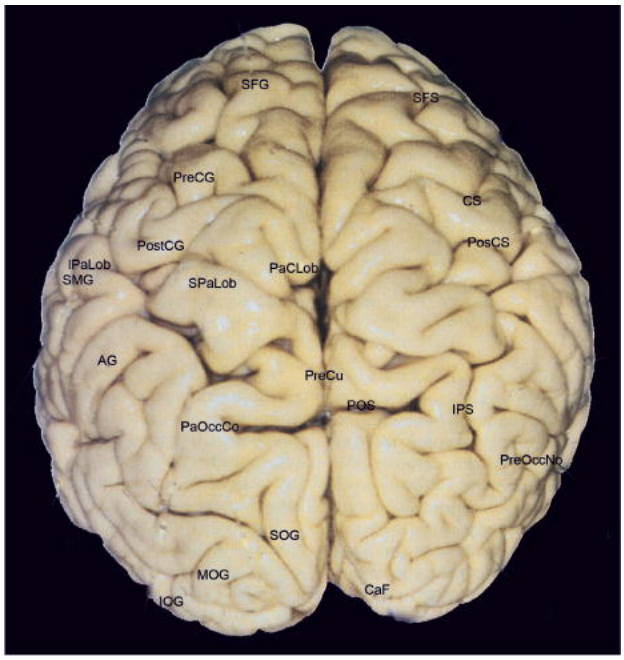


**Figure 1.7**. Superior view of the cerebral hemispheres. AG = angular gyrus; CaF = calcarine fissure; CS = central sulcus; IOG = inferior occipital gyrus; IPaLob = inferior parietal lobule; IPS = intraparietal sulcus; MOG = middle occipital gyrus; PaCLob = paracentral lobule; PaOccCo = parietooccipital arch; POS = parietooccipital sulcus; PosCS = postcentral sulcus; PostCG = postcentral gyrus; PreCG = precentral gyrus; PreCu = precuneus; PreOccNo = preoccipital notch; SFG = superior frontal gyrus; SFS = superior frontal sulcus; SMG = supramarginal gyrus; SOG = superior occipital gyrus; SPaLob = superior parietal lobe. By permission of JNS Publishing Group

The superior parietal lobule is quadrangular and typically connected to the postcentral gyrus via a connection that transects the most superior portion of the postcentral sulcus and, occasionally, via another fold that more inferiorly interrupts the postcentral sulcus. The superior parietal lobule is delineated laterally by the intraparietal sulcus; medially, it is continuous with the precuneus gyrus along the superomedial border (Fig. 1.5); and, posteriorly, it continues to the superior occipital gyrus via the prominent and arched superior parietooccipital fold that surrounds the external perpendicular fissure, which represents the depth of the parietooccipital sulcus over the superolateral cerebral surface (Fig. 1.7). In some brains, there is also a small sulcus, designated the superior parietal sulcus, emerging from the interhemispheric fissure, between the postcentral sulcus and the external perpendicular fissure, over the superior parietal lobule.[137]

The inferior parietal lobule consists of, anteriorly, the supramarginal gyrus, which is a curved gyrus surrounding the distal portion of the sylvian fissure, and, posteriorly, the angular gyrus, which encircles the horizontal distal portion of the superior temporal sulcus. The supramarginal and angular gyri characterize the cranial parietal tuberosity, or bossa. Those 2 gyri are separated by the intermediate sulcus (of Jensen), which is an inferior vertical branch of the intraparietal sulcus or a distal and superior vertical branch of the superior temporal sulcus or both (Fig. 1.1).

Anteriorly, the supramarginal gyrus is connected to the postcentral gyrus via a fold that lies around the inferior portion of the postcentral sulcus; inferiorly, it consistently encircles the terminal portion of the sylvian fissure and continues to the superior temporal gyrus; and posteriorly, it occasionally rounds the inferior border of the intermediate sulcus, connecting to the angular gyrus (Figs. 1.1 and 1.2). In turn, the angular gyrus typically curves anteriorly around a distal horizontal branch of the superior temporal sulcus, also known as the angular sulcus,[137] continuing to the middle temporal gyrus and giving rise to a posterior fold that connects it to the middle occipital gyrus. (Broca, basing his ideas on the work of Gratiolet, considered the supramarginal and angular gyri to be folds connecting the parietal lobe with the temporal lobe. From Broca's perspective, the supramarginal gyrus, which wraps around the distal portion of the sylvian fissure, corresponded to Gratiolet's superior marginal fold, and the angular gyrus, which wraps around the distal portion of the superior temporal sulcus, corresponded to the inferior marginal fold, or curved fold.[187,188]

Therefore, the intraparietal sulcus delineates superiorly the supramarginal and angular gyri with a slightly arciform and inferiorly concave course, and, anteriorly, it typically continues to the inferior portion of the post- central sulcus. Posteriorly, the continuation of the intra-parietal sulcus becomes the intraoccipital sulcus,[45,132] also known as the superior occipital sulcus[187] or transverse occipital sulcus,[137] which separates the (more vertical) superior occipital gyrus from its (more horizontal) middle counterpart.[45,137,187,188] Along its length, the intraparietal sulcus typically gives rise to 2 vertical folds: a smaller, superior fold located anterior to the external perpendicular fissure, known as the transverse parietal sulcus of

Brissaud, and another inferior, more developed fold that constitutes the previously mentioned intermediate sulcus of Jensen, which separates the supramarginal gyrus from the angular gyrus.[187,188,206] The superior parietal lobule, supramarginal gyrus, and angular gyrus are also known as P1, P2, and P3, respectively.

On the medial surface of each hemisphere, the precuneus gyrus is a medial extension of the superior parietal lobule along the superomedial border of the brain and corresponds to the medial portion of the parietal lobe (Fig. 1.5). The precuneus is also quadrangular, delineated anteriorly by the marginal branch of the cingulate sulcus, posteriorly by the parietooccipital sulcus, and inferiorly by the subparietal sulcus. Inferiorly to the subparietal sulcus, the precuneus is connected to the isthmus of the cingulate gyrus and the parahippocampal gyrus.

The Occipital Lobe

On the superolateral cerebral surface, the occipital lobe is situated posterior to the imaginary line that connects the point of emergence of the parietooccipital sulcus (on the superomedial border of the cerebral hemisphere) with the preoccipital notch. The sulci and gyri of the occipital lobe have greater anatomical variation as compared with other lobes. Despite being less well defined and less anatomically constant than gyri in other dorsal cortical areas, the occipital gyri of the superolateral cerebral surface tend to consist of 3 gyri that are, for the most part, arrayed longitudinally in relation to the interhemispheric fissure and converge posteriorly to form the occipital pole of each hemisphere. As is the case for the frontal and temporal lobes, the occipital gyri of the superolateral surface are usually designated superior, middle, and inferior,[45,187] or O1, O2, and O3, respectively. While the superior occipital gyrus is arranged more vertically along the interhemispheric fissure, the middle and inferior occipital gyri are arranged more horizontally and parallel to the inferior cerebral margin (Fig. 1.7).

On the medial surface, the occipital lobe is particularly well defined anatomically. It is separated from the parietal lobe by the parietooccipital sulcus and is composed of the cuneal and lingual gyri, which are separated by the calcarine fissure (Fig. 1.5). The basal, or inferior,

surface of the occipital lobe, in turn, is contiguous with the basal surface of the temporal lobe (Fig. 1.8).

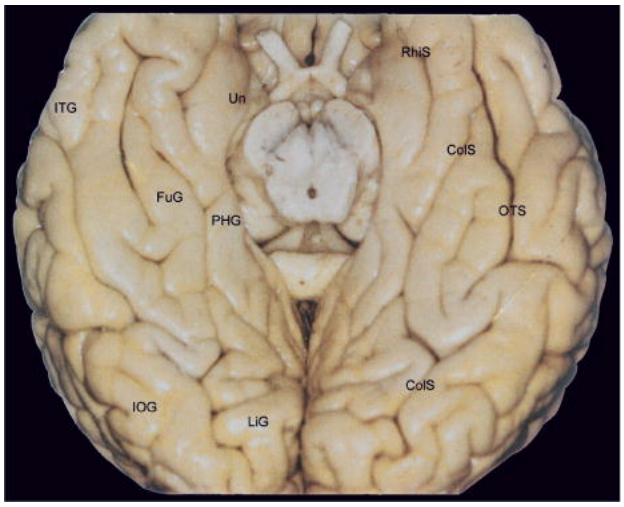


**Fig. 1.8.** The basal temporooccipital surface. ColS = collateral sulcus; FuG = fusiform gyrus; IOG = inferior occipital gyrus; ITG = inferior temporal gyrus; LiG = lingual gyrus; OTS = occipitotemporal sulcus; PHG = parahippocampal gyri; RhiS = rhinal sulcus; Un = uncus. By permission of JNS Publishing Group

On the superolateral surface, whereas the superior and middle occipital gyri are separated by the intraoccipital sulcus,[45,132,187] which is the continuation of the intraparietal sulcus and is also known as the superior occipital sulcus[45,132,187] and transverse occipital sulcus,[137] the middle and inferior occipital gyri are separated by the less well defined inferior occipital sulcus,[45,132,187] also known as the lateral occipital sulcus.[137] When present, the so-called lunate sulcus is typically oriented vertically, immediately facing the occipital pole.[45,137] Given the shallow depth and discontinuity as well as the (often) multiple branches of the 2 principal occipital sulci, the occipital gyri are not always well defined and are typically joined by various anastomotic folds, and thus constitute a cortical surface that is difficult to characterize morphologically. (According to the description given by Gratiolet, the parietal and temporal lobe connections with the occipital lobe are made via 4 folds [2 parietooccipital and 2 temporooccipital]: 1) the first and more superior parietooccipital fold, which surrounds the external perpendicular occipital fissure and connects the superior parietal lobule with the superior occipital gyrus; 2) the second and more inferior parietooccipital fold, composed of a posterior extension of the angular gyrus, which converges with the

middle occipital gyrus and also occasionally with the superior occipital gyrus; 3) the first temporooccipital fold, characterized by the union of the middle temporal gyrus and the inferior occipital gyrus; and 4) the second temporooccipital fold, characterized by the union of the inferior temporal gyrus and the inferior occipital gyrus.[187,188]

Superiorly, the superior occipital gyrus extends along the superior border of the cerebral hemisphere, thus continuing along the medial surface to the cuneal gyrus. Inferiorly, the inferior occipital gyrus extends along the inferolateral margin, and its basal surface is lateral to the medial temporooccipital gyrus, also known as the lingual gyrus, as well as to the collateral sulcus that separates the two.

On the medial surface of the cerebral hemisphere, as previously mentioned, the occipital lobe is delineated and characterized by its well-defined and anatomically constant sulci and gyri. Its principal sulcus is the calcarine fissure, which is located just above the inferomedial margin of the cerebral hemisphere. The calcarine fissure starts over the splenium of the corpus callosum, delineating inferiorly the isthmus of the cingulate gyrus from the parahippocampal gyrus, and continues posteriorly as a gentle and superior convex curvature from whose apex emerges, superiorly, the parietooccipital sulcus, which in turn delineates anteriorly the occipital lobe on the medial surface of the cerebral hemisphere. Posteriorly, the calcarine fissure occasionally crosses the superomedial margin and extends along the occipital pole to the superolateral surface of the cerebral hemisphere.

The point of emergence of the parietooccipital sulcus divides the calcarine fissure into its proximal and distal parts. Superior to the proximal portion of the calcarine fissure and anterior to the parietooccipital sulcus is the precuneal gyrus, which is part of the parietal lobe. Superior to its distal part and posterior to the parietooccipital sulcus is the cuneus, or cuneal gyrus, so designated because of its wedge shape.

Inferiorly and along the entire length of the calcarine fissure is the medial temporooccipital gyrus, or lingual gyrus, which anteriorly continues to the parahippocampal gyrus and constitutes the mediobasal portion of the occipital lobe, which is supported on the cerebellar

tentorium. The lingual gyrus is therefore delineated superiorly by the calcarine fissure and inferiorly by the collateral sulcus, which is a deep and generally continuous sulcus situated at the cerebral base, extending from the occipital pole to the temporal lobe and running parallel to the calcarine fissure.

The parietooccipital sulcus and calcarine fissure appear continuous on the surface. However, when their borders are retracted, it is obvious that they are separated by one or more small gyri. These gyri are composed of extensions of the cuneus and are known as the cuneolingual gyri.

The proximal part of the calcarine fissure is classified as a complete sulcus because its depth creates a rise in the medial wall of the occipital horn of the lateral ventricle, designated the calcar avis, and the distal part is considered an axial sulcus given that its axis runs along the visual cortex. Only the distal part includes the primary visual cortical areas, which are located on its superior (cuneal) and inferior (lingual) surfaces.

On the basal surface of the cerebral hemisphere, lateral to the lingual gyrus, is the medial temporooccipital gyrus or fusiform gyrus, situated between the collateral sulcus and the temporooccipital sulcus. The temporooccipital sulcus lies lateral and parallel to the collateral sulcus, rarely extends to the occipital pole, and in general is interrupted and divided into 2 or more parts. Anteriorly, the temporooccipital sulcus often bends medially and joins the collateral sulcus. The fusiform gyrus, in turn, extends to the basal surface of the temporal lobe, and lateral to its posterior portion lies the inferior occipital gyrus, whose lateral aspect constitutes the inferior most portion of the lateral surface of the occipital lobe.

The Temporal Lobe

The temporal lobe is situated inferior to the sylvian fissure and delineated posteriorly by the imaginary line running from the superomedial portion of the parietooccipital sulcus to the preoccipital notch. Its lateral surface is composed of the superior, middle, and inferior temporal gyri—also respectively known as T1, T2, and T3— which are separated by the

superior and inferior temporal sulci, parallel to the lateral or sylvian fissure (Fig. 1.1). Anteriorly, the middle temporal gyrus is generally shorter, causing the superior and inferior temporal gyri to come together, and thereby forming the temporal pole.

The superior temporal sulcus is always a very well defined and deep sulcus and often presents as a continuous sulcus because of its parallelism with the sylvian fissure. In fact, in the past it was called the parallel sulcus. The inferior temporal sulcus is usually discontinuous and composed of various parts. Both of the temporal sulci start at the proximal portion of the temporal pole and end posterior to its borders. Whereas the posterior portion of the sylvian fissure typically terminates as an ascending curve that penetrates the supramarginal gyrus, the superior temporal sulcus always terminates at a point posterior to the end of the sylvian fissure (posterior sylvian point). In general, the superior temporal sulcus then bifurcates into an ascending sulcal segment, which separates the supramarginal gyrus from the angular gyrus, and corresponds to the intermediate sulcus of Jensen, and a distal and horizontal segment that penetrates the angular gyrus.[137,159,162] Given this configuration of the sulci, the superior temporal gyrus always continues posteriorly to the supramarginal gyrus, encircling the terminal portion of the sylvian fissure. The middle temporal gyrus is often partially connected to the angular gyrus beneath the dis- tall and horizontal portion of the superior temporal sulcus that penetrates the angular gyrus proper and inferiorly is often connected to the inferior occipital gyrus. In turn, the inferior temporal gyrus continues to the inferior occipital gyrus, over the preoccipital notch that posteriorly delineates the temporal lobe. Inferiorly, the inferior temporal gyrus extends along the inferolateral margin of the cerebral hemisphere. Medially, its basal surface lies along the lateral temporooccipital gyrus, or fusiform gyrus, and along the temporooccipital sulcus that separates the 2 gyri (Fig. 1.8).[214]

The superior temporal gyrus constitutes the temporal operculum and covers the inferior aspect of the insular surface, and its superior, or opercular, surface (Fig. 1.9), which is within the sylvian fissure, is composed of various transverse gyri that emerge from the superior temporal gyrus and are directed obliquely toward the inferior part of the circular insular sulcus.[198,214]

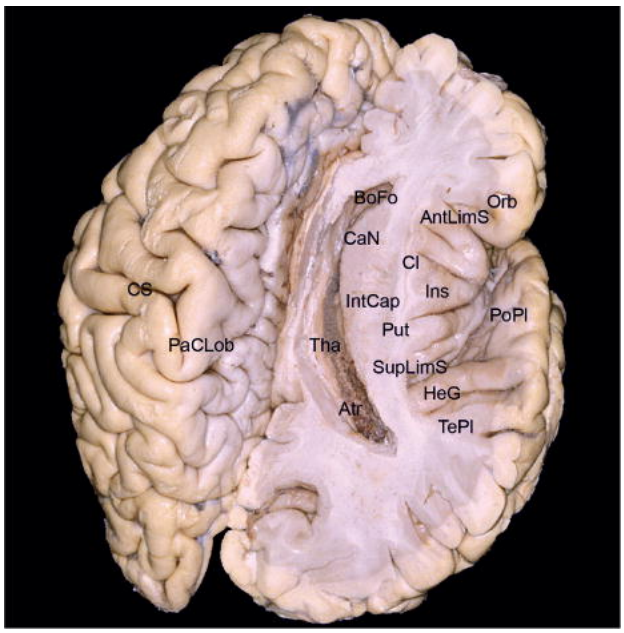


**Fig. 1.9.** The temporal opercular surface, the insula, and the central core of the brain. AntLimS = anterior limiting sulcus; Atr = atrium of lateral ventricle; BoFo = body of fornix; CaN = caudate nucleus; Cl = claustrum; CS = central sulcus; HeG = Heschl gyrus; Ins = insula; IntCap = internal capsule; Orb = orbital part of inferior frontal gyrus; PaCLob = paracentral lobule; PoPl = polar plane of the opercular temporal surface; Put = putamen; SupLimS = superior limiting sulcus of insula; TePl = temporal plane; Tha = thalamus. By permission of JNS Publishing Group

Chief among these temporal gyri of the operculum is a much more voluminous transverse gyrus that originates in the posterior most portions of the superior temporal gyrus and is oriented diagonally toward the posterior vertex of the floor of the sylvian fissure and toward the ventricular atrium. This gyrus is designated the transverse gyrus of Heschl. In some brains, 1 or 2 sulci divide this gyrus; and in such cases, 2 or 3 gyri are also featured. Together with the posterior most aspect of the superior temporal gyrus, the most anterior transverse gyrus of Heschl constitutes the primary auditory cortical area.[198,216] This gyrus has particular topographical importance because it underlies the opercular surface of the postcentral gyrus, its longest axis is oriented toward the ventricular atrium, and it divides the temporal opercular surface into 2 planes: an anterior plane called the polar plane and a posterior plane known as the temporal plane (Fig. 1.9).[214]

The floor of the polar plane is composed of short transverse gyri at oblique angles, and the lower border of the plane is defined by the inferior portion of the circular insular sulcus that runs along the bottom of the sylvian fissure. The temporal plane is triangular with an internal vertex that exactly corresponds to the posterior vertex at the bottom of the sylvian fissure, where the superior part of the circular insular sulcus comes into contact with its inferior part. The temporal plane is oriented horizontally and faces the inferior surface of the supramarginal gyrus as if supporting its anteriormost portion. Whereas the sylvian fissure appears oblique in coronal slices taken in the polar plane, it appears horizontal in those taken in the temporal plane.

The basal surface of the temporal lobe is continuous with the basal surface of the occipital lobe and is situated over the floor of the middle cranial fossa, anterior to the petrous portion of the temporal bone, whereas the basal occipital surface lies over the superior surface of the cerebellar tentorium. The temporal lobe is composed laterally of the inferior surface of the inferior temporal gyrus and the anterior portion of the lateral temporooccipital gyrus, or fusiform gyrus, and medially of the inferior surface of the parahippocampal gyrus. The fusiform gyrus is situated lateral to the parahippocampal and lingual gyri, between the collateral and temporooccipital sulci. Its temporal portion presents a slight basal prominence due to its adaptation to the concavity of the middle cranial fossa. Its anterior aspect is typically curved or pointed, because the anteriormost portion of the temporooccipital sulcus frequently presents a medial curvature toward the collateral sulcus (Fig. 1.8). The anterior border of the fusiform gyrus, in general, corresponds medially to the level of the mesencephalic peduncle; as a whole, it constitutes the floor of both the atrium and the inferior horn of the lateral ventricle.

The parahippocampal gyrus and the anterior portion of the collateral sulcus have been described as limbic lobe structures.

The Insular Lobe

On the publication of the fourth edition of the Paris Nomina Anatomica in 1975,[4] the insula came to be considered a cerebral lobe. The insular surface is composed of the so-called mesocortex, which is anatomically situated between the allocortex, which is older and topographically more medial (comprising the amygdala and hippocampus), and the isocortex, which is phylogenetically younger and topographically more lateral (comprising the neocortex of the cerebral hemispheres).

Embedded between the frontal and temporal lobes of each cerebral hemisphere and constituting the base of each sylvian cistern, the insula has an anterior surface and a lateral surface (Fig. 1.10) that are encased in their respective opercular convolutions,[198] which correspond to the regions of the cerebral hemispheres that have lately become more fully developed. The anterior surface of the insula is covered by the frontoorbital operculum (comprising the posterior portion of the posterior orbital gyrus and the orbital part of the inferior frontal gyrus), whereas its lateral surface is covered superiorly by the frontoparietal operculum (triangular and opercular parts of the inferior frontal gyrus, subcentral gyrus, and anterior and basal part of the supramarginal gyrus) and inferiorly by the temporal operculum (superior temporal gyrus; Figs. 1.2 and 1.3). [198,216,223]

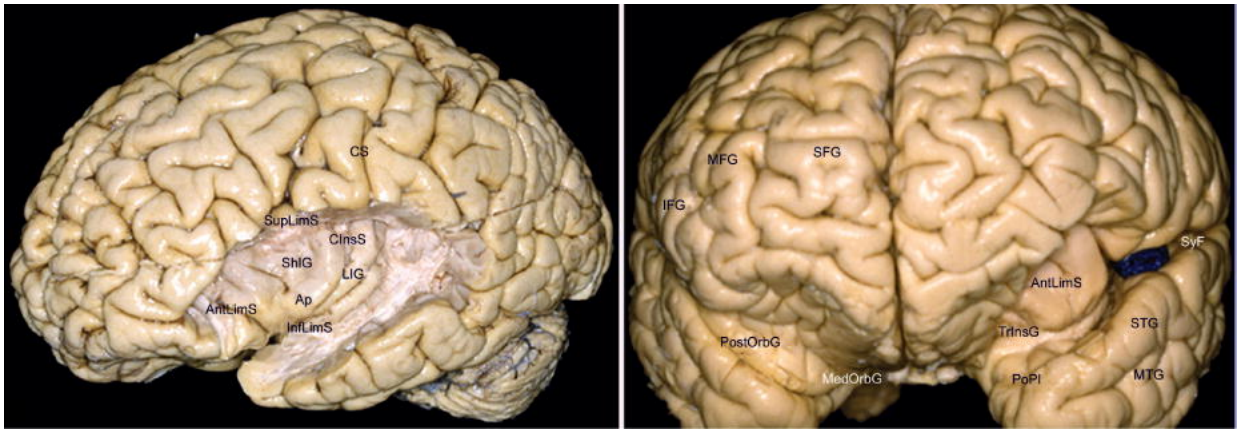


**Fig. 1.10.** The lateral (left) and anterior (right) surfaces of the insula. AntLimS = anterior limiting sulcus; Ap = insular apex; CInsS = central insular sulcus; CS = central sulcus; IFG = inferior frontal gyrus; InfLimS = inferior limiting sulcus; ITG = inferior temporal gyrus; LIG= long insular gyri; MedOrbG= medial orbital gyrus; MFG= middle frontal gyrus; MTG= middle temporal gyrus; PoPl = polar plane of the opercular temporal surface; PostOrbG = posterior orbital gyrus; SyF= sylvian fissure; SFG = superior frontal gyrus; ShIG = short insular gyri; STG = superior temporal gyrus; SupLimS = superior limiting sulcus of insula; TrInsG = transverse insular gyrus. By permission of JNS Publishing Group

The lateral surface of the insula is characterized as a pyramid with a triangular base, whose anteroinferior vertex constitutes the limen insulae, and is divided by the oblique central sulcus of the insula into an anterior portion and a posterior portion, with the former having a larger area. The anterior portion is typically composed of 3 short gyri that originate at the apex of the insula, which corresponds to the most prominent aspect of the insular pyramid, with the anteriormost aspect extending over the anterior surface of the insula; and the posterior portion, in general, is composed of 2 long gyri not originating at the apex but oriented obliquely and in parallel. The transverse and accessory insular gyri, which together constitute the insular pole, also originate from the apex of the insula.[198,199] The transverse insular gyrus, which is situated more inferiorly, runs along the limen insulae and is connected to the posteromedial orbital lobule, which is composed of the posterior portion of the medial orbital gyrus and the medial portion of the posterior orbital gyrus[198,222] and is located anterior and along the lateral olfactory stria.

The insular surface is delineated peripherally by the circular sulcus of Reil,[45,186] or periinsular sulcus,[188,198] which is interrupted by the previously mentioned transverse insular gyrus. Given the triangular shape of the insula, its circular, or periinsular, sulcus is usually divided into 3 parts, that is, the anterior, superior, and inferior periinsular sulci,[198] also designated the anterior, superior, and inferior limiting sulci of the insula.[158]

To understand the periinsular spaces more fully, one should remember that the insula has a lateral surface and an anterior surface. The superior and inferior limiting sulci are morphologically categorized as true sulci that delineate the respective transitions and deflections occurring among the lateral insular surface and the frontoparietal operculum, and the lateral insular surface and the temporal operculum. The so-called anterior limiting sulcus of the insula, on the other hand, is considerably deeper and morphologically characteristic of a true fissure or space that separates the anterior surface of the insula from the posterior surface of the posterior orbital gyrus. The upper half of the fundus of the anterior limiting sulcus is separated from a true anterior ventricular recess at the head of the caudate nucleus only by the fibers of the thin anterior limb of the internal capsule,

whereas the fundus of the lower half continues to the ventral striato-pallidal region (Fig. 1.11).

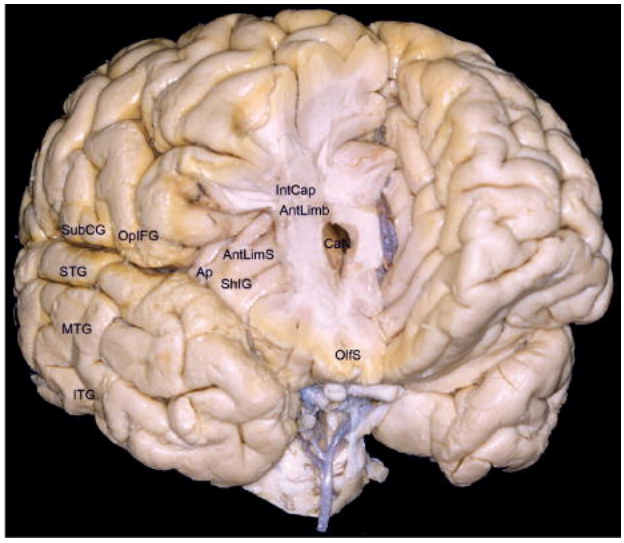


**Fig 1.11.** The anterior surface of the insula and the anterior horn of the lateral ventricle. AntLimb = anterior limb of the internal capsule; AntLimS = anterior limiting sulcus; Ap = insular apex; CaN = caudate nucleus; IntCap = internal capsule; ITG = inferior temporal gyrus; MTG = middle temporal gyrus; OlfS = olfactory sulcus; OpIFG = opercular part of the inferior frontal gyrus; ShIG = short insular gyri; STG = superior temporal gyrus; SubCG = subcentral gyrus. By permission of JNS Publishing Group

From a morphological and topographical perspective, the surface of the insula clearly represents the external shield of a true central core of the brain,57 quite well defined anatomically. This central core of the brain comprises, in each cerebral hemisphere, the insula proper, the basal nuclei, the thalamus, and the internal capsule (Fig. 1.12). The anterior half of the lateral surface of the insula corresponds internally to the head of the caudate nucleus, whereas the posterior half corresponds to the thalamus and the body of the caudate nucleus. Each central core of each cerebral hemisphere, composed of all the structures mentioned above, is incorporated into the corresponding half of the mesencephalon, morphologically characterizing a brainstem with 2 heads that correspond to the 2 central cores (Fig. 1.13).


**Fig. 1.12.** The insular lateral surface corresponds to an external shield of the central core of the brain. AntLimS = anterior limiting sulcus of insula; BodCaN = body of the caudate nucleus; ChPl = choroid plexus; Fo = fornix; HeG = Heschl gyrus; Ins = insula; IntCap = internal capsule; PoPl = polar plane of the opercular temporal surface; SupLimS = superior limiting sulcus of insula; Tha = thalamus. By permission of JNS Publishing Group

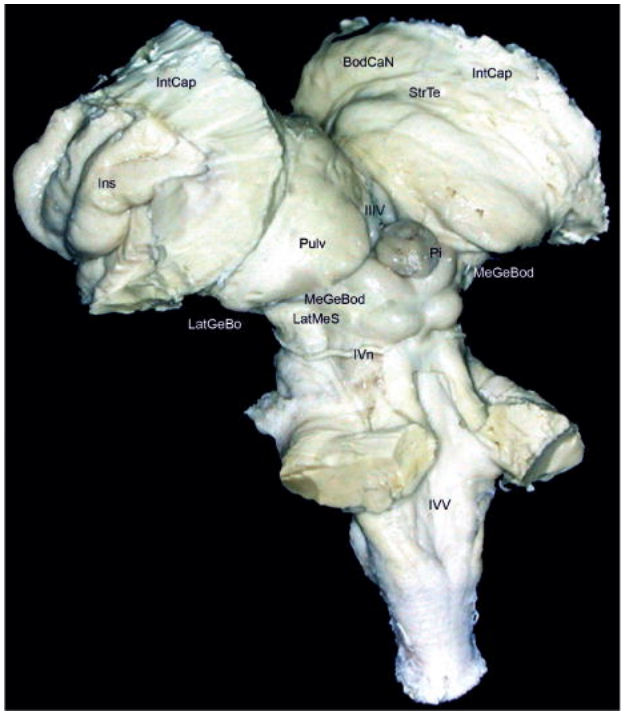


**Fig. 1.13.** Each central core of the brain corresponds to a head of each half of the brainstem. BodCaN = body of the caudate nucleus; Ins = insula; IntCap = internal capsule; LatGeBo = lateral geniculate body; LatMeS = lateral mesencephalic sulcus; MeGeBod = medial geniculate body; Pi = pineal gland; Pulv = pulvinar of thalamus; StrTe = stria terminalis; IIIV = third ventricle; IVn = trochlear nerve; IVV = fourth ventricle. By permission of JNS Publishing Group

Under the insular cortex and its respective subcortical white matter, also known as the extreme capsule, is the fine lamina of gray matter that constitutes the claustrum. Underneath that is the putamen, enclosed within its external and internal capsules. The thin external capsule is composed of fibers that cover only the lateral portion of the putamen and are bereft of major functional importance, whereas the internal capsule consists of important projection fibers that originate from, and are directed toward, the cerebral cortex as a whole. Since the area of the putamen is slightly smaller than that of the lateral surface of the insula,[198] and given the shape of the internal capsule, the recesses of the anterior, superior, and inferior limiting sulci are practically adjacent to the fibers of the internal capsule

## 1.3 Macroscopic, microscopic and functional anatomy of the precuneus

Despite recent intense interest in the functional significance of the precuneus, the details of its cytoarchitecture and connections have remained a relatively unexplored topic of brain mapping, largely due to its inaccessible location along and in the depths of the longitudinal fissure.[140] Moreover, since in vivo axonal tracing techniques cannot be applied to the human brain, our knowledge about the connectivity of the posteromedial parietal lobe is based mainly on axonal tracing studies in the macaque brain.[232]

The associative cortices, to which the precuneus belongs, have undergone a gradual increase in the complexity of their organization during the course of primate and hominid evolution. As a consequence of this, in the cebida (New World monkey) the superior parietal and precuneate regions are poorly developed[33]; on the other hand, the posteromedial cortex of the macaque (Old World monkey) has been shown to share its main architectonic patterns with Homo sapiens.[100,205] Overall, the medial aspect of the parietal lobe of the chimpanzee and other apes closely resembles the general appearance of the same structures in the human brain.[6] However, it should be pointed out that the precuneus has received relatively little attention even in the most comprehensive comparative neuroanatomy treatises (e.g. Nieuwenhuys et al., 1998)[134], thus indicating a need for further comparative studies specifically addressing this cortical area.

Topographical anatomy

The medial aspect of the posterior parietal lobe has historically been referred to as the precuneus, or quadrate lobule of Foville (1844).[54] This nomenclature follows the topographical location and geometrical appearance of this cortical area, situated immediately in front of the triangular-shaped convolution of the cuneus, on the medial surface of the occipital lobe. The precuneus is limited anteriorly by the marginal branch of the cingulate sulcus, posteriorly by the medial portion of the parieto-occipital fissure and inferiorly by the subparietal (i.e. postlimbic) sulcus. Figure 1.14 shows the medial surface of

the human brain with the main landmarks of the precuneus according to the traditional anatomical descriptions (Critchley, 1953).

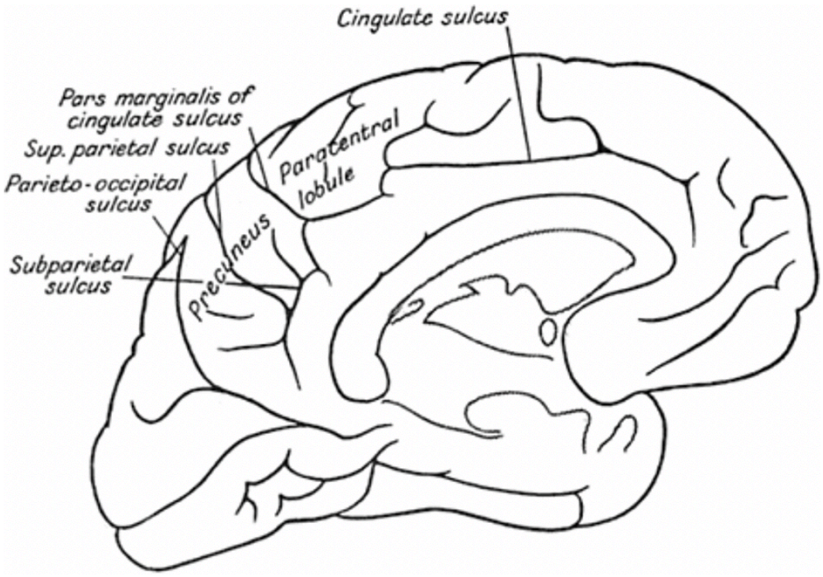


**Figure 1.14** A drawing of the medial surface of the human brain; the precuneus and its traditional anatomical landmarks are labelled [after Critchley (1953)]

The variable boundaries of the precuneus have been recently described in detail by Salamon et al. (2003)[167], who also highlighted some correlations with neuroimaging findings. In summary, the cingulate sulcus ends upward with the ramus marginals, which marks the division of the brain between the precuneus and the primary sensory and motor areas. The parieto-occipital fissure has a limited extension on the upper part of the brain and ends at the level of the upper bend of the calcarine fissure, or slightly more anteriorly. Its shape is variable: straight, T-shaped or more complex with three branches. The subparietal sulcus constitutes the inferior margin of the precuneus and continues its course around the posterior part of the cingulum. Most often, this sulcus is not represented as a single line, but as a complete or incomplete H shape, with one to three ascending branches along its course. The vasculature of this region shows remarkable interindividual variability. The main arterial supply of the precuneus stems from the posterior cerebral artery, with

predominance from the P2 segment. The occipito-parietal artery, a terminal branch of the internal occipital artery, principally supplies the precuneate and anteromedial occipital cortices.

Cytoarchitectonics

Numerous cytoarchitectonic and myeloarchitectonic maps of the posteromedial portion of the parietal cortex have been proposed since the beginning of the past century. However, its exact parcellation remains the subject of discussion, since the existing maps differ considerably concerning the number and size of individual brain areas. The cytoarchitectonic map of Brodmann (1909)[18] still dominates our present concepts of the structural organization of the human cerebral cortex, since it serves, via a popular brain atlas,[183] as an anatomical reference for functional imaging studies. The territory of the precuneus mainly corresponds to the mesial extent of BA 7, which also occupies most of the lateral parietal cortex above the intraparietal sulcus (IPS). [100,232] In addition, an adjacent cytoarchitectonic region has been proposed to be a part of the precuneus: according to some authors[55,201] BA 31, which is positioned between the cingulate and splenial sulci, includes both posterior cingulate and precuneate cortices. However, throughout this study we explicitly confined our analysis to the precuneus in its more restricted sense, i.e. the medial aspect of BA 7. The rationale for choosing BA 7 instead of broader anatomical descriptions, including the superior portion of BA 31, was because different BAs with different cytoarchitectonic structures and connectivity patterns are likely to differ in terms of their subserved functions as well. The medial surface of BA 7 is easily distinguished from adjacent posterior cingulate and retrosplenial cortices by its representative parietal cytoarchitecture, characterized by fully differentiated isocortex: a columnar pattern with conspicuous layers II, IV, V and VI, and a noticeable thinning of cortex as a whole. [140] BA 31, on the other hand, appears to be a cortical transition zone from the medial parietal areas to the posterior cingulate, presenting an apparent shift in cytoarchitecture from parietal isocortex to limbic cortex.

Brodmann described gradual rostrocaudal architectonic changes within area 7; thus, he defined the existence of two main subdivisions, which he named 7a and 7b, although he did

not define a clear border between them.[232] Von Economo and Koskinas[207] summarized the previous efforts made by Brodmann and others[24,180] and described a practically identical location for their area PE, which was subdivided into the anterior area PEm, with a more pronounced magnocellular appearance, and the relatively smaller-celled posterior area PEp. PEm and PEp are probably equivalent to Brodmann's subdivisions 7a and 7b, respectively; yet, since Brodmann did not provide a cytoarchitectonic description or a micrograph of BA 7, comparisons with the maps of other authors can be performed only on the basis of topography.[232] Figure 1.15 compares the cytoarchitectonic maps of the precuneus as defined for the scope of the present review (i.e. mesial BA 7) and the adjacent areas of the human medial parietal lobe after Brodmann[18] and von Economo and Koskinas[207]. A number of subsequent cytoarchitectonic studies[140,168,205] adopted or further developed Brodmann's and von Economo and Koskinas' parcellation schemes. Table 1.1 summarizes the different labels proposed for the precuneate cortex, according to the major cytoarchitectonic maps. Interested readers are referred to the recent paper by Zilles and Palomero-Gallagher[233] for a historical overview of the cytoarchitectonic parcellation of human parietal cortex and further anatomical details. It has been pointed out that the classical cortical maps fail to explain the more detailed aerial organization of the posterior parietal cortex, as revealed by recent functional imaging studies.[15] As a consequence, these cytoarchitectonic and myeloarchitectonic studies can only be considered as guidelines for future multimodal and observer-independent quantitative architectonic analyses.[232]

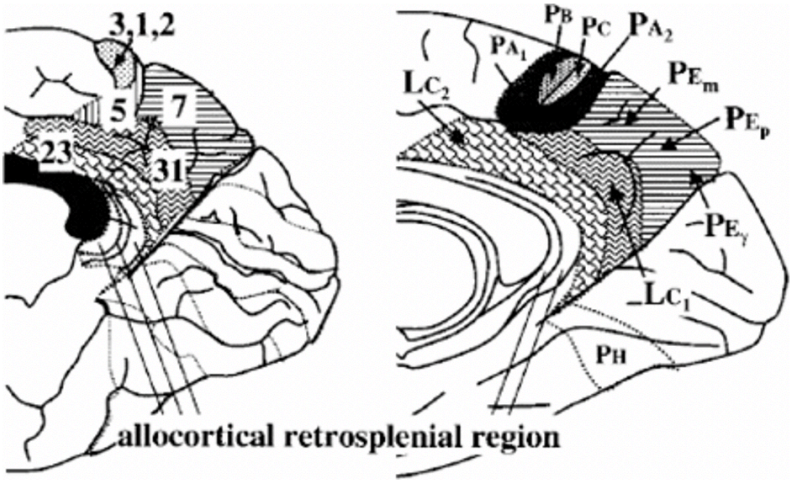


**Figure 1.15** Comparison of the cytoarchitectonic maps of the human medial parietal isocortex after Brodmann (1909) (left) and von Economo and Koskinas (1925) (right); for the scope of the present review, the precuneus corresponds to mesial BA 7 and PE, respectively (horizontally shaded areas) [reprinted with permission from Zilles and Palomero-Gallagher (2001)].

**Table 1.1** Nomenclature of the precuneus according to the major cytoarchitectonic cortical maps

| Author | Area |
|---|---|
| Brodmann[18] | 7 (7a, 7b) |
| von Economo and Koskinas[207] | PE (PEm,PEp) |
| von Bonin and Baile[205] | PE |
| Pandya and Seltzer[140] | PGm |
| Cavada and Goldman-Rakic[29] | 7m |

Cortical and subcortical connectivity

Quite recently, Leichnetz [100] studied the afferent and efferent connections of the precuneus in Cebus apella (New World monkey) and Macaca fascicularis (Old World monkey) using the retrograde and anterograde capabilities of the horseradish peroxidase technique and compared his findings with those of previous tracing studies.[11,60,127,140,144,148] Figure 1.16 summarizes the main cortical and subcortical projections of the precuneus.

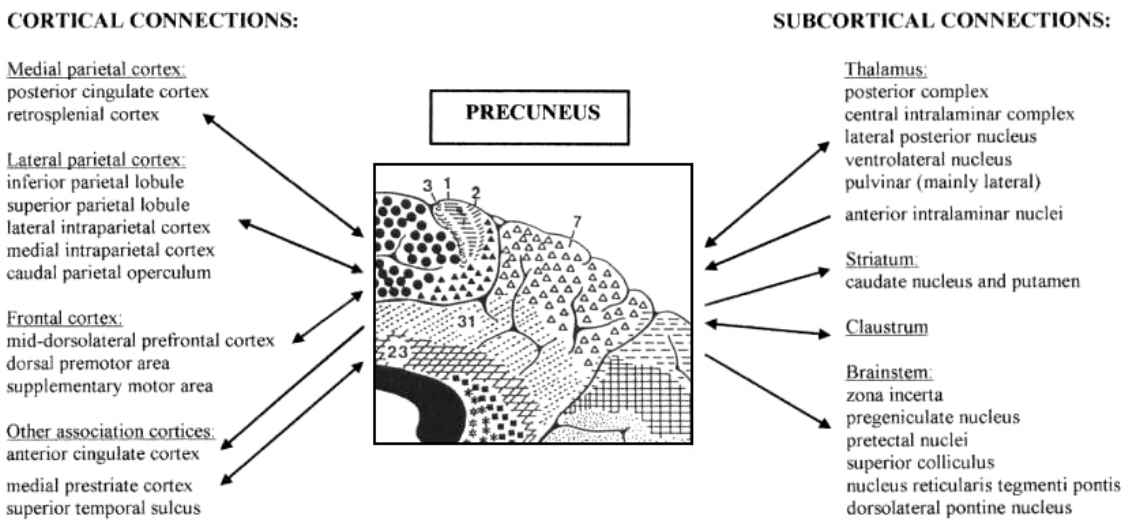


**Fig. 1.16.** Summary of the cortical (left) and subcortical (right) connections of the precuneus. Bidirectional arrows indicate reciprocal projections; unidirectional arrows indicate afferent/efferent projections.

The precuneus has reciprocal corticocortical connections with the adjacent areas of the posteromedial cortex, namely the posterior cingulate and retrosplenial cortices. This intimate interconnection is also bilateral, bridging homologous components of the two hemispheres, and to some extent providing an anatomical basis for their functional coupling. The precuneus is also selectively connected with other parietal areas, namely the caudal parietal operculum, the inferior and superior parietal lobules (SPLs), and the IPS, known to be involved in visuo-spatial information processing.[29,100,174]

The principal extraparietal corticocortical connections of the precuneus are with the frontal lobes. The precuneus and prefrontal cortex have been demonstrated to be strongly interconnected, and these projections tend to concentrate at the level of BA 8, 9 and 46. There are also extensive connections between the precuneus and the dorsal premotor area, the supplementary motor area (SMA) and the anterior cingulate cortex.[29,60,100,144] The results of the tracer injection studies of Leichnetz and colleagues[98-100] and Tian and Lynch[193,194] in macaque and cebus monkeys strongly support the existence of a topographical organization in the reciprocal parieto- frontal connections, such that the precuneus has

connections with oculomotor-related cortical regions, including the frontal eye fields. Neurophysiological studies in non-human primates provided further evidence for the selective functional coupling of medial parietal and frontal cortices. Thier and Andersen[190] were able to elicit saccades by direct low-current electrostimulation of the medial aspect of the posterior parietal cortex in the monkey, raising the hypothesis that the brain of these primates contains a 'medial parietal eye field'[189] involved in the control of eye movement and 'visual reaching'[76], in addition to the already known 'lateral parietal eye field', located in the lateral bank of the IPS[5]. Likewise, the corticocortical projections from the precuneus to the lateral parietal areas and premotor cortex[29,76,77,217] seem to play a pivotal role in the visual guidance of hand movements, i.e., hand–eye coordination[50] and reaching[22,23].

Other reciprocal cortical connections involve the medial prestriate cortex, with the parietooccipital visual area and the caudomedial lobule, and the cortex buried in the superior temporal sulcus, known as temporoparietooccipital cortex (TPO)[11,100]. The association cortices of the TPO form a heteromodal higher associative cortical network, which is involved in the integration of auditory, somatosensory and visual information.

The thalamic projections of the precuneus target mostly the dorsum of the thalamus, which contains nuclei connected with higher association cortices, the ventrolateral thalamic nucleus, the central nuclei of the intralaminar complex and the lateral pulvinar.[171,225,226] All these nuclei send projections back to the precuneus; in addition, the precuneus receives unilateral projections from the 'non-specific' anterior intralaminar nuclei. Interestingly, the lack of connections with the sensory thalamic nuclei, such as the ventral posterior lateral nucleus, suggests that the precuneus does not share the thalamic connectivity pattern of the parietal somatosensory cortical regions.

Other major subcortical connections of the precuneus include the claustrum, corticostriate projections to the dorsolateral caudate nucleus and putamen, and efferent projections to the zona incerta and brainstem structures with strongly 'oculomotor' characteristics, such as the pretectal area, the superior colliculus and the nucleus reticularis tegmenti pontis.[100,227] Finally, projections from each cytoarchitectonic area of the posteromedial cortex to the

basis pontis target different domains of this structure, and because each domain of the basis pontis recruits a specific set of cerebellar territories, the precuneus can gain access to multiple cerebellar circuits.

Overall, the extent of the connectivity of the precuneus is widespread and involves higher association cortical and sub- cortical structures. Notably, no direct connections with the primary sensory regions have been observed. Therefore, it seems reasonable to assume that precuneus activity influences an extensive network of cortical and subcortical structures involved in elaborating highly integrated and associative information, rather than directly processing external stimuli. Material reused from Cavanna AE & Trimble MR. The precuneus: a review of its functional anatomy and behavioural correlates, Brain, 2006, 129, 3, by permission of Oxford University Press [2]

## **1.4** Aims of Thesis

During the last years anatomical investigations by early scientists have sparked interest in cerebral subcortical anatomy and paved the way for a fundamental change in our perception of the white matter; from being regarded as an amorphous mass, to actually represent a complex network of tracts that interconnect adjacent and distant cortical and subcortical areas [172] Later, the introduction of Klingler's technique refined the anatomical investigation of white matter microstructure through the fixation of brains in a formalin solution followed by a freeze-thaw process, which facilitates meticulous dissections and enhances the delineation of fiber pathways [81,82]. Further, the recent advent of diffusion-weighted magnetic resonance imaging has allowed for a fast and non-invasive investigation of the white matter architecture *in vivo* and has provided valuable insights on the intrinsic white matter anatomy and its 3D representation [7,27,28,96,129,173].

From a functional standpoint, evidence from stroke studies combined with data stemming from pathologic processes mainly affecting white matter structures, such as multiple sclerosis, have led to the appreciation of a broad clinical significance of the cerebral white matter [51,52]. Keeping with this, functional neuroimaging [106,117,149,220] and human brain mapping studies [42,44,125,152,169,181] reflect the concept of a cortico-subcortical correlation and integration, thus emphasizing on a hodotopical network approach to understand higher cerebral processing [26,35]. To this end, advances in decoding the anatomical basis of cerebral processing along with the availability of the non-invasive diffusion tensor imaging (DTI) technique, led to a special research interest on the white matter architecture and brain connectivity. Due to specific technical limitations of DTI and tractography, data had to be validated through classical anatomic descriptions of white matter tracts [37,111] or alternatively be compared to relevant studies on non-human primates [113]. However, especially with regard to novel tracts, neither of the two aforementioned approaches seems to be accurate [87,163]. Hence, the Klingler's technique is currently considered the gold standard method through which DTI results can be verified.[120]

The anatomy of the human precuneus exhibits significant variability and has remained one of the less accurately mapped areas of the human.[31] The location of the precuneus renders this anatomical region particularly difficult to study as it is hidden in the interhemispheric fissure and in a very tight anatomical relationship with the sagittal sinus and bridging veins.[31] Additionally, strokes, accidents or tumors involving the postero-medial parietal cortices are rare and therefore data coming from patients with lesions localized in the precuneus remain scarce.[31,104] Nevertheless, its' strategic location and vast connections suggest that the precuneus is a major association area that may subserve a variety of behavioral functions. Findings in healthy individuals suggest that the precuneus is the core structure of the default mode network.[56,200] Moreover, the precuneal lobule is consistently found to activate in a broad range of high-order functions such as navigation, memory retrieval, attention, intelligence comparison, visuo-spatial imagery, representational similarity analysis (RSA) and transitive reasoning.[2,121,139,165,215] In the same vein, data stemming from a recent repetitive transcranial magnetic stimulation (rTMS) study documented the precuneus to be involved in the process of updating place representations during self-motion.[130]

During the last decade a growing body of evidence has advocated the functional connectivity of the precuneus with multiple eloquent areas of the cerebral cortex. [69,119] This synergy is a basic component of our default mode network, which is activated when the brain is in the condition of "resting consciousness", and allegedly sub-serves high order functions such as planning, volition, episodic memory, attention, spatial updating, error detection, social intelligence, intelligence comparison and verbal creativity.[21,46,121,151,177,182,196,200] Stronger connectivity of these regions is positively correlated with higher cognitive performance,[229] while in neurological and psychiatric conditions the activation of this circuitry is markedly altered.[105,211,231] Although the functional connectivity of the aforementioned cerebral regions and its significance have been repeatedly reported, the anatomical constraints of underlying structural circuits need to be further elucidated.

Given the functional significance, anatomical complexity and its uncharacterized connectivity, we opted to study the architecture of the precuneus through a combined

approach entailing mapping of the cortical surface and white matter anatomic dissections. To this end, we are studying the surface anatomy of the precuneus and by employing the fiber micro-dissection technique in formalin fixed brains we focus our study on the structural architecture of a recently identified fiber tract known as the sledge runner fasciculus which is believed to interconnect the precuneus with the occipital lobe,[9,63] a long association fiber tract, previously described as the Cingulum bundle V (CB-V), which is believed to interconnect the precuneus with areas of the temporal lobe,[218] the dorsal component of the Superior Longitudinal Fasciculus (SLF-I) which has been thus far depicted as a long association subcortical pathway connecting the precuneus with the dorsal premotor cortex and the SMA complex, and the middle longitudinal fasciculus which is believed to interconnect the precuneus with the temporal lobe[113]. We provide direct anatomical evidence on the tracts' invariable existence, morphological silhouette, termination pattern and spatial relationship with adjacent fiber tracts. Our results aim to document and refine current knowledge on structural brain connectivity and organization in terms of cortical and subcortical axonal interactions. Moreover, useful insights are provided allowing the study of high-level functioning circuits residing in the posteromedial cortices in greater detail; thus, paving the way towards a more comprehensive understanding of these networks both in normal and pathological brain conditions. Lastly, surgical comments and functional considerations on the involvement of the aforementioned tracts in operative trajectories designed to access lesions in and around the ventricular trigone are pointed out.

# Materials and Methods

## 2.1 Mapping the surface cortical anatomy of the precuneus

To study the regional surface anatomy of the precuneus, we reviewed the relevant literature, mainly focusing on contemporary studies conducted during the past 30 years. The variable and inconsistent anatomical nomenclature used for the sulcal pattern of the precuneus was documented to detect varying or overlapping terminologies. Moreover, we studied the relevant surface anatomy in cadaveric hemispheres. We studied forty-one (41) normal, adult, cadaveric hemispheres (20 right, 21 left) fixed in a 15% formalin solution for 2 months. We meticulously removed the arachnoid membrane and vessels of the area of the occipital lobe under the microscope (Carl Zeiss OPMI) and the sulcal morphology was systematically recorded in the area of the precuneus. Using a Nikon DSLR camera and a macro lens, we obtained multiple photographs from different angles in order to vividly illustrate the regional surface anatomy. We identified and recorded the regional sulcal anatomy consisting of the parieto-occipital sulcus (demarcating the precuneus and isthmus of the cingulate gyrus from the cuneus), calcarine fissure (demarcating the cuneus from the lingual gyrus) and the marginal ramus of the cingulate sulcus (demarcating the precuneus and frontal lobe). We categorized the patterns and variations of the SpS and POS and their branches according to the previously described landmarks and terminology introduced by Ono et al. and recently utilized by Gürer et al.[65,137]

## 2.2 Fiber Dissection Technique to Study the Sledge Runner Fasciculus

We studied the Sledge Runner Fasciculus (SRF) in twenty (20) normal, adult, cadaveric cerebral hemispheres (11 right hemispheres – 9 left hemispheres) obtained from 20 different cadavers previously fixed in a 10% -15% formalin solution for a minimum period of 8 weeks. We carefully removed the arachnoid membrane and vessels and prepared all specimens according to the Klingler's procedure (freeze-thaw process). We then investigated the specimens using the fiber dissection technique and the microscope (Carl Zeiss OPMIR Plus, Carl Zeiss AG, Oberkochen, Germany). as described.[83-86,89-91] The Sledge Runner fasciculus resides in the depth of the medial and medio-basal occipital lobe. [9,63,203] Therefore, we performed medial to lateral fiber micro-dissections focused on the occipital lobe in all twenty (20) hemispheres.

Prior to the dissection process, the surface anatomy of the medial cerebral surface was recorded in detail. Specifically the parieto-occipital sulcus (delineating the precuneus and isthmus of the cingulate gyrus from the cuneus), calcarine fissure (delineating the cuneus from the lingual gyrus) and their common stem (delineating the lingual and posterior parahippocampal gyri from the isthmus of the cingulate gyrus) the collateral sulcus (delineating the parahippocampal from the fusiform gyrus) and sub-parietal sulcus (delineating the isthmus of the cingulate gyrus from the precuneus) (Figures 2.1 & 2.2).

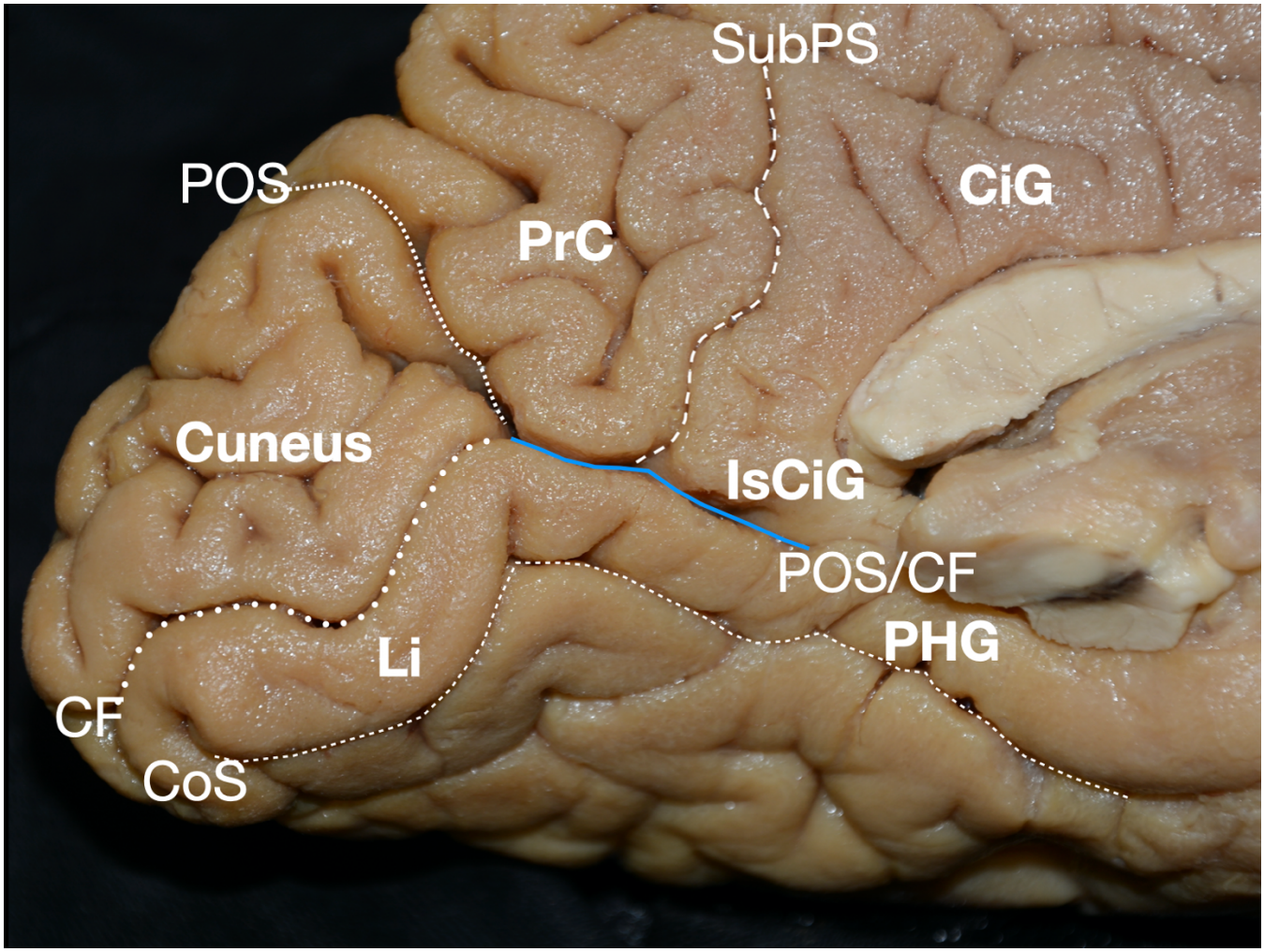


**Figure. 2.1** Surface anatomy of the postero-medial surface of a left hemisphere. The parieto-occipital sulcus is demonstrated on a white dashed line delineating the precuneus, isthmus of the cingulate gyrus and cuneus, the calcarine fissure is demonstrated on a white dotted line delineating the lingual gyrus and the cuneus, their common stem is demonstrated on a blue line delineating the lingula, posterior parahippocampal gyrus and the isthmus of the cingulate gyrus, the collateral sulcus is demonstrated on a white dashed line delineating the parahippocampal and fusiform gyri and sub-parietal sulcus is demonstrated on a white dashed line delineating the isthmus of the cingulate gyrus and the precuneus. C= Cuneus, CiG= Cingulate gyrus, CF= Calcarine fissure, CoS= Collateral sulcus, IsCiG= Isthmus of the Cingulate gyrus, Li= Lingual gyrus, PHG= Parahippocampal gurus, POS= Parieto-occipital sulcus, POS/CF= Parieto-occipital sulcus & Calcarine Fissure common stem, PPA= Parahippocampal Place Area, PrC= Precuneus, RSC= Retrosplenial Cortex, SubPS= Sub-Parietal Sulcus

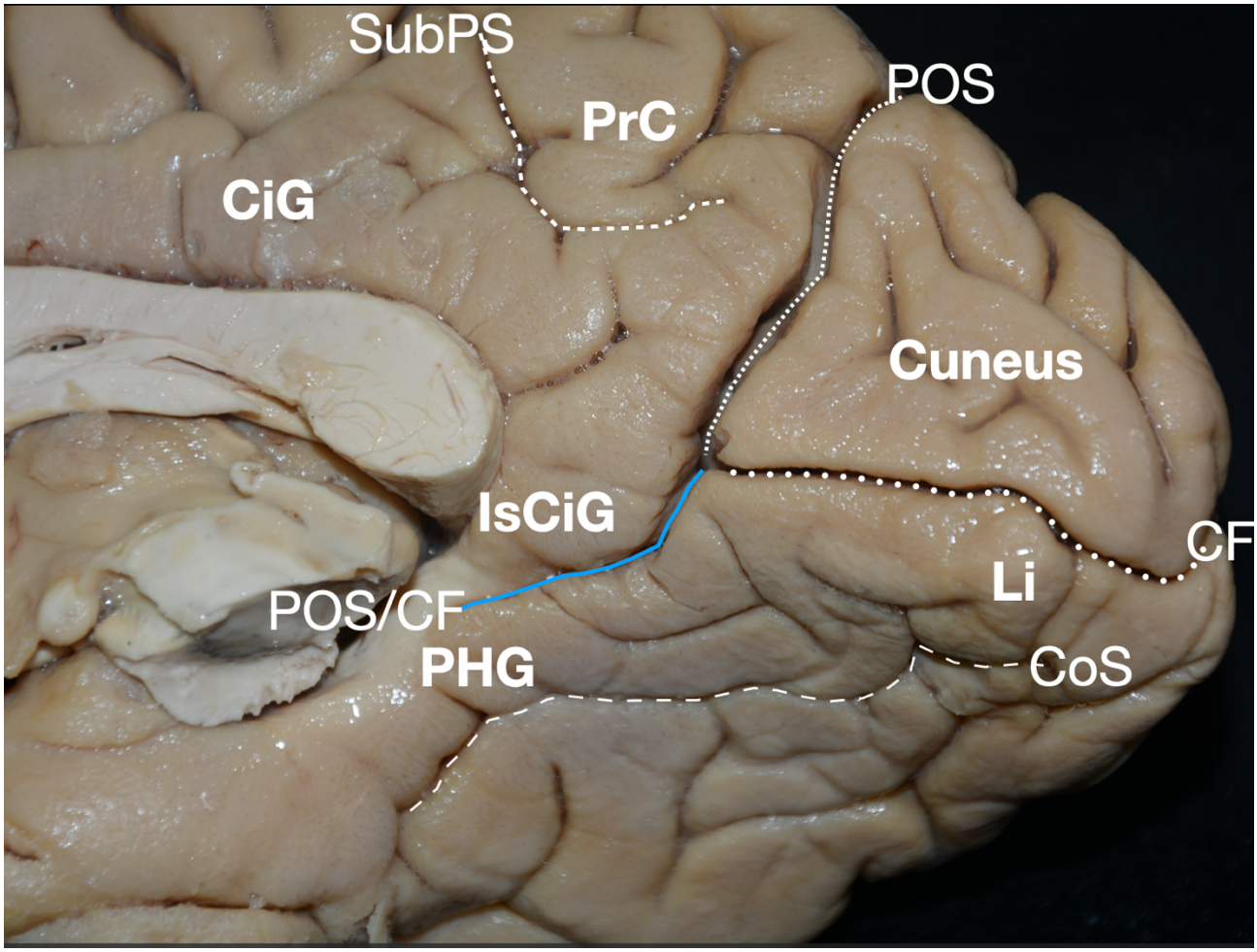


**Figure 2.2** Surface anatomy of the postero-medial surface of a right hemisphere. The parieto-occipital sulcus is demonstrated on a white dashed line delineating the precuneus, isthmus of the cingulate gyrus and cuneus, the calcarine fissure is demonstrated on a white dotted line delineating the lingual gyrus and the cuneus, their common stem is demonstrated on a blue line delineating the lingula, posterior parahippocampal gyrus and the isthmus of the cingulate gyrus, the collateral sulcus is demonstrated on a white dashed line delineating the parahippocampal and fusiform gyri and sub-parietal sulcus is demonstrated on a white dashed line delineating the isthmus of the cingulate gyrus and the precuneus. C= Cuneus, CiG= Cingulate gyrus, CF= Calcarine fissure, CoS= Collateral sulcus, IsCiG= Isthmus of the Cingulate gyrus, Li= Lingual gyrus, PHG= Parahippocampal gurus, POS= Parieto-occipital sulcus, POS/CF= Parieto-occipital sulcus & Calcarine Fissure common stem, PPA= Parahippocampal Place Area, PrC= Precuneus, RSC= Retrosplenial Cortex, SubPS= Sub-Parietal Sulcus

To study and record the anatomy, morphology, and measurements of the sledge runner fasciculus, we initially confined our fiber microdissections within the region of the cuneus and lingual gyrus and subsequently we extended them to the adjacent cerebral region of the cingulate isthmus, posterior half of the precuneus and posterior part of the parahippocampal gyrus (Figure 2.1 &2.2). Furthermore, we studied the correlative anatomy of the sledge

runner fasciculus with the ventricular compartments, relevant sulci, gyri and adjacent white matter pathways

For the fiber microdissections, we utilized fine metallic periosteal elevators, various sized anatomical forceps, and micro-scissors.[88] We obtained photographs during every stage of the cadaveric dissections to illustrate the regional cortical and subcortical anatomy. Notably the dissection photos included in this study have not been edited by picture enhancing software so that they closely resemble the anatomy encountered during standard fiber micro-dissections in the setting of a microneurosurgery laboratory.[88]

## 2.3 Fiber Dissection Technique to Study the Dorsal Component of the Superior Longitudinal Fasciculus

We studied the SLF-1 in twenty (15) normal, adult, cadaveric cerebral hemispheres (7 right hemispheres - 8 left hemispheres) previously fixed in a 10% -15% formalin solution for a minimum period of 8 weeks. We carefully removed the arachnoid membrane and vessels and prepared all specimens according to the Klingler's procedure (freeze-thaw process). We then investigated the specimens utilizing the fiber microdissection technique by using micro-dissectors, various anatomical micro-forceps, micro-scissors and the microscope (Carl Zeiss OPMIR Plus, Carl Zeiss AG, Oberkochen, Germany). [83-86,89-91]

Taking into account that the SLF-1 is located within the medial surface of the hemisphere (Figure 2.3), we performed fiber microdissections in a medial to lateral direction, starting from the area of the anterior cingulate cortex and extending posteriorly towards the area of the precuneus. The posterior limit of our dissections was delineated by the parieto-occipital sulcus.

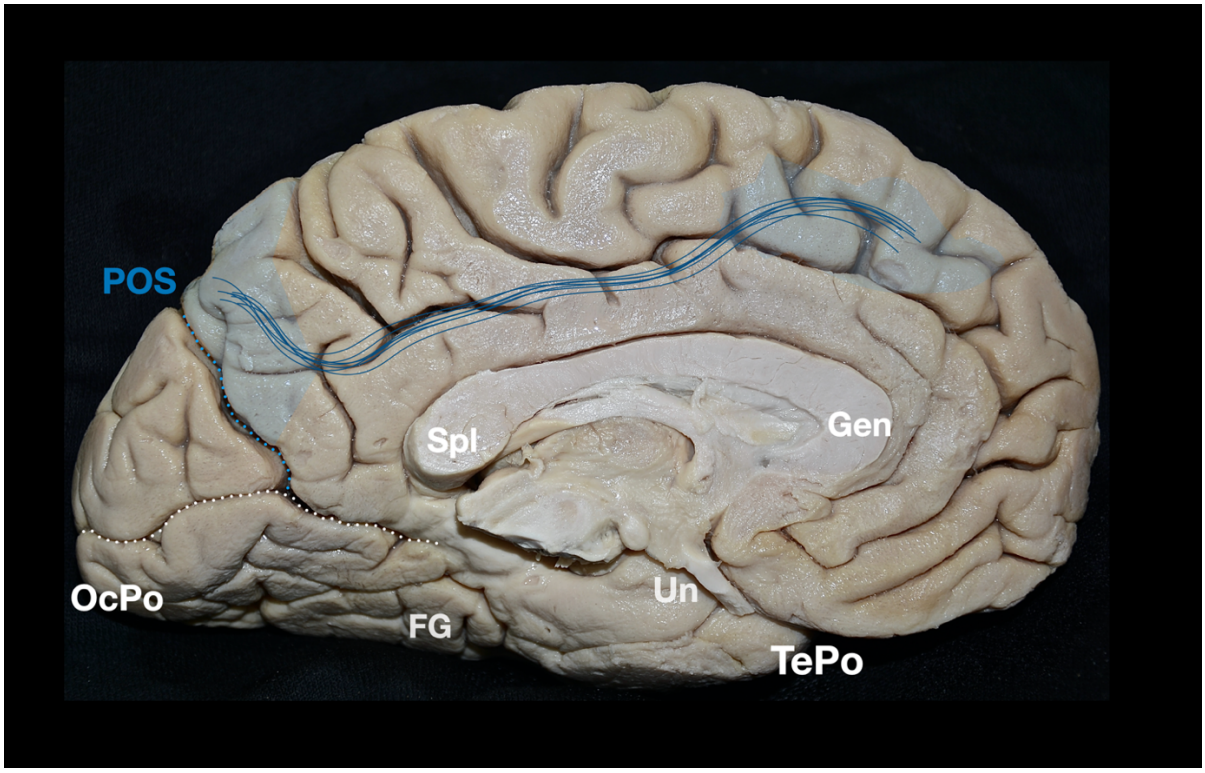


**Figure 2.3** Medial aspect of a left hemisphere showing the SLF-1 trajectory projected on the surface anatomy. Blue dotted line, parietooccipital sulcus; white dotted line, calcarine fissure; dark blue continuous lines, SLF-1 trajectory; highlighted light blue = SLF-1 Cortical Projections; CaF, calcarine fissure; Gen, genu of corpus callosum; FuG, fusiform gyrus; OcPo, occipital pole; PPA, parahippocampal place area; POS, parietooccipital sulcus; Spl, splenium of corpus callosum; TePo, temporal pole; Un, uncus.

Prior to the dissection process, the surface anatomy of the medial cerebral surface was recorded in detail. (Figure 2.4) The cingulate sulcus marked the superior limit of the cingulate gyrus and therefore proved to be a useful superficial landmark that delineated the subcortical boundaries of the superior arm of the cingulum. Special attention was paid to the medial aspect of the superior frontal gyrus as well as to the paracingulate sulcus and gyrus - when present- since the fibers representing what has been described as the SLF I are usually encountered just under the superficial U fibers of this area and therefore can be easily disrupted. In 5 out of the 15 studied hemispheres we proceeded with a multi-layered dissection in which a part of the lateral aspect of the frontal lobe and frontoparietal operculum was included in order to understand and demonstrate the correlative anatomy

of the SLF I, SLF II and SLF III. Notably, the medial aspect of the superior frontal gyrus represents a complex area where several subcortical pathways originating from the cingulate gyrus, the SMA complex and paracentral lobule converge, thus rendering the preservation of the structural white matter integrity particularly difficult.

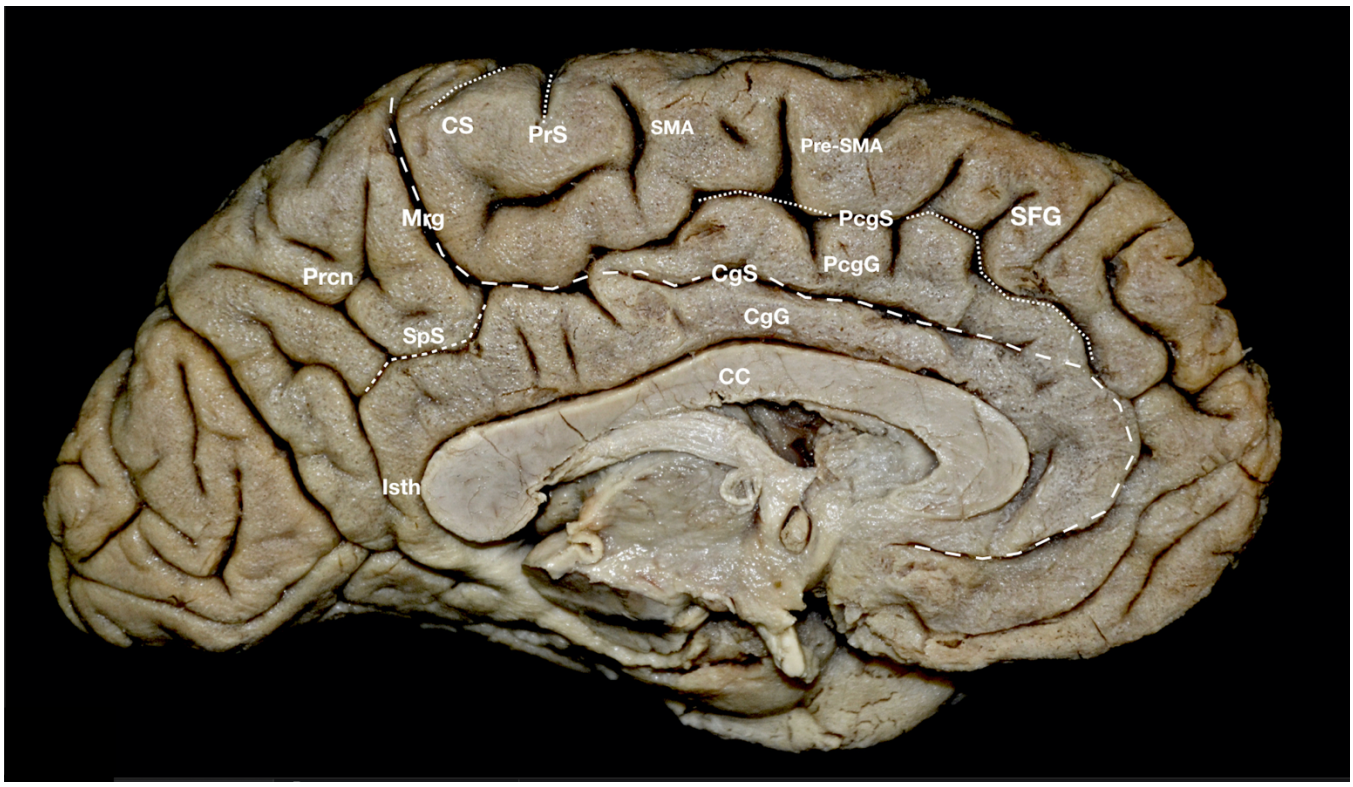


**Figure 2.4.** left hemisphere illustrating surface relevant surface anatomy of the medial surface. Note the presence of the paracingulate gyrus and sulcus. CC= Corpus Callosum, CgG= Cingulate Gyrus, Cgs= Cingulate Sulcus, Cgsa= Cingulum Superior Arm, CR= Callosal Radiations, CS= Central Sulcus, Mrg= Marginal ramus of the cingulate sulcus, PcgG= Paracingulate gyrus, PcgS= Paracingulate sulcus, Prcn= Precuneus, PrCn(a)= Anterior Precuneus, Pre-SMA= Pre-Supplementary Motor Area, PrG= Precentral Gyrus, PrS= Precentral Sulcus, PtG= Postcentral Gyrus, SFG= Superior Frontal Gyrus, SLF-Ia= Superior Longitudinal Fasciculus I – anterior segment, SLF-Ip= Superior Longitudinal Fasciculus I – posterior segment, SMA= Supplementary Motor Area, SpS= Subparietal sulcus. Reprinted from Komaitis et al.[84] by permission of JNS publishing group

Digital photographs were obtained in a stepwise fashion in different dissection stages and angles to illustrate more vividly the topographical architecture and spatial relationship of the regional white matter tracts. All figures included in this study are un-enhanced in order

to closely resemble the white matter fiber tract anatomy encountered in standard laboratory settings.

## 2.4 Fiber Dissection Technique to Study the middle longitudinal fasciculus

To investigate the MdLF, we studied twenty (20) normal, adult, cadaveric cerebral hemispheres (9 right hemispheres - 11 left hemispheres) previously fixed in a 10% -15% formalin solution for a minimum period of 8 weeks. We carefully removed the arachnoid membrane and vessels and prepared all specimens according to the Klingler's procedure (freeze-thaw process). After carefully removing the arachnoid membrane and vessels, all hemispheres underwent the Klingler's procedure and were subsequently dissected using the white matter fiber micro-dissection technique. [83-86,89-91]

According to current literature, the MdLF runs in the lateral aspect of the hemisphere and participates in the axonal connectivity of the superior temporal gyrus (STG) and the parietal and occipital lobes. [32,113-116,118,126,210] We, therefore, performed lateral to medial anatomic dissections with special emphasis on the aforementioned area. To better illustrate the subcortical correlative anatomy, we further dissected the entire temporal lobe, insula and fronto-parietal operculum. Prior to the dissection process, the sulcal and gyral anatomy of the lateral aspect of the hemisphere was recorded in detail (Figure 2.5)

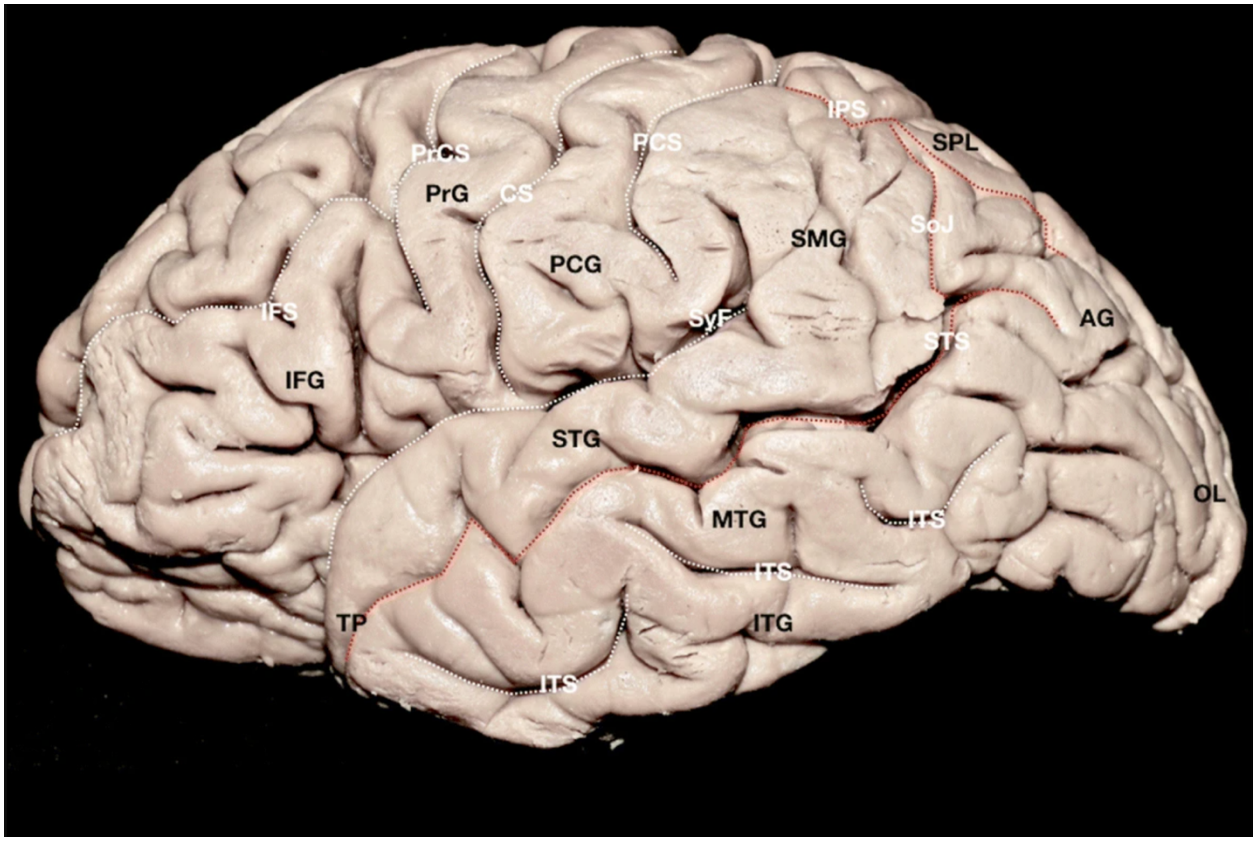


**Figure 2.5** Sulcal and Gyral anatomy of the lateral surface of a left hemisphere. The STS (demarcating the STG and the MTG), IPS (demarcating the SPL and the IPL) and SoJ (demarcating the SMG and AG) are marked with red dotted lines. The illustrated sulci of the lateral surface are marked with white dotted lines. AG angular gyrus, CS central sulcus, HG Heschl's gyrus, IFG inferior frontal gyrus, IFS inferior frontal sulcus, IN insula, IPS intraparietal sulcus, ITG inferior temporal gyrus, ITS inferior temporal sulcus, MTG middle temporal gyrus, OL occipital lobe, PCG postcentral gyrus, PCS postcentral sulcus, PrCS precentral sulcus, PrG precentral gyrus, PTA posterior transverse area, SLF/AF Superior Longitudinal Fasciculus/Arcuate Fasciculus Complex, SMG supramarginal gyrus, SoJ sulcus of jensen, SPL superior parietal lob- ule, STG superior temporal gyrus, STS superior temporal sulcus, SyF sylvian fissure, TP temporal pole, TTS transverse temporal sulcus. Reprinted from Kalyvas et al[79] by permission of Springer Nature [3]

## 2.5 Fiber Dissection Technique to Study the inferior fronto-occipital fasciculus

To investigate the IFOF. We studied twenty (9) normal, adult, cadaveric cerebral hemispheres (4 right hemispheres - 5 left hemispheres) previously fixed in a 10% -15% formalin solution for a minimum period of 8 weeks. We carefully removed the arachnoid membrane and vessels and prepared all specimens according to the Klingler's procedure (freeze-thaw process). After carefully removing the arachnoid membrane and vessels, all hemispheres underwent the Klingler's procedure and were subsequently dissected using the white matter fiber micro-dissection technique. [83-86,89-91]

According to current literature, the IFOF resides in the lateral aspect of the hemisphere and participates in the axonal connectivity of the frontal, parietal and occipital lobes.[68,122,142] Therefore, we performed lateral to medial micro-dissections focusing on the aforementioned area. To better illustrate the subcortical correlative anatomy, we further dissected the entire temporal lobe, insula and fronto-parietal operculum. Prior to the dissection process, the sulcal and gyral anatomy of the lateral aspect of the hemisphere was recorded in detail. (**Figure 2.5**) Our aim was to disclose the IFOF and to determine whether the most superior part of the IFOF reaches the precuneus.

## 2.6 Fiber Dissection Technique to Study the precuneual claustrocortical fibers

To investigate the claustrocortical fibers terminating on the precuneus, we studied twenty (22) normal, adult, cadaveric cerebral hemispheres previously fixed in a 10% -15% formalin solution for a minimum period of 8 weeks. We carefully removed the arachnoid membrane and vessels and prepared all specimens according to the Klingler's procedure (freeze-thaw process). After carefully removing the arachnoid membrane and vessels, all hemispheres underwent the Klingler's procedure and were subsequently dissected using the white matter fiber micro-dissection technique. [83-86,89-91]

According to current literature, the claustrocortical reside in the lateral aspect of the hemisphere and participates in the axonal connectivity of the claustrum with the superior frontal, precentral, postcentral, and posterior parietal cortices.[14,48,49] Therefore, we performed lateral to medial micro-dissections focusing on the aforementioned area. To better illustrate the subcortical correlative anatomy, we further dissected the entire temporal lobe, insula and fronto-parietal operculum. Prior to the dissection process, the sulcal and gyral anatomy of the lateral aspect of the hemisphere was recorded in detail. (Figure 2.5)

## 2.7 Fiber Dissection Technique to Study the Fifth Component of the Cingulum Bundle

To investigate the fifth component of the cingulum bundle CB-V, fifteen (15) normal, adult, cerebral hemispheres were obtained from 8 different individuals in routine autopsy and were fixed in a 10% formalin solution for 8 weeks. Upon meticulous dissection of the arachnoid membrane and vessels, all specimens were prepared according to the Klingler's method and investigated through the fiber micro-dissection technique. The operating microscope and (Carl Zeiss OPMIR Plus, Carl Zeiss AG, Oberkochen, Germany) surgical micro-instruments such as fine metallic periosteal elevators, various sized anatomical forceps, and micro-scissors were used as previously described.[83-86,89-91] All dissections were focused deep to the parieto-occipital sulcus (POS), distal calcarine fissure and medial temporal lobe as this was the area of interest. Prior to dissection, the regional sulcal anatomy consisting of the parieto-occipital sulcus, proximal calcarine fissure, distal calcarine fissure, collateral sulcus, occipitotemporal sulcus and sub-parietal sulcus was studied in all cases. (Figure 2.6)

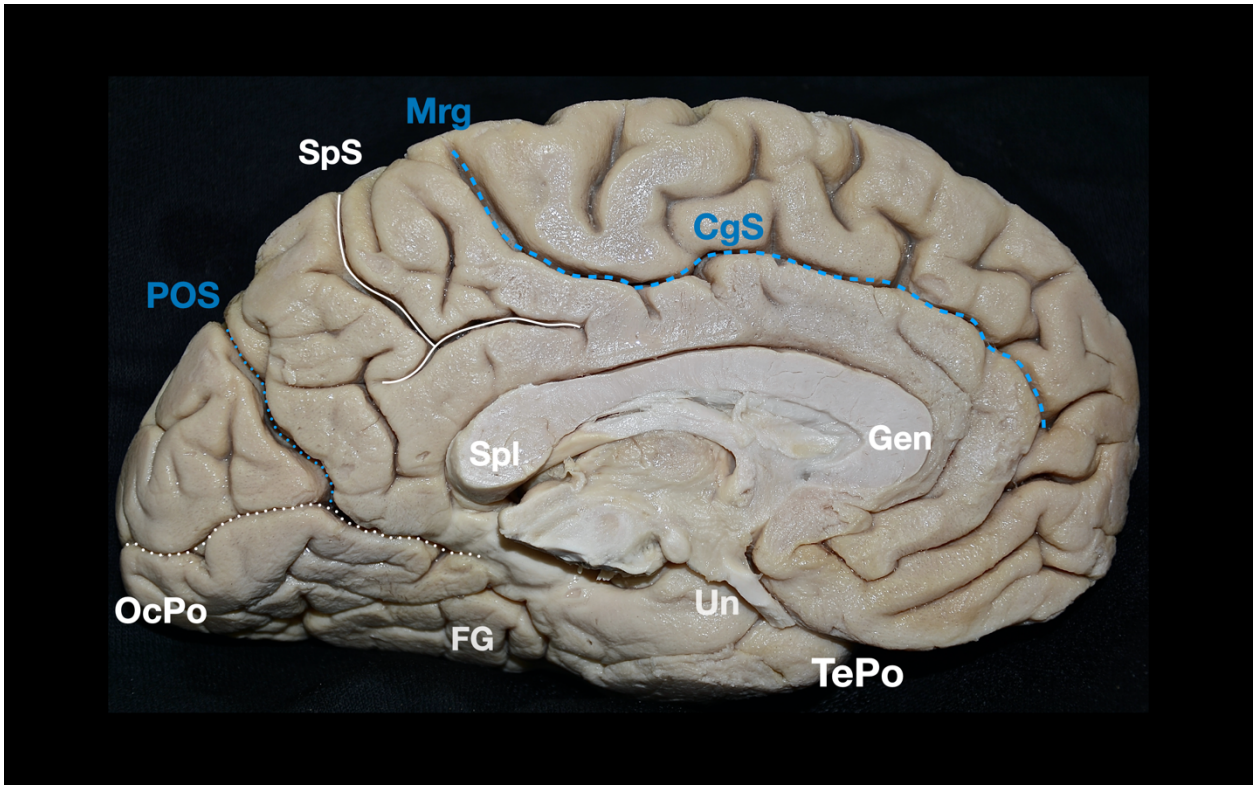


**Figure 2.6** Medial aspect of a left hemisphere illustrating the surface anatomy. The parieto-occipital sulcus is demonstrated on a blue dotted line delineating the precuneus, and cuneus, the calcarine fissure is demonstrated on a white dotted line delineating the lingual gyrus and the cuneus, the lingula, posterior parahippocampal gyrus and the isthmus of the cingulate gyrus. The subparietal is demonstrated on a white dashed line delineating the parahippocampal and fusiform gyri and sub-parietal sulcus is demonstrated on a white dashed line delineating the isthmus of the cingulate gyrus and the precuneus Blue dotted line parietooccipital sulcus; white dotted line, calcarine fissure; CaF, calcarine fissure; Gen, genu of corpus callosum; FuG, fusiform gyrus; OcPo, occipital pole; PPA, parahippocampal place area; POS, parietooccipital sulcus; Spl, splenium of corpus callosum; TePo, temporal pole; Un, uncus; Cgs= Cingulate Sulcus, Mrg= Marginal ramus of the cingulate sulcus, SpS= Subparietal sulcus.

We then started the dissection process by carefully peeling away the cortex and underlying short association fibers known as arcuate or “U” fibers - at the level of the parieto-occipital sulcus and up until the distal end of the calcarine sulcus. Cortical and white matter fiber dissections gradually proceeded to include the cuneus, precuneus, posterior cingulate cortex, retrosplenial area, ventral and medial temporal lobe and basal temporo-occipital area to map and record the topography, morphology, termination pattern and correlative anatomy of the CB-V.

Digital photographs were obtained in a stepwise fashion in different dissection stages and angles to illustrate more vividly the topographical architecture and spatial relationship of the regional white matter tracts. All figures included in this study are un-enhanced in order to closely resemble the white matter fiber tract anatomy encountered in standard laboratory settings.

# Results

## 3.1 The cortical surface anatomy of the precuneus

The precuneus constitutes the medial part of the superior parietal lobule and is located on the medial surface of the hemisphere. It is delineated by the parietooccipital sulcus posteriorly, the marginal ramus of the cingulate sulcus anteriorly, and the subparietal sulcus inferiorly. [160] Inferiorly to the subparietal sulcus, the precuneus is connected to the isthmus of the cingulate gyrus and the parahippocampal gyrus. We identified the SpS as a short main sulcus following the original course of the cingulate sulcus posteriorly from where the marginal ramus of the cingulate sulcus bends superiorly and also separating the precuneus superiorly from the posterior segment of the cingulate gyrus. We identified the POS coursing inferiorly form the vertex to merge with the distal part of the calcarine sulcus. The SpS and POS displayed the following patterns:

Patterns of the SpS

We recorder the H-pattern in 21 out of 41 hemispheres (11R/10L); Split H pattern in 3 out of 41 hemispheres (3R/0L); oblique pattern in 2 out of 41 hemispheres (1R/1L); single upward branch pattern in 7 out of 41 hemispheres (5R/2L); triple upward branch pattern in 6 out of 41 hemispheres (0R/6L); double horizontal pattern in 2 out of 41 hemispheres (1R/1L) (Figure 3.1).

Patterns of the POS

We recorded the POS as an uninterrupted sulcus in 40 out of 41 the hemispheres (20L/20R) examined and as an interrupted sulcus in 1 out of 41 the hemispheres (1L/0R).

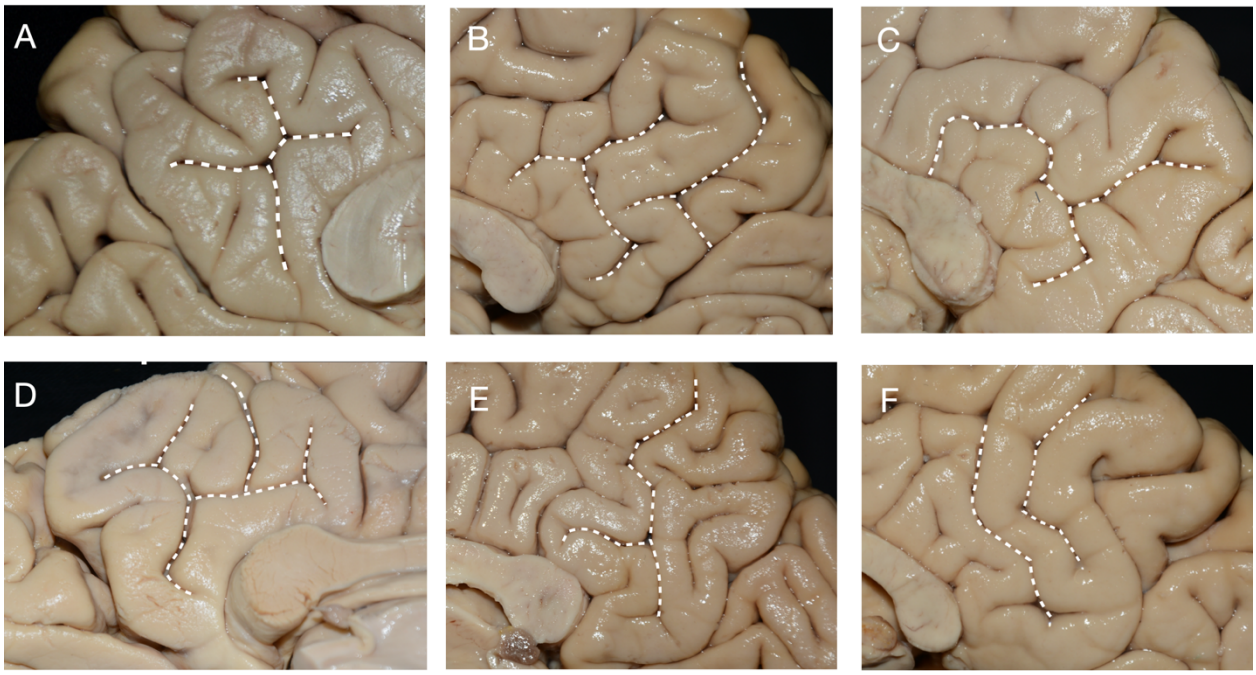


**Figure 3.1** (A) H pattern (B) Split H pattern (C) Oblique pattern (D) Triple upward branch pattern (E) Single upward branch pattern (F) Double horizontal pattern

## 3.2 The Sledge Runner Fasciculus

*Microanatomic dissection*

To investigate and record the morphology, axonal connectivity, and topographical anatomy of the sledge runner fasciculus we performed medial to lateral fiber microdissections focused on the area of the posteromedial cortex; specifically, we focused our microdissections to the area of the cuneus, posterior precuneus, lingual gyrus, isthmus of the cingulate gyrus and posterior parahippocampal gyrus (Fig. 3.2). We peeled away the cortex of the aforementioned gyri, exposing the arcuate or U fibers (Fig. 3.2D). We gradually dissected the local U fibers, revealing the Sledge Runner fasciculus along with fibers of the cingulum. We also exposed the stratum calcarinum at the depth of the calcarine fissure, a distinct group of fibers displaying a vertical trajectory (Fig. 3.3).

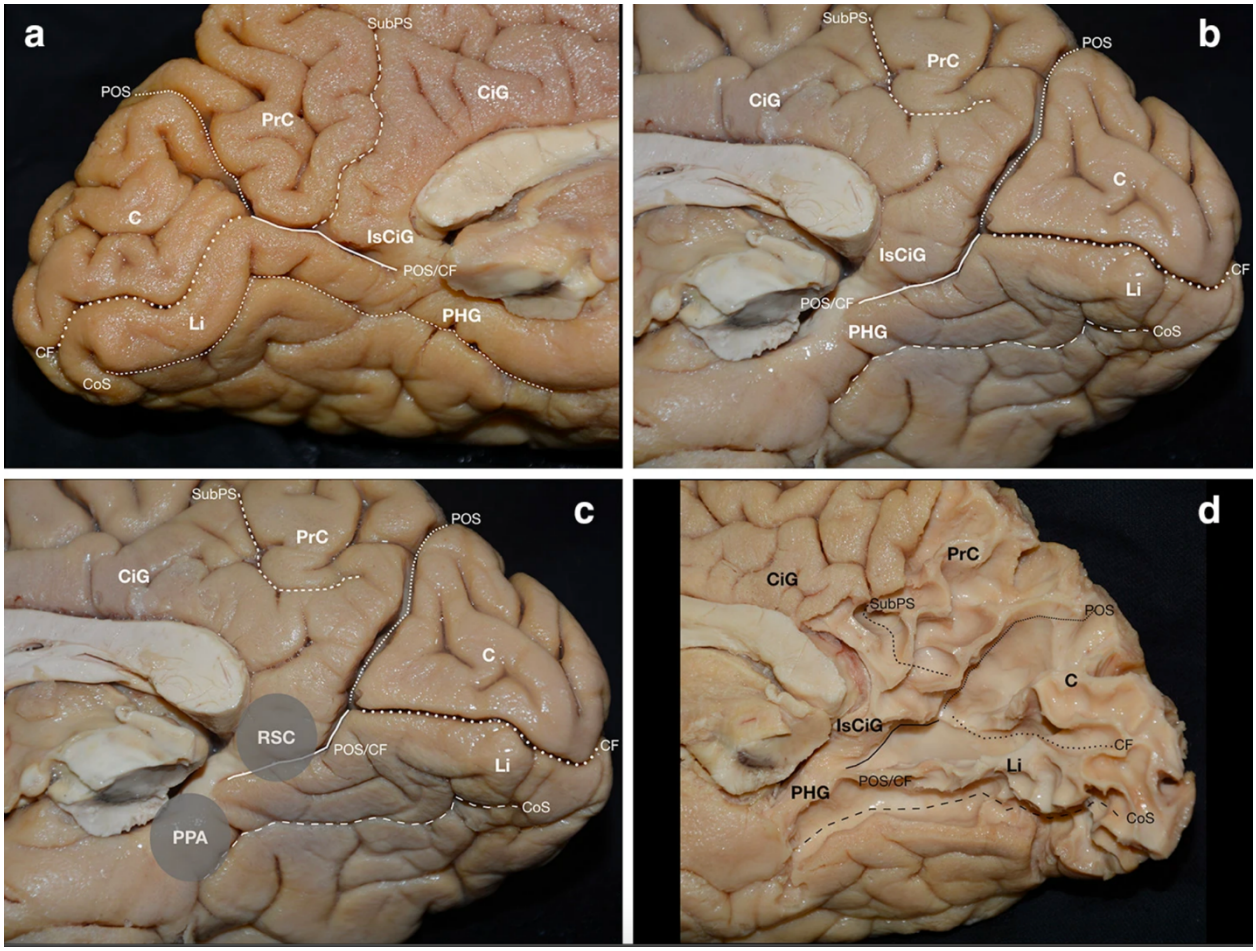


**Figure 3.2** Sulcal and gyral anatomy of the medial and basal cerebral surface of a left (a) and right (b) hemisphere. The parieto-occipital sulcus (demarcating the precuneus, isthmus of the cingulate gyrus and cuneus), the calcarine fissure (demarcating the cuneus and the lingual gyrus), their common stem (demarcating the lingula posterior parahippocampal gyrus and the isthmus of the cingulate gyrus), the collateral sulcus (demarcating the parahippocampal and fusiform gyri) and sub-parietal sulcus (demarcating the isthmus of the cingulate gyrus and the precuneus) are illustrated. c The cerebral areas known as the Retrosplenial Cortex (RSC) and Parahippocampal Place Area are demarcated in the specimen shown in b to correlate the anatomical landmarks to their functional equivalent. d The arcuate or U fibers of the medial surface of a right hemisphere are depicted. The plane of the parieto-occipital sulcus, calcarine fissure, their common stem and sub-parietal sulcus is marked for better orientation. C cuneus, CiG cingulate gyrus, CF calcarine fissure, CoS collateral sulcus, IsCiG isthmus of the cingulate gyrus, Li lingual gyrus, PHG parahippocampal gurus, POS parieto-occipital sulcus, POS/CF parieto-occipital sulcus and calcarine fissure common stem, PPA parahippocampal place area, PrC precuneus, RSC retrosplenial cortex, SubPS sub-parietal sulcus. Reprinted from Koutsarnakis et al[86] by permission of Springer Nature [6]

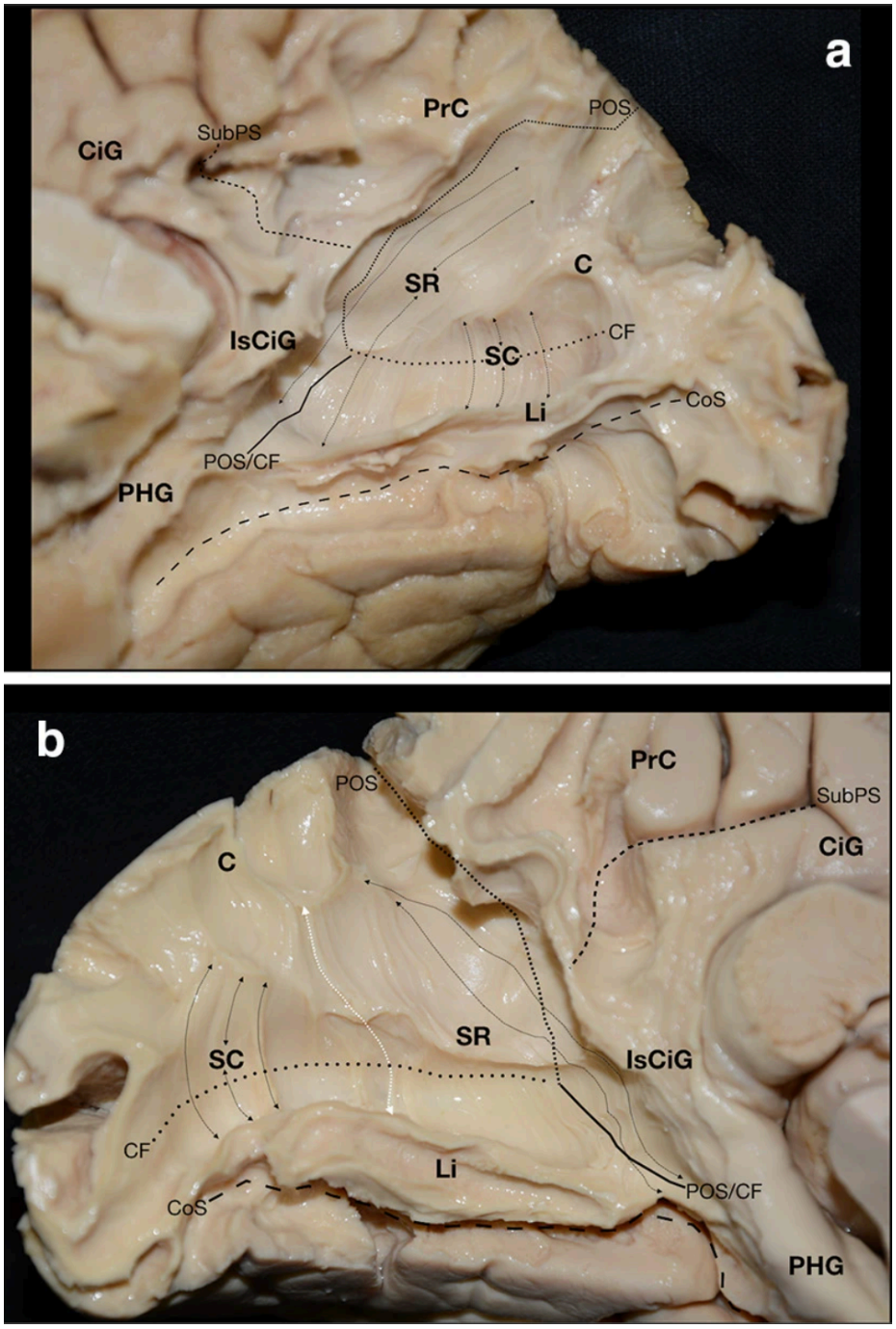


**Figure 3.3** Dissecting the U-fibers of a right (a) and a left (b) hemisphere reveals the fibers of the sledge runner fasciculus (SRF), the fibers of the cingulum arching over the splenium of the corpus callosum and a group of vertically oriented fibers located at the depth of the calcarine fissure, corresponding to the tract known as the "stratum calcarinum". a Right hemisphere: the SRF is seen to course in an oblique direction- just under the U-fibers of the medial cerebral surface- connecting the cuneus, the anterior part of the lingual gyrus, the cingulate isthmus and the posterior part of the parahippocampal gyrus. Note the fibers of the stratum calcarinum connecting the superior and inferior banks of the calcarine fissure. The direction and trajectory of the SRF and stratum calcarinum (SC) are marked with curved arrows. This white matter morphology of both the SRF and SC was consistently encountered in all studied specimens. b Left hemisphere: The anatomical silhouette of the SRF and SC is delineated with curved arrows. Note how the most anterior fibers of the SRF cross the plane of the parieto-occipital sulcus as they travel ventrally towards the isthmus of the cingulum and posterior part of the parahippocampal gyrus. Note also the clear anatomical boundary between the fibers of the SRF and SC in this specimen (distance between the most anterior black curved arrows placed on the SC and the posteriorly placed white arrow on the SR). C cuneus, CiG cingulate gyrus, CF calcarine fissure, CoS collateral sulcus, IsCiG isthmus of the cingulate gyrus, Li lingual gyrus, PHG parahippocampal gurus, POS parieto-occipital sulcus, POS/CF parieto-occipital sulcus and calcarine fissure common stem, PrC precuneus, SC stratum calcarinum, SRF sledge runner fasciculus, SubPS Sub-parietal sulcus Reprinted from Koutsarnakis et al[86] by permission of Springer Nature [6]

*Connectivity of the Sledge Runner Fasciculus (SRF)*

We consistently found and recorded the Sledge Runner fasciculus (SRF) as a distinct group of fibers travelling deep to the U-fibers of the occipital lobe. The SRF was consistently interconnecting the areas of the anterior cuneus, anterior half of the lingual gyrus, cingulate isthmus and posterior parahippocampal gyrus (Figure 3.3). We did not found fibers of the SRF connecting any area of the precuneus.

*Trajectory and Configuration of the Sledge Runner Fasciculus (SRF)*

We consistently recorded a dorsomedial to ventrolateral direction with two medial curves or knees. We recorded one curve at the level of the major forceps and one at the level of the inferior margin of the medial wall of the ventricular atrium. (Figure 3.4). We also consistently found the SRF to exhibit a superior narrow silhouette superiorly at the level of the superior cuneus, and a broader silhouette inferiorly at the level of lingual gyrus (Figure 3.4).

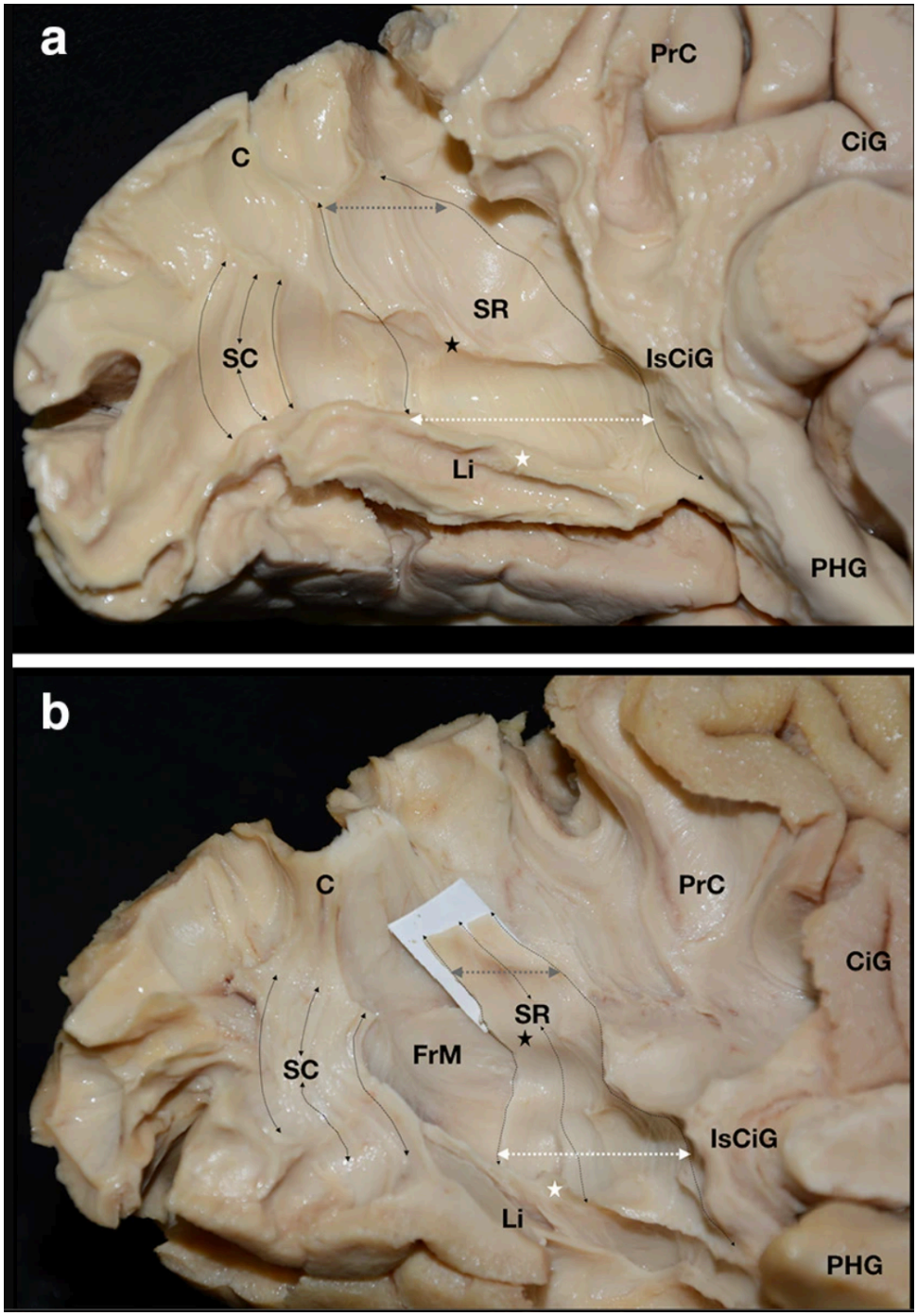


**Figure 3.4** The morphology and configuration of the SRF is illustrated in two left hemispheres (a,b). The standard and consistent dorsomedial–ventrolateral direction of the SRF is depicted in both specimens. Note how the tract progressively widens from its dorsal narrow part, corresponding to the area of the cuneus (marked with the grey arrow), to its wider ventral part at the area of the cingulum and posterior parahippocampal gyrus (marked with the white arrow). During its course the SRF usually exhibits two medially directed curves, as seen and marked with black and white stars in these specimens. In the specimen included in b, we preserved the fibers of the SRF (marked with the white strap) while deepening the dissection plane posteriorly and exposing the more medially located fibers of the forceps major, thus illustrating the upper curve to lie at the level of the major forceps (marked in both specimens with the black star). The lower curve, marked with the white star, roughly corresponds to the level of the infero-medial wall of the ventricular atrium. C cuneus, CiG cingulate gyrus, FrM forceps major, IsCiG isthmus of the cingulate gyrus, Li lingual gyrus, PHG parahippocampal gurus, PrC precuneus, SC stratum calcarinum, SRF sledge runner fasciculus. Reprinted from Koutsarnakis et al[86] by permission of Springer Nature [6]

*Surface correlative anatomy of the SRF*

We found the superior fibers of the SRF residing deep to the posterior bank of the superior 2/3rds of the parieto-occipital sulcus. We found the inferior fibers of the SRF more anteriorly, at the level of the inferior 1/3rd of the parieto-occipital sulcus. We did not found fibers of the SRF fibers residing deep to the plane of the sub-parietal sulcus or entering the white matter of the precuneus.

Deep to the calcarine fissure, we found the SRF fibers to cross the fissure in an almost vertical fashion, interconnecting the cuneus with the lingual gyrus (anterior half). Deep to the common trunk formed by the proximal parts of the calcarine fissure and the parieto-occipital sulcus (also referred to as distal calcarine fissure), we found the SRF fibers to follow the trajectory of the sulcus, up to the level of the cingulate isthmus and posterior part of the parahippocampal gyrus, (Figure 3.3). In relationship with the gyral anatomy, we found the SRF to reside deep to the anterior half of cuneus, anterior half of the lingual gyrus, isthmus of cingulate gyrus and posterior parahippocampal gyrus.

*Subcortical correlative anatomy of the SRF*

<u>Cingulum</u>

The cingulum is also a tract that resides within the parietooccipital sulcus. We consistently found fibers of the SRF adjacent to Cingulum fibers. Specifically, the relationship between the two distinct aforementioned fiber tracts was particularly close in the anteroinferior part of the SRF and the mid anteroinferior part of the Cingulum, which runs deep to the isthmus of the cingulate gyrus and posterior part of the parahippocampal gyrus. We also found SRF fibers to cross the deep segment of the POS and share common terminations in the PPA area. We found the anteroinferior fibers of the SRF to reside medial and posterior to the fibers of the Cingulum. Fibers of the SRF exhibited a postero-supero-medial to antero-infero-lateral direction while the fibers of the Cingulum exhibited an antero-supero-medial to postero-infero-lateral direction. (Fig. 3.5).

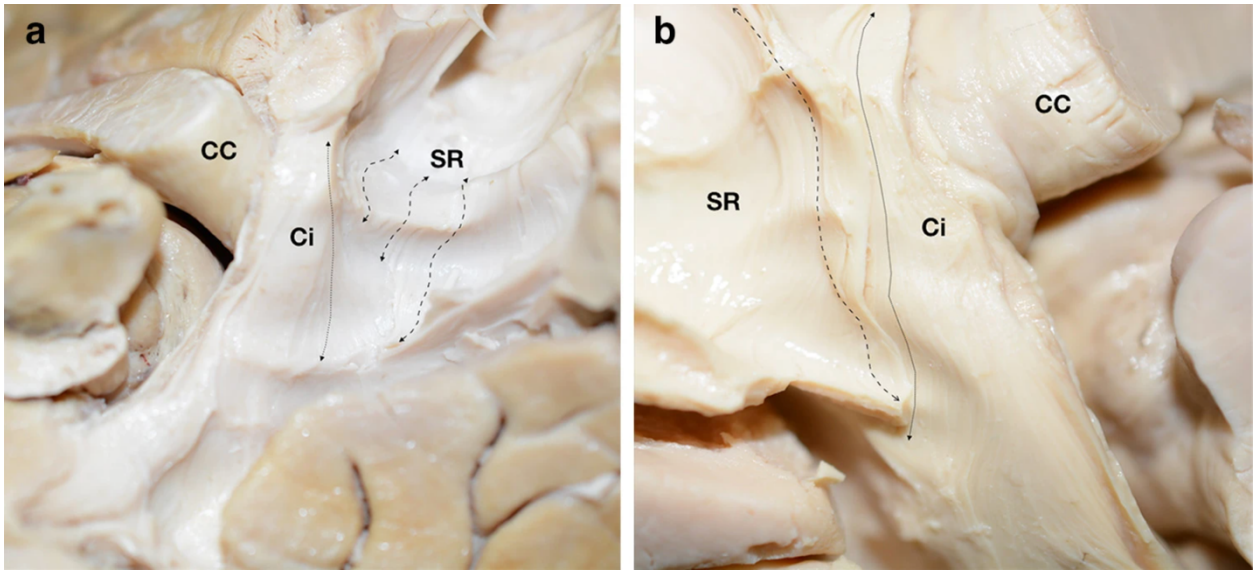


**Figure 3.5** Photos of a right (a) and left (b) cerebral hemisphere zooming in the correlative topography of the SRF with regard to the fibers of the cingulum. In both figures, the anatomical vicinity between the most anteriorly descending fibers of the SRF and the fibers of the inferior arm of the cingulum is illustrated. The different trajectories of the aforementioned fibers are marked with arrows. Note that the SRF travels in a postero-supero-medial to antero-infero-lateral direction while the fibers of the cingulum take an antero-supero-medial to postero-infero-lateral course. CC corpus callosum, Ci cingulum, SR Sledge runner fasciculus. Reprinted from Koutsarnakis et al[86] by permission of Springer Nature [6]

Stratum calcarinum

We consistently identified the stratum calcarinum deep to the plane of the calcarine fissure. We found this distinct group of vertically oriented fibers between the superior and inferior banks of the calcarine fissure interconnecting the superior and inferior lips of the calcarine cortex. We found the stratum calcarinum posterior to the SRF. In 12/20 of the studied specimens (60%) we found the stratum calcarinum delineated from the SRF (Fig. 3 SRF results). In the remaining 8/20 of hemispheres (40%) we found the fibers of the stratum calcarinum to blend with the fibers of the SRF anteriorly in a "kissing pattern" fiber distribution. However, the Stratum calcarinum displayed a vertical trajectory whereas the SRF displayed an oblique trajectory (Figure 3.6).

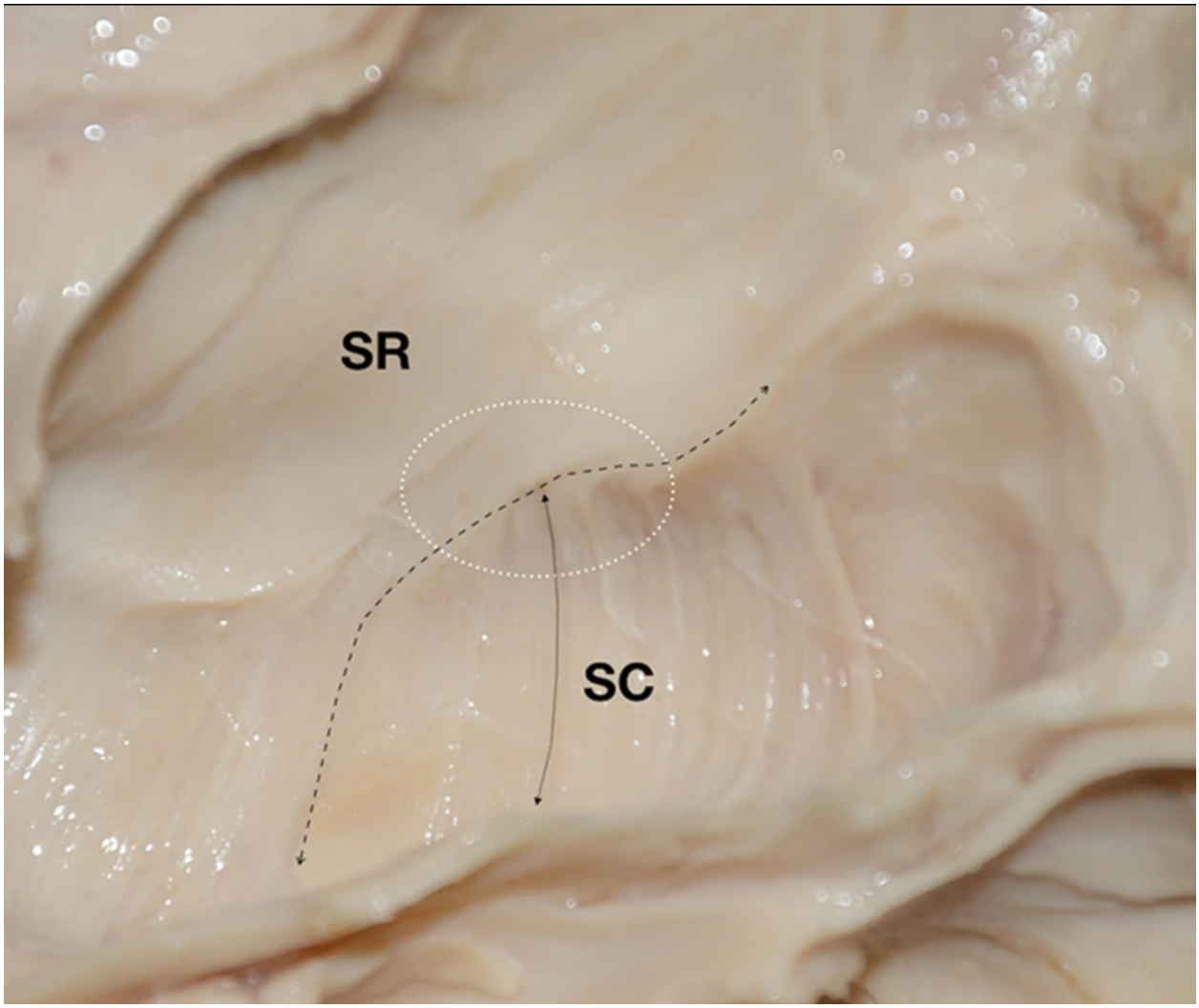


**Figure 3.6** High magnification of the regional anatomy of a right hemisphere at the level of the SRF and SC fasciculi i.e. just under the U fibers of the medial surface of the occipital lobe. Note the tight anatomical relationship between the fibers of the SR and SC illustrated with the white circle. Continuous and dashed arrows delineate the trajectory of the SR and SC respectively. SC stratum calcarinum, SRF sledge runner fasciculus. Reprinted from Koutsarnakis et al[86] by permission of Springer Nature [6]

Forceps Major

Advancing our microdissections, we encountered fibers of the forceps major, travelling from the splenium of the corpus callosum to the atrium and occipital horn (Figure 3.7). We identified and recorder the superior part of the SRF medial to the forceps major. In terms of their trajectory, we observed that the fibers of the SRF vertical in relation to the trajectory of the fibers of the forceps major.

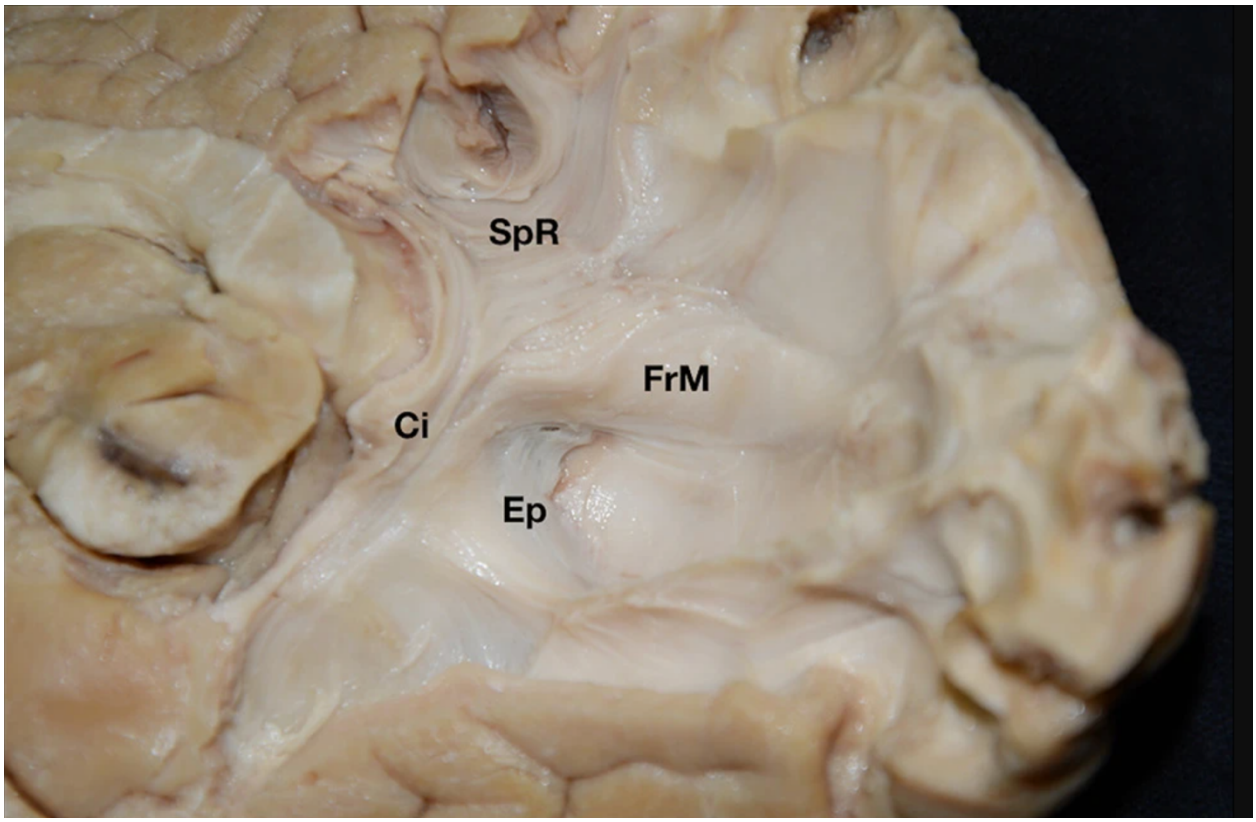


**Figure 3.7.** Oblique view of a right hemisphere. Gradual white matter dissection exposes the fibers of the major forceps and the ventricular ependyma of the medial wall of the atrium. *Ci* cingulum, *Ep* ependyma, *FrM* forceps major, *SpR* splenial radiations Reprinted from Koutsarnakis et al[86] by permission of Springer Nature [6]

### 3.3 The dorsal component of the Superior Longitudinal Fasciculus (SLF-I)

*Microanatomic Dissection*

We performed stepwise dissections, starting from the area of the anterior cingulate sulcus and moving posteriorly towards the marginal ramus. After removing the cortical grey matter, the U-fibers of the medial aspect of the hemisphere become apparent. (Fig 3.8B, Fig3.9B) These U-fibers interconnect adjacent gyri and represent the most superficial layer of the white matter encountered. At this point, we placed special attention to the proper and careful dissection of the U-fibers that radiate from the area of the anterior part of the cingulum and curve under the cingulate sulcus towards the area of the paracingulate or medial frontal gyrus. In 20% (3/15) of the studied specimens where the paracingulate sulcus was not evident, removing these U fibers revealed a longitudinal group of axons running deep to the plane of the cingulate sulcus and dorsal to the superior arm of the cingulum. These fibers correspond to the anterior part of the SLF-I. In the remaining twelve hemispheres (80%), this tract was found just under the superficial U-fibers of the paracingulate area, with the paracingulate sulcus and gyrus actually demarcating the silhouette of the anterior part of the SLF-I. (Figure3.8C.) Therefore, in all specimens studied, the anterior part of the SLF-I was recorded to lie in a slight supracingulate plane within the white matter of the cingulate or paracingulate gyrus. Attention should be placed on the fact that because the axons of the SLF-I and the overlying U-fibers that radiate from the cingulum, run in overlapping but perpendicular directions, it is easy to remove the fibers of the SLF-I along with the u-fibers of the cingulum. This is, allegedly, the main pitfall for not preserving the SLF-I fibers during standard medial to lateral dissections. In addition, while removing the U fibers that run superior to the plane of the SLF- I, it is important to recognize and preserve the regional cortical terminations. To this end, we observed the anterior portion of the SLF-I to receive a number of fibers originating from the anterior cingulate cortex (BA32), the medial part of the superior frontal gyrus (BA8 and 9), the pre-SMA, SMA proper (BA6) and paracentral lobule (BA1,2,3,4) (Figure 3.10). These fibers converge in an almost perpendicular manner to the SLF-I and form a number of knots that, in our sample, varied from 2 to 4.

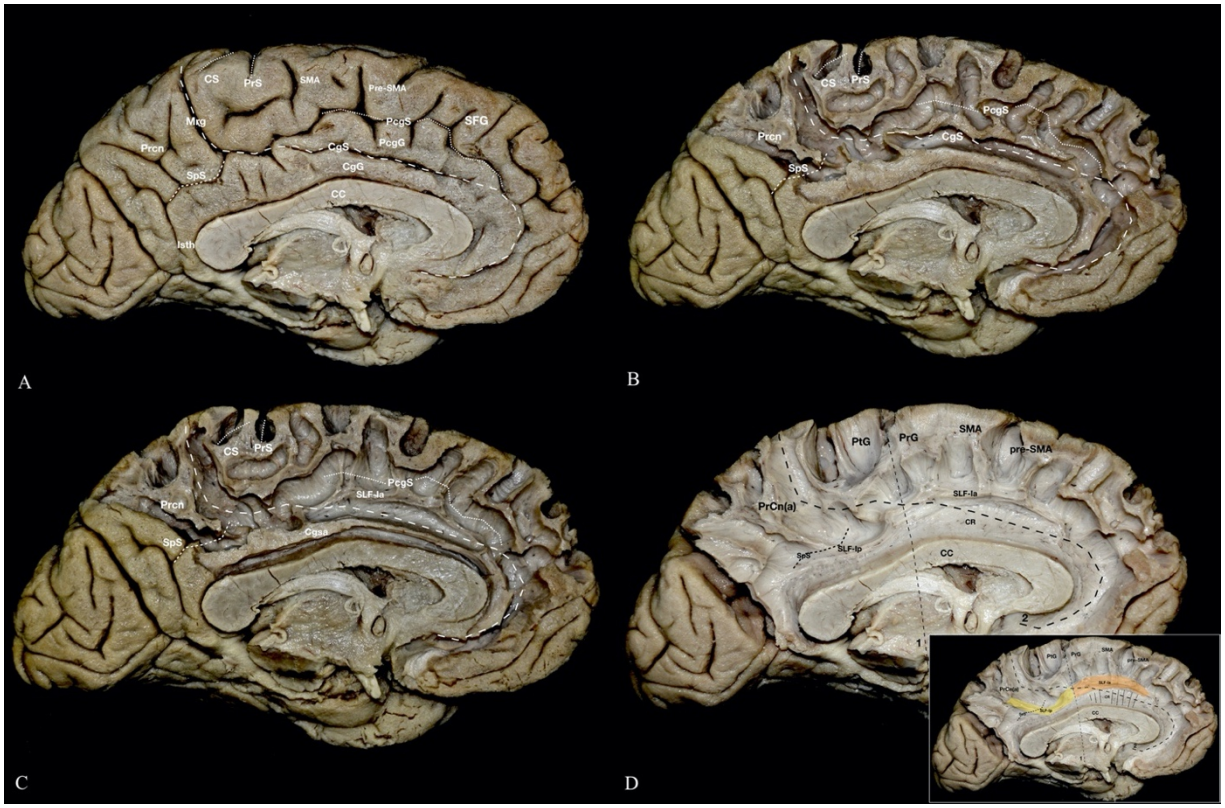


**Figure 3.8.** Progressive dissection of a left hemisphere illustrating the structural architecture of the SLF-I. (A): The medial surface anatomy is depicted. Note the presence of the paracingulate gyrus and sulcus. (B): the superficial U-fibers are shown after removing the grey matter. The silhouette of the main sulci is marked for better orientation (C): The superficial U-fibers at the area of the paracingulate gyrus are removed revealing a group of longitudinal axons that correspond to the anterior segment of the SLF-I. These fibers lie dorsal to the level of the cingulate sulcus. The superior arm of the cingulum is seen to run parallel to these fibers and inferior to the level of the cingulate sulcus. (D): Progressive dissection reveals the silhouette and terminations of the SLF-I. The two segments of the SLF-I are illustrated with the point of their transition to lie approximately at the level of the anterior paracentral lobule. The anterior segment (SLF-Ia) gives axons to the anterior cingulate cortex, pre-SMA, SMA proper and precentral gyrus while the posterior segment (SLF-Ip) terminates to the postcentral gyrus and precuneus (especially its anterior part). The SLF-Ip crosses the depth of the subparietal sulcus before arching towards the precuneus. (Inset): The SLF is highlighted using orange and yellow color for the anterior and posterior segment respectively. 1= Imaginary line bisecting the paracentral lobule, 2= Cingulate Sulcus, CC= Corpus Callosum, CgG= Cingulate Gyrus, Cgs= Cingulate Sulcus, Cgsa= Cingulum Superior Arm, CR= Callosal Radiations, CS= Central Sulcus, Mrg= Marginal ramus of the cingulate sulcus, PcgG= Paracingulate gyrus, PcgS= Paracingulate sulcus, Prcn= Precuneus, PrCn(a)= Anterior Precuneus, Pre-SMA= Pre-Supplementary Motor Area, PrG= Precentral Gyrus, PrS= Precentral Sulcus, PtG= Postcentral Gyrus, SFG= Superior Frontal Gyrus, SLF-Ia= Superior Longitudinal Fasciculus I – anterior segment, SLF-Ip= Superior Longitudinal Fasciculus I – posterior segment, SMA= Supplementary Motor Area, SpS= Subparietal sulcus.

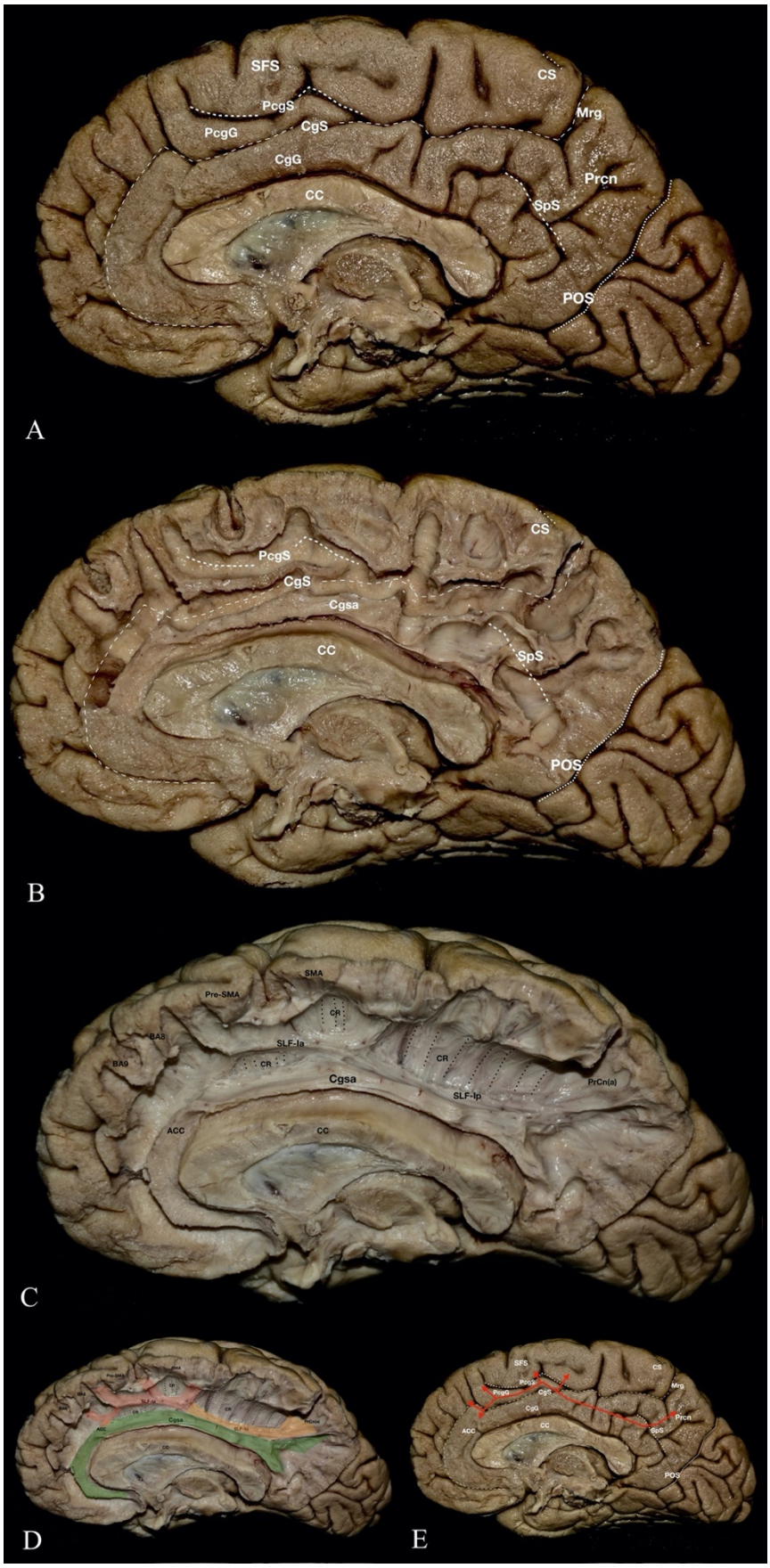


**Fig. 3.9** Progressive dissection of a right cerebral hemisphere, illustrating the SLF-I and its correlative anatomy to the superior arm of the cingulum. (A): The surface anatomy of the medial cerebral aspect is depicted (B): Grey matter is removed revealing the superficial U-fibers of the medial surface. The silhouette of the main sulci is marked for proper orientation. (C): Dissecting the u-fibers reveals the SLF-I and cingulum, running parallel to each other anteriorly and in a tangential line posteriorly. The fibers of the posterior segment of the SLF-I travel in a lateral and superior trajectory to those of the superior arm of the cingulum and terminate in the area of the anterior precuneus. (D): In order to illustrate the correlative anatomy, the cingulum is highlighted in green color, the anterior segment of the SLF-I in red and the posterior segment of the SLF-I in orange. (E): Trajectory and terminations of the SLF-I superimposed to the superficial anatomy. ACC= Anterior Cingulate Cortex, BA= Brodmann Area, CC= Corpus Callosum, CgG= Cingulate Gyrus, Cgs= Cingulate Sulcus, Cgsa= Cingulum Superior Arm, CR= Callosal Radiations, CS= Central Sulcus, Mrg= Marginal ramus of the cingulate sulcus, PcgG= Paracingulate gyrus, PcgS= Paracingulate sulcus, POS= Parieto-occipital sulcus, Prcn= Precuneus, PrCn(a)= Anterior Precuneus, Pre- SMA= Pre-Supplementary Motor Area, SFG= Superior Frontal Gyrus, SLF-Ia= Superior Longitudinal Fasciculus I – anterior segment, SLF- Ip= Superior Longitudinal Fasciculus I – posterior segment, SMA= Supplementary Motor Area, SpS= Subparietal sulcus.

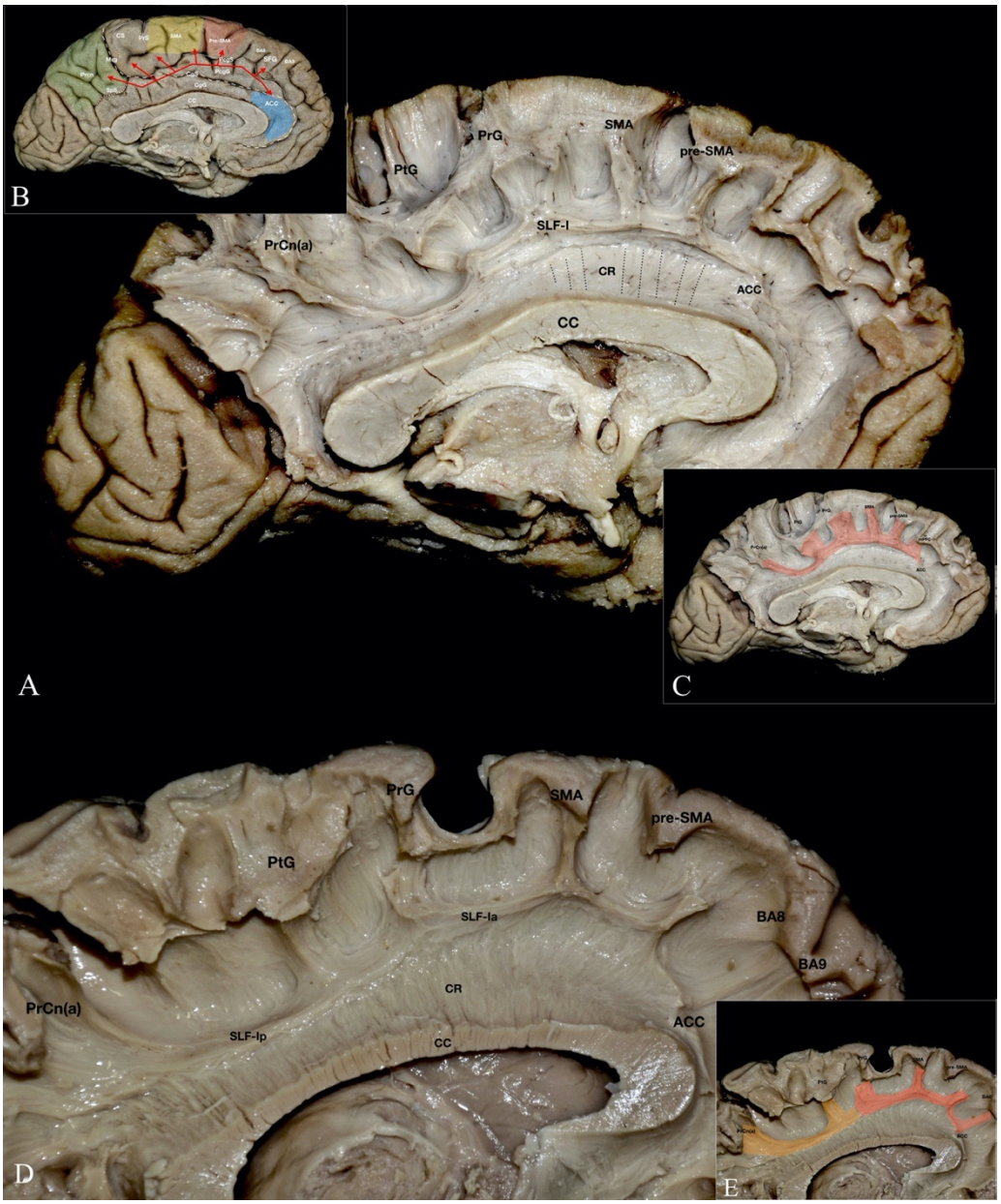


**Figure3.10.** Morphology, connectivity and termination pattern of the SLF-I. (A): Left hemisphere. The SLF-I is seen running from the level of dorsomedial frontal gyrus towards the precuneus. Along its course, 6 knots corresponding to 6 sets of terminating fibers can be noticed. Three groups of terminating fibers curve towards the superior frontal gyrus, at the territory of the medial prefrontal cortex, the dorsal premotor cortex, SMA and pre-SMA, two groups of fibers terminate towards the superior and medial aspect of the central lobe, while the basic posterior termination of the SLF-I consists of fibers curving towards the precuneus. Anteriorly the stem of the SLF-I terminates in the area of the anterior cingulate cortex. (B): The trajectory of the SLF-I superimposed on the superficial anatomy of the medial aspect is delineated. The areas corresponding to the anterior cingulate cortex, pre-SMA, SMA proper and precuneus are highlighted in blue, red, yellow and green respectively. (C): The SLF-I with and its terminations are highlighted in red color. (D): A left cerebral hemisphere at the final step of the dissection process. The S-shaped morphology of the SLF-I is illustrated. The anterior segment terminates in the territory of the anterior cingulate cortex, medial frontal gyrus (BA 8 and 9) the pre-SMA, SMA proper and Precentral Gyrus. The posterior segment terminates in the area of the postcentral gyrus and the anterior precuneus. The radiating callosal fibers can be seen running deep to the level of the SLF-I. (E): The anterior and posterior segments of the SLF-I along with terminations are highlighted in red and orange color respectively. ACC= Anterior Cingulate Cortex, BA= Brodmann Area, CC= Corpus Callosum, CR= Corona Radiata, PrCn(a)= Anterior Precuneus, Pre-SMA= Pre-Supplementary Motor Area, PrG= Precentral Gyrus, PtG= Postcentral Gyrus, SLF-I= Superior Longitudinal Fasciculus I, SLF-Ia= Superior Longitudinal Fasciculus I – anterior segment, SLF-Ip= Superior Longitudinal Fasciculus I – posterior segment, SMA= Supplementary Motor Area

During the next dissection stage, we removed the remaining U fibers of the posterior part of the medial aspect of each hemisphere up until the marginal ramus of the cingulate sulcus. At the level of the anterior paracentral lobule, the fibers of the SLF-I were consistently recorded to course in an almost tangential line to the cingulum (Figure3.8D), following a slight dorsal and lateral trajectory. Due to this tight anatomical proximity, it becomes unclear whether fibers of the SLF-I intermingle with the cingulum (Figure 3.9C). Following the SLF fibers posteriorly, we identified their cortical termination at the area of the anterior precuneus.

*Morphology and Connectivity of the SLF I*

In our sample, the SLF-I had a mean length of 107mm (range 100-115mm) and was invariably recorded to travel just under the U fibers of the paracingulate or cingulate gyrus, exhibiting an "S-shaped" configuration with two prominent bends: an anterior bend facing upwards and a posterior one facing downwards. These curves represent two distinct segments of the SLF-I: an anterior segment (SLF-Ia) and a posterior segment (SLF-Ip), with the point of their transition lying approximately at the level of the anterior paracentral lobule (Figure 3.8D, Figure 3.10B).

The anterior segment of the SLF-I was always seen to course within the paracingulate gyrus, when this gyrus is present, or within the anterior part of the cingulate gyrus and deep to the cingulate sulcus in any other instance. The mean length of this segment was 45mm (range 43-47mm), while its mean distance from the superior arm of the cingulum was 6mm (range 5-8mm). The SLF-Ia is characterized by the presence of 2-4 knots that represent the fibers terminating at the area of the, medial part of the superior frontal gyrus (BA8 and 9) pre-SMA and SMA proper (medial aspect of BA6), precentral (BA 4) and post-central(BA1,2,3) area.(Fig 3.10) The terminations to the pre-SMA and SMA proper area were invariably present (100% of the studied hemispheres). The terminations towards the medial paracentral lobule (1-2 groups of fibers) where evident in 8 out 15(53%) of the hemispheres. In 4 out of 15 hemispheres (27%) the SLF-Ia terminated towards the medial aspect of BA8(Frontal Eye Fields) and BA9(Medial Prefrontal Cortex) (Fig3.10). Finally, in 6 out of 15

hemispheres (40%) the stem of the SLF-I terminated in the area of the anterior cingulate cortex (BA 32) (Fig3.9C, Fig3.9D, Fig3.10).

The fibers of the posterior segment of the SLF-I in turn were always found to lie within the cingulate gyrus, travelling tangentially to the superior arm of the cingulum – thus exhibiting a paracingulate trajectory- before crossing the plane of the subparietal sulcus to arch towards and consistently terminate at the superior parietal lobule and mainly the anterior part of the precuneus (BA5 and 7) (Fig3.8D, Fig3.9C, Fig3.10). The mean length of SLF-Ip was 57mm (range 55-60mm).

*Subcortical correlative anatomy of the SLF-I*

SLF-I and Cingulum.

During the microanatomic dissections, we identified the SLF-I and the superior arm of the cingulum as two almost parallel, longitudinal fiber tracts that exhibit a distinct boundary up to the level of the anterior paracentral lobule. In this area, the SLF-I dives towards the cingulum, coursing in a tight and seemingly indiscrete anatomical trajectory to it, before bending again upwards to terminate to the precuneus. Aiming to define whether a cleavage plane between these white matter pathways in the region of the anterior paracentral lobule exists, we attempted to dissect apart the fibers of the cingulum from those of the SLF-I, focusing on the preservation of their anatomical integrity. Indeed, and despite their proximity, we were able to distinguish a clear dissection plane between these two tracts in all studied specimens proving that they are discrete anatomical entities (Fig 3.11).

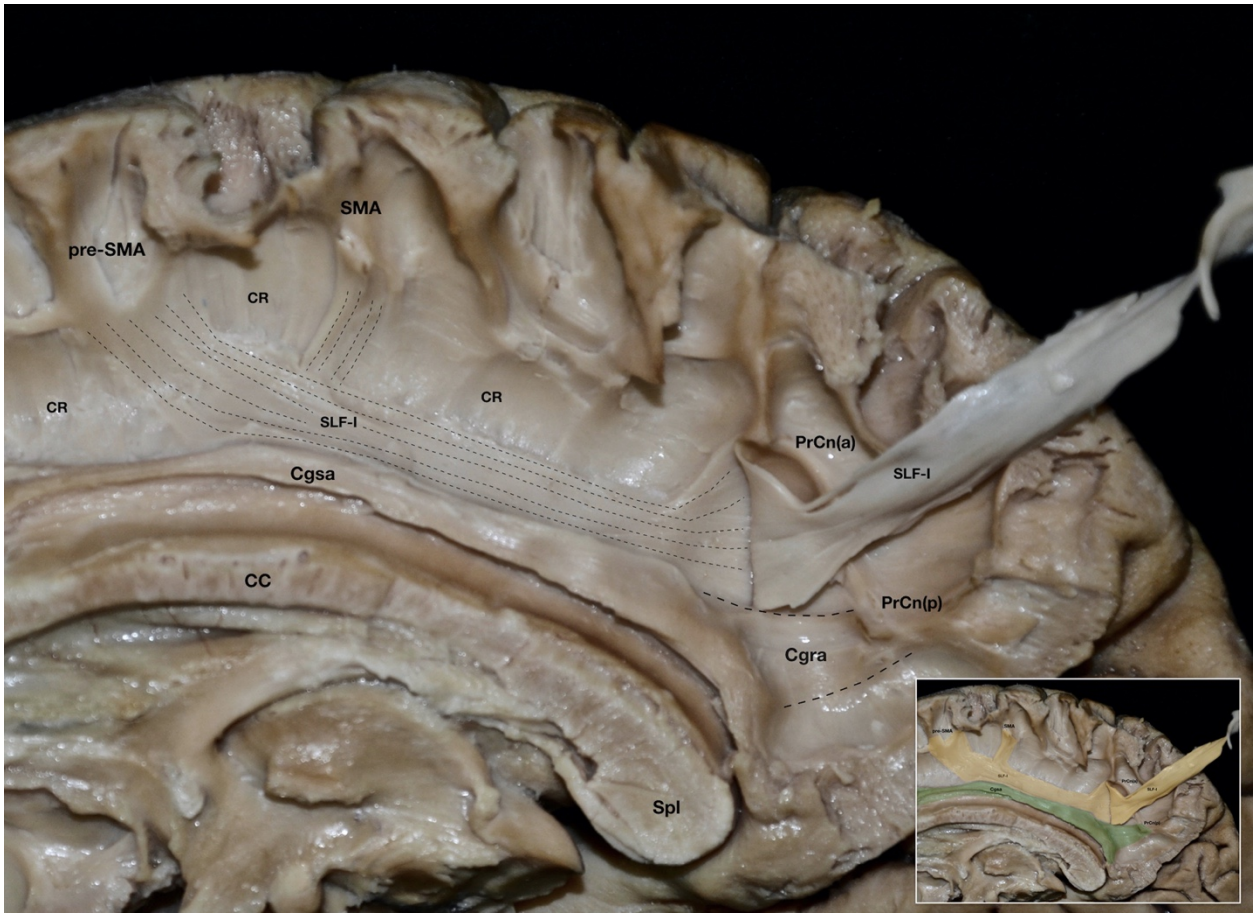


**Figure 3.11**. Medial view of a right cerebral hemisphere illustrating the superior arm of the cingulum and SLF-I. The fibers of the SLF-I are followed posteriorly along their course I.e. from the SMA towards the precuneus. In this way, the different trajectories of these discrete fiber pathways can be appreciated. The fibers of the SLF-I can be adequately removed under the microscope without interrupting the integrity of the superior arm of the cingulum at any point during its course. (inset): The SLF-I and superior arm of the cingulum highlighted in yellow and green respectively. Cgra= Radiations of the cingulum towards the precuneus, Cgsa= Superior arm of the cingulum, CR= Callosal Radiations, PrCn(a)= Anterior Precuneus, PrCn(p)= Posterior Precuneus, SLF-I= Superior Longitudinal Fasciculus I, SMA= Supplementary Motor Area.

## Relationship between the SLF-I and SLF-II.

In order to investigate the anatomical relationship between the SLF-I and SLF-II and given that the SLF-II lies in the white matter of the lateral aspect of the cerebral hemisphere, we further shifted our direction of dissection on the lateral cerebral aspect in three (3) hemispheres. After removing the gray matter and U fibers of the frontal lobe up to the level of the precentral sulcus, we encountered the axons of the SLF-II coursing superficial to the Corona Radiata (CR), at the level of the Middle Frontal Gyrus (M2). Focusing our dissection

on the white matter intervening between these two tracts, we revealed a 4-6mm layer of fibers coursing in a vertical trajectory and stemming from the Callosal Radiations and Corona Radiata. (Figure 3.12) These fibers were consistently recorded to run in a perpendicular direction to the fibers of the SLF II and SLF I without intermingling with them at any point. Therefore, our results support the argument that the SLF-I and SLF-II are two long association fibers tracts that run parallel to each other without maintaining any anatomical connection and should be deemed as discrete anatomical entities.

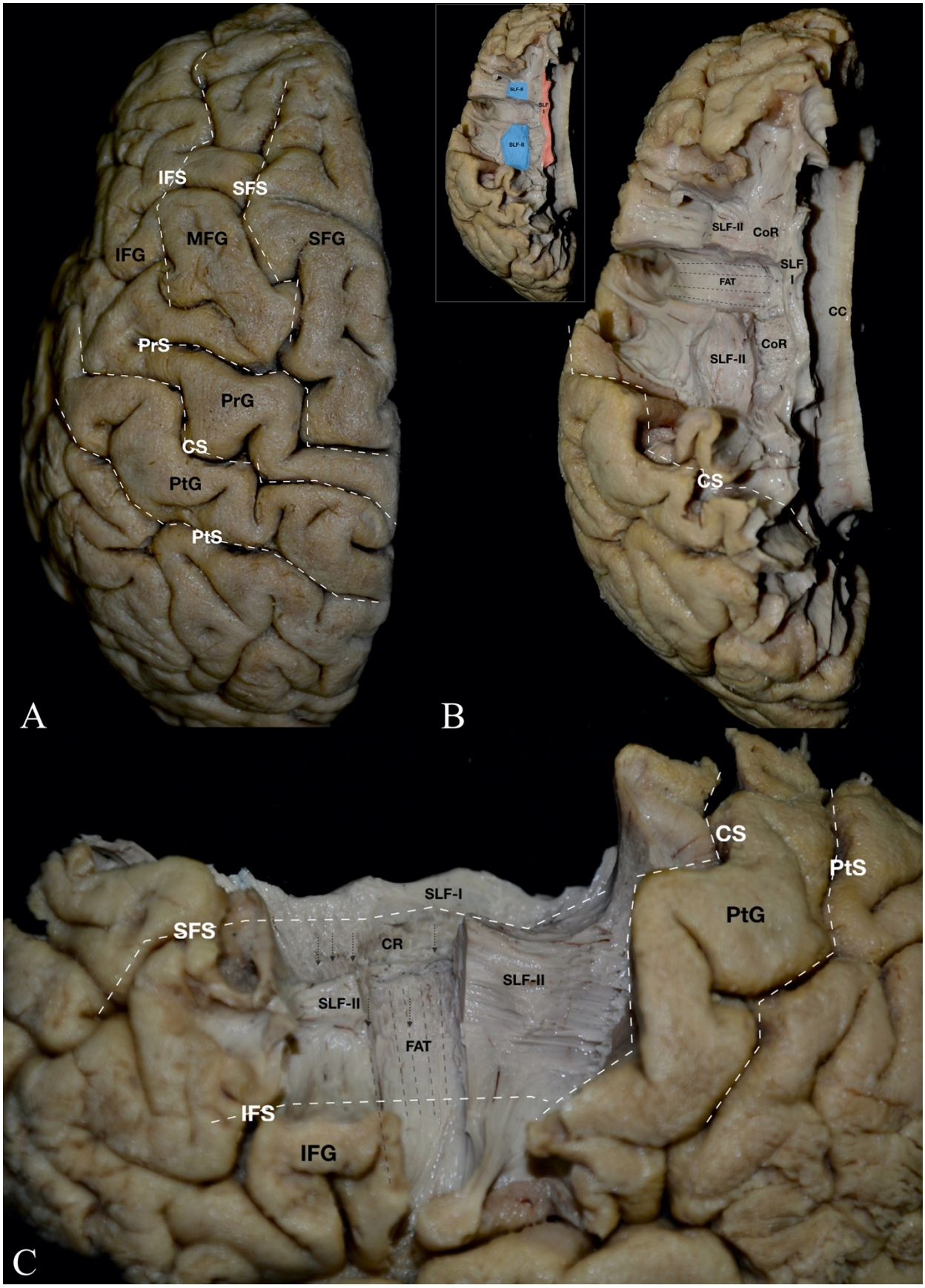
IFS
SFS
MFG
SFG
IFG
PrS
PrG
CS
PtG
PtS
A
SLF-II
SLF I
SLF-II
CoR
SLF I
FAT
CC
CoR
SLF-II
CS
B
CS
PtS
PtG
SLF-I
SFS
CR
SLF-II
SLF-II
FAT
IFS
IFG
C

**Figure 3.12**. Superior and lateral views of a left hemisphere showing the relationship between the SLF-I and the SLF-II. (A): Superior view illustrating the surface anatomy. (B): Same hemisphere after a standard medio-lateral dissection which was further extended on the lateral cerebral surface by removing the u-fibers of the superior, middle and inferior frontal gyri. The SLF-I and SLF-II are demonstrated. Progressive meticulous dissection reveals the fibers of the Frontal Aslant Tract, travelling from the SMA to the inferior frontal gyrus, along with the projecting fibers of the corona radiata, both of which are seen to intervene between the SLF-I and SLF-II. (inset): The SLF-I and SLF-II in red and blue color respectively. (C): lateral view of the correlative anatomy in the same hemisphere. CC= Corpus Callosum, CoR= Corona Radiata, CS= Central Sulcus, FAT= Frontal Aslant Tract, IFG= Inferior Frontal Gyrus, IFS= Inferior Frontal Sulcus, MFG= Middle Frontal Gyrus, PrG= Precentral Gyrus, PrS= Precentral Sulcus, PtG= Postcentral Gyrus, PtS= Postcentral Sulcus, SFG= Superior Frontal Gyrus, SFS= Superior Frontal Sulcus, SLF-I= Superior Longitudinal Fasciculus I, SLF-II= Superior Longitudinal Fasciculus II

## Relationship between the SLF I and SLF III.

In two specimens, we employed the same procedure as above but further focused our dissections on the inferior frontal and supramarginal gyri, in order to demonstrate the relationship between the SLF-I and SLF-III. We additionally removed the middle and superior frontal gyri to illustrate the regional correlative anatomy. (Figure 3.13) Again, a 14-17mm vertical layer of fibers stemming from the Corona Radiata -just above its transition area to the internal capsule - and the Callosal Radiations was observed to separate the two subcomponents of the SLF system. Neither the SLF-I nor the SLF-III mix or intermingle with these fibers at any point during their course. As previously seen with regard to the SLF-II, the SLF-I and SLF-III run in parallel directions and do not exhibit any direct anatomical connection, therefore constituting two discrete anatomical entities.


**Figure 3.13.** Superior and medial views of a dissected left hemisphere depicting the relationship between the SLF-I and the SLF-III. (Left): Superior view of a left hemisphere after a standard medial to lateral dissection process, which we further extended over the lateral aspect of the central lobe, parietal lobe and part of the central core. The areas of the rolandic operculum and frontoparietal operculum were dissected in order to reveal the ventral component of the SLF, namely the SLF-III. Progressive dissection of the fibers of the corona radiata up to the central core allowed a clear view of the anatomical relationship between the SLF-I and SLF-III. This white matter layer of Corona Radiata fibers clearly separates the two components of the Superior Longitudinal Fasciculus. (inset): Fiber tracts highlighted in different colors: Superior arm of the cingulum (green color), SLF-I (red color), Corona Radiata (blue color), SLF-III (yellow color). (Right): Medial view of the same hemisphere. CC= Corpus Callosum, CdN = Caudate Nucleus (body), Cgsa= Superior arm of the cingulum, CoR= Corona Radiata, CR= Callosal Radiations, Fpo= Frontoparietal Operculum, IntCps= Internal Capusle, SLF-I= Superior Longitudinal Fasciculus I, SLF- III= Superior Longitudinal Fasciculus III, Th= Thalamus

Material reused from Komaitis S et al.[84] by permission of JNS Publishing Group.

### 3.4 The Middle Longitudinal Fasciculus (MdLF)

*Microanatomic dissections*

Starting the dissection from the superior temporal sulcus (STS) and gyrus (STG), including the transverse gyri, we moved our plane posteriorly and superiorly towards the parieto-occipital area. Following the removal of cortical grey matter, the arcuate or U-fibers of the lateral aspect of the hemisphere are evident (Step 1) (Figure 3.14).

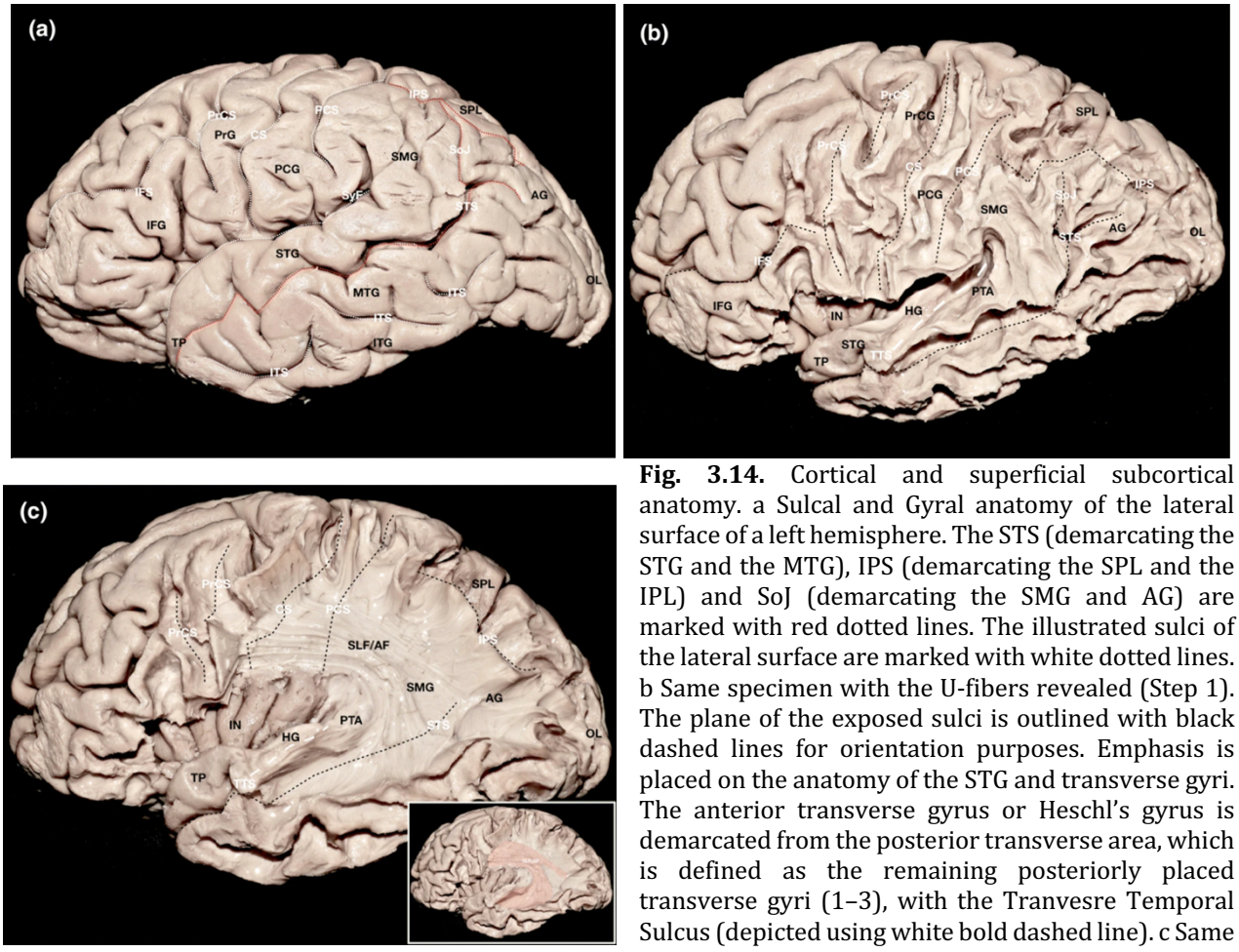


**Fig. 3.14.** Cortical and superficial subcortical anatomy. a Sulcal and Gyral anatomy of the lateral surface of a left hemisphere. The STS (demarcating the STG and the MTG), IPS (demarcating the SPL and the IPL) and SoJ (demarcating the SMG and AG) are marked with red dotted lines. The illustrated sulci of the lateral surface are marked with white dotted lines. b Same specimen with the U-fibers revealed (Step 1). The plane of the exposed sulci is outlined with black dashed lines for orientation purposes. Emphasis is placed on the anatomy of the STG and transverse gyri. The anterior transverse gyrus or Heschl's gyrus is demarcated from the posterior transverse area, which is defined as the remaining posteriorly placed transverse gyri (1–3), with the Tranvesre Temporal Sulcus (depicted using white bold dashed line). c Same specimen illustrating the SLF/AF complex (Step 2). The U-fibers of the inferior central lobe, IPL and TPO junction have been dissected and the SLF/AF complex, connecting the IFG, MFG and central lobe with the IPL and temporal lobe is illustrated. The inner fibers of the "C" shaped part of the SLF/AF complex terminating at the STG and STS should be removed with caution in order to preserve the underlying MdLF fibers. The Transverse Temporal Sulcus plane is depicted using a white bold dashed line, while the rest of the sulci with black dashed lines. Inset: the SLF/AF complex highlighted in red. AG angular gyrus, CS central sulcus, HG Heschl's gyrus, IFG inferior frontal gyrus, IFS inferior frontal sulcus, IN insula, IPS intraparietal sulcus, ITG inferior temporal gyrus, ITS inferior temporal sulcus, MTG middle temporal gyrus, OL occipital lobe, PCG postcentral gyrus, PCS postcentral sulcus, PrCS precentral sulcus, PrG precentral gyrus, PTA posterior transverse area, SLF/AF Superior Longitudinal Fasciculus/Arcuate Fasciculus Complex, SMG supramarginal gyrus, SoJ sulcus of jensen, SPL superior parietal lobule, STG superior temporal gyrus, STS superior temporal

sulcus, SyF sylvian fissure, TP temporal pole, TTS transverse temporal sulcus. Reprinted from Kalyvas et al[79] by permission of Springer Nature [3]

These fibers connect adjacent gyri and form the most superficial layer of white matter. Removing the U-fibers of the inferior central lobe, inferior parietal lobule (IPL) and temporo-parieto-occipital (TPO) junction, discloses the superior longitudinal fasciculus (SLF)/arcuate fasciculus (AF) complex, which essentially connects the IFG and middle frontal gyrus (MFG) with the IPL and temporal lobe (Step 2) (Figure 3.14). Dissecting the U-fibers of the STG and STS unveils a distinct group of fibers that originate from the temporal pole (TP) and anterior segment of the STS/STG and exhibit a horizontal trajectory, corresponding to the anterior part of the MdLF (Step 3) (Figure 3.15).

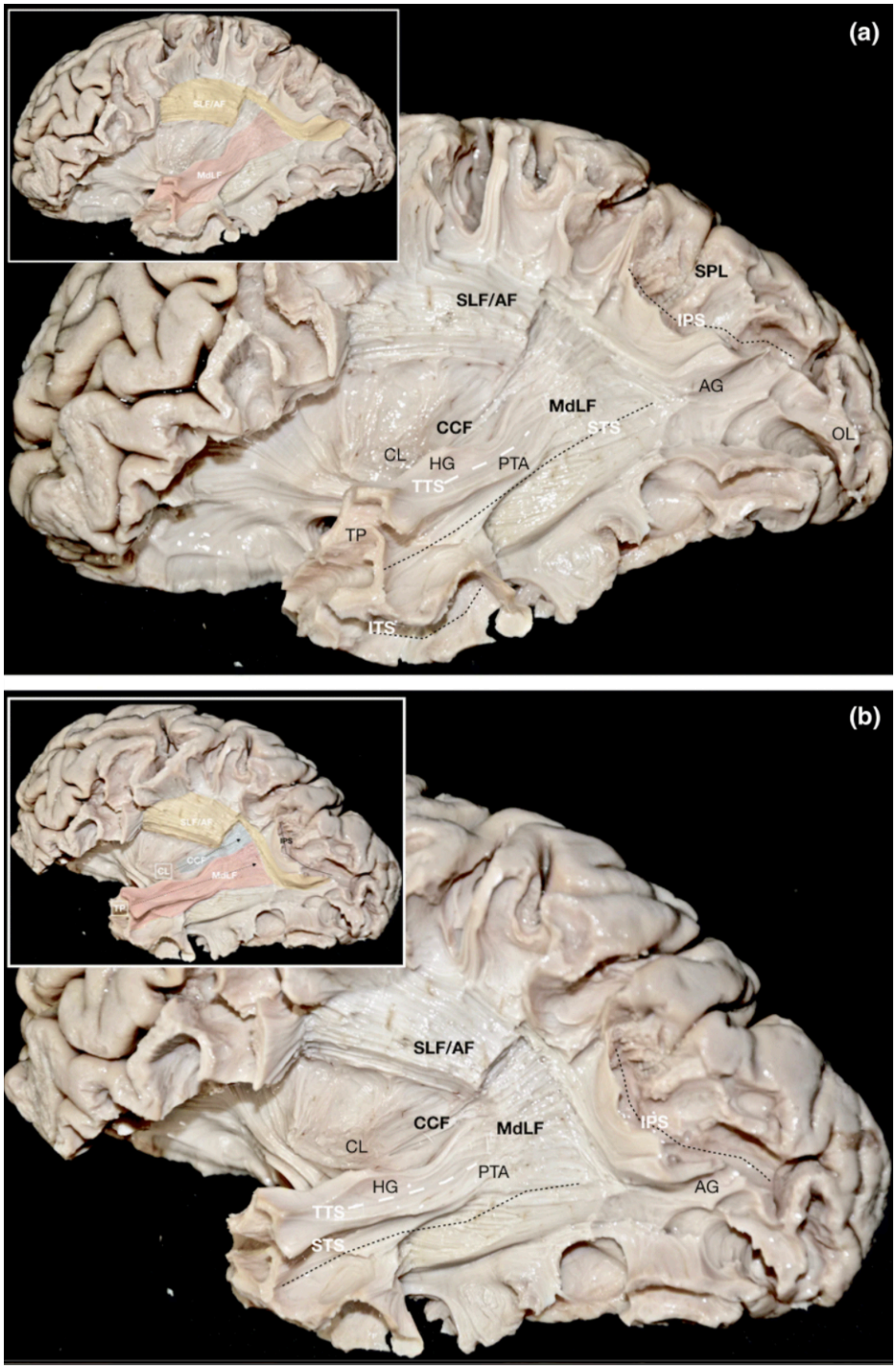


**Fig. 3.15.** Relationship between the MdLF and the IPL. Correlative anatomy with respect to the SLF and CCF (Step 3). a Same specimen as in Fig. 2. The temporal part of the MdLF is found under the fibers of the SLF/AF complex. The majority of the MdLF fibers were seen to enter the transverse gyri and course upwards and posteriorly, just medial to the SLF/AF complex. The U-fibers of the insula are dissected in order to expose the claustrum, delineate the claustrocortical fibers of the dorsal external capsule and distinguish them from the MdLF. The U-fibers of the IPS and TPO junction are preserved to illustrate the MdLF relationship with the IPL. Inset: the MdLF is highlighted in red and the remaining SLF/AF complex fibers in yellow. b Superolateral view of the same specimen. MdLF fibers and CCF fibers of the dorsal external capsule are illustrated. The MdLF lies postero-laterally with respect to the dorsal external capsule. The fibers of the MdLF can be tracked down to the TP; while those of dorsal external capsule are followed up to the claustrum. The MdLF passes deep to the IPS and continues towards the SPL and occipital lobe. The transverse temporal sulcus plane is depicted using white bold dashed line, while the rest of the exposed sulci using black dashed lines. Inset: The MdLF, SLF/AF complex and CCF are highlighted in red, yellow and blue, respectively. AG angular gyrus, CCF claustro-cortical fibers, CL claustrum, HG Heschl's gyrus, IPS intraparietal sulcus, ITS inferior temporal sulcus, MdLF middle longitudinal fasciculus, OL occipital lobe, PTA posterior transverse area, SLF/AF superior longitudinal fasciculus/arcuate fasciculus complex, SPL superior parietal lobule, STS superior temporal sulcus, TP temporal pole, TTS transverse temporal sulcus. Reprinted from Kalyvas et al[79] by permission of Springer Nature [3]

The majority of the MdLF fibers were found to enter the transverse gyri and course upwards and posteriorly, just under the SLF/AF complex. Removing the SLF/AF complex helps to identify and record the parietal course of the MdLF. In this step, the insula and the most anterior part of the inferior frontal gyrus (IFG) were also included in the dissection with the aim to reveal the dorsal external capsule, the UF and IFOF and to differentiate them from the MdLF. More specifically, the U-fibers of the insula are dissected away in order to delineate the claustrocortical fibers of the dorsal external capsule and to distinguish them from the MdLF. The U-fibers of the intraparietal sulcus (IPS) and TPO junction were preserved to determine whether MdLF fibers change trajectory and terminate at the AG and SMG or instead head towards the SPL and occipital lobe. Not unexpectedly, MdLF fibers can be readily identified and differentiated from the dorsal external capsule fibers. Although these tracts exhibit the same direction (antero-inferior to postero-superior), the MdLF lies postero-laterally with respect to the dorsal external capsule, while their anterior origin is completely different i.e. claustrum for the dorsal external capsule and STG for the MdLF. None of the MdLF fibers was seen to change trajectory and terminate to the angular gyrus (AG) and supramarginal gyrus (SMG). On the contrary, we found this part of the MdLF to pass deep to the IPL and to continue towards the SPL and occipital lobe. Interestingly, fibers stemming from the SLF were seen travelling through the IPS and finally terminating at the AG. Dissecting away the U-fibers of the IPS, reveals fibers of the MdLF reaching the postero-superior part of the SPL and the parieto-occipital arcus (POA) [3,118,157]. Removing the U-fibers of the TPO junction, unveils MdLF fibers continuing further posteriorly to enter the occipital lobe (Step 4) (Figure 3.16).

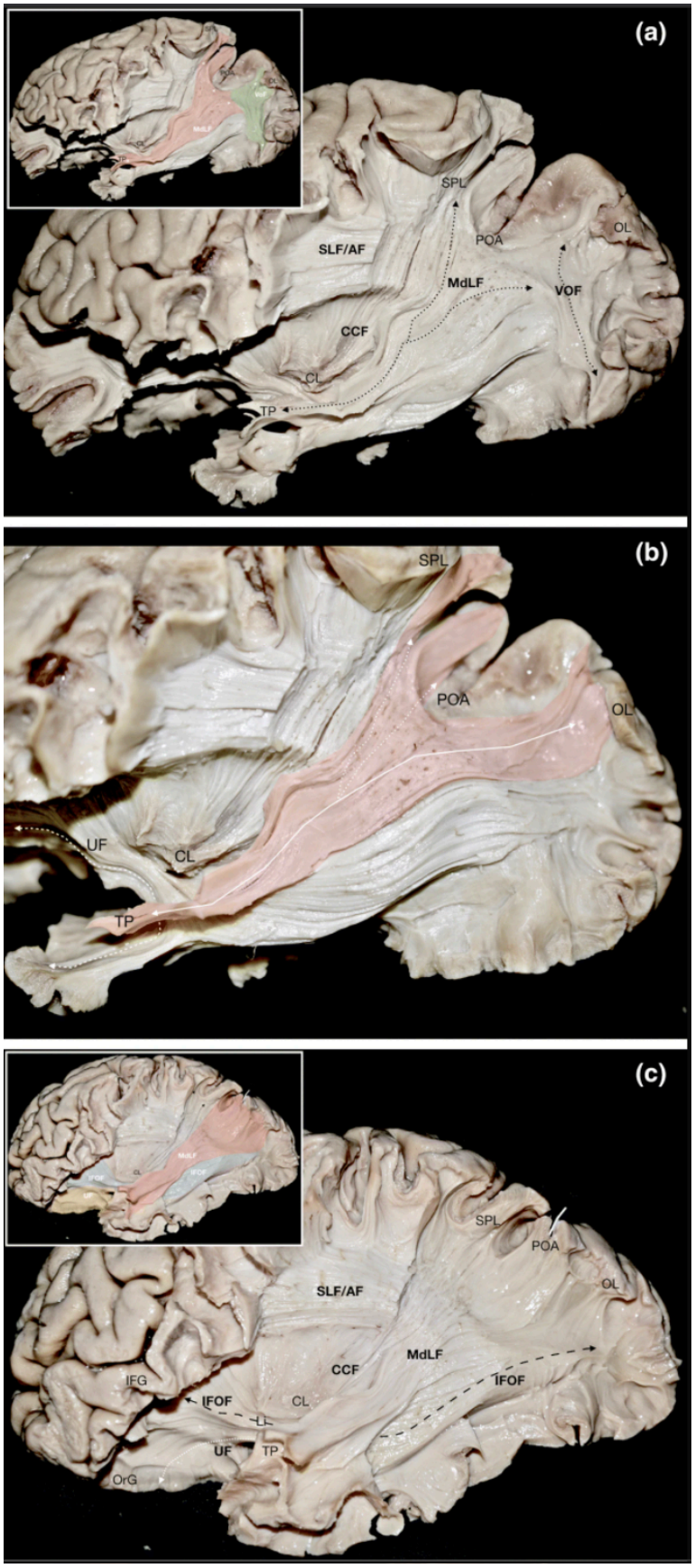


**Fig. 3.16** Illustration of the temporo-parietal and temporo-occipital connections of the MdLF. a Different specimen. Left lateral side. The MdLF temporo-parietal connection is delineated (Step 4) extending up to the postero-superior part of the SPL/PrC and the parieto-occipital area. Dissecting away the U-fibers of the TPO junction exposes fibers of the MdLF continuing posteriorly to enter the occipital lobe. The VOF, running under the U-fibers of the occipital lobe and exhibiting a vertical trajectory can be also identified. Inset: the MdLF is highlighted in red and the VOF in Green. The trajectories of the MdLF and VOF are outlined with black dotted arrows. b Same specimen as in (a). Following dissection of the VOF, the MdLF temporo-occipital connection reaching the posterior border of the occipital lobe/cuneus is illustrated (Step 5). The silhouette of the MdLF is highlighted in red. The temporo-occipital connection is indicated with the white arrow and the temporo-parietal connection with the white dotted arrows. The UF is outlined with white dashed arrowed line. The UF lies medially to the MdLF at the anterior temporal lobe and terminates more anteriorly and inferiorly in the temporal pole. c Same specimen as in Fig. 2. Relationship between the MdLF, IFOF and UF. The MdLF is seen to reach the anterior part of the STG and the TP. It is also clearly distinguished from the UF and IFOF, which travel in a deeper dissection plane as they form the ventral external capsule at the level of limen insula. The trajectory of the IFOF is demonstrated with the black dashed arrow as it courses ventromedial to the MdLF at the level of the temporal lobe and the sagittal stratum. The orbito-frontal part of the UF is depicted with the white dotted arrow. Inset: The MdLF, IFOF and UF are highlighted in red, blue and yellow, respectively. CCF claustro-cortical fibers, CL claustrum, IFG inferior frontal gyrus, IFOF inferior fronto-occipital fasciculus, Li limen insula, MdLF middle longitudinal fasciculus, OL occipital lobe, OrG orbital gyri, POA parieto-occipital arcus, SLF/AF superior longitudinal

fasciculus/arcuate fasciculus complex, SPL superior parietal lobule, TP temporal pole, UF uncinate fasciculus, VOF vertical occipital fasciculus. Reprinted from Kalyvas et al[79] by permission of Springer Nature [3]

In this dissection step we recorded a discrete group of fibers, which were seen to run under the U-fibers of the occipital lobe and exhibit a vertical trajectory, corresponding to the Vertical Occipital Fasciculus (VOF). After removing the VOF, the stem of the MdLF was observed to course vertically and medially, in relation to the VOF, and was seen to reach the posterior border of the occipital lobe (Step 5) (Figure 3.16) With regard to the anterior part of the MdLF, special attention was placed to the proper and careful dissection of the U-fibers of the anterior IFG and the anterior-most part of the temporal pole. Our aim was to disclose the UF, IFOF and ILF and to determine whether the most anterior part of the MdLF reaches the TP. Interestingly, the MdLF was consistently found to reach the anterior segment of the STG and the dorsal TP, while it was clearly demarcated and distinguished from the UF, IFOF and ILF. Following the complete exposure of the MdLF in the lateral cerebral aspect, we meticulously dissected, detached and retracted its fibers, starting from the TP and anterior STG, with the goal to record its connectivity and possibly identify a segmentation pattern (Step 6) (Figure 3.17).

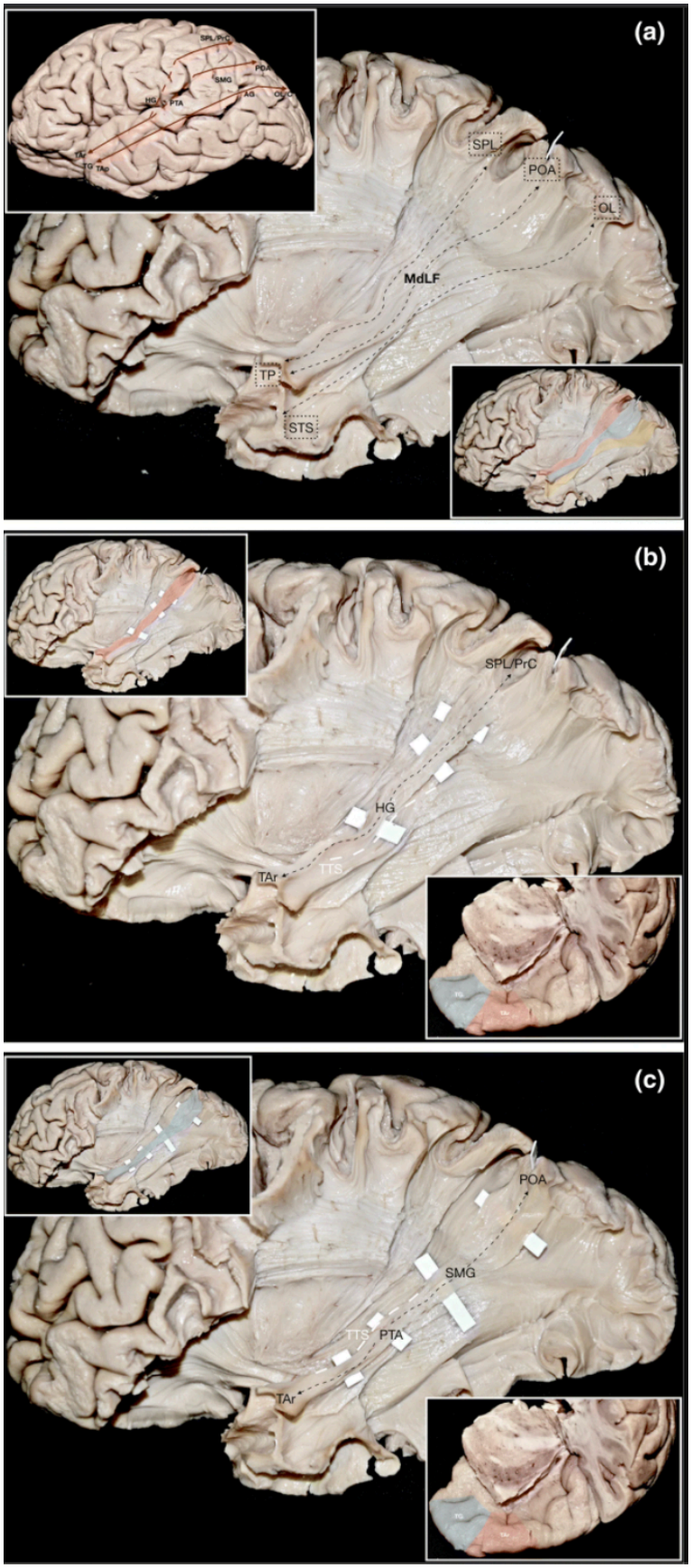


**Fig. 3.17** Connectivity and segmentation pattern (Step 6). a Left hemisphere—Same as in Fig. 2. The MdLF is consistently recorded to connect various segments of the TP and STG with the SPL/PrC, POA and occipital lobe/cuneus, by passing through the transverse gyri and the IPL (SMG and AG). The fibers originating at the dorsolateral TP were seen to travel through the transverse gyri to reach the SPL and the parieto-occipital arcus (MdLF-I and MdLF-II). The fibers originating at the anteriormost STS and TP, reach the occipital lobe/cuneus (MdLF-III) without travelling through the transverse gyri. Upper inset: Connectivity and terminations of the MdLF (red line and arrows) superimposed on the superficial anatomy, Lower inset: Trajectory and terminations of the three segments of the MdLF; MdLF-I, MdLF-II and MdLF-III highlighted in red, blue and yellow, respectively. b Same specimen, Hyper-Selective dissection of the fibers of the MdLF-I. MdLF fibers that originate from the dorsolateral TP, corresponding to the area TAr, enter the Heschls's Gyrus (anterior to the plane of Transverse Temporal Sulcus) and follow a superior trajectory to terminate at the supero-posterior part of the SPL/PrC. The trajectory and connectivity of MdLF is marked with the black dashed arrow. Upper inset: The MdLF-I highlighted in red. Lower inset: a superolateral view of the exposed dorsal TP and superior STG on a left hemisphere, after cutting though the temporal stem and disconnecting the frontal lobe. The TG and TAr areas are highlighted in blue and red, respectively. Note the axial cut on the central core. c Same specimen as above, Hyper-selective dissection of the MdLF-II. The MdLF-I has been carefully removed and the trajectory and connectivity of the MdLF-II is vividly illustrated. MdLF fibers originating from the dorsolateral TP, corresponding to the area TAr, are seen to travel through the posterior transverse area (posterior to the plane of transverse temporal sulcus) and to course obliquely in the depths of SMG, finally reaching the parieto-occipital arcus, i.e., the area folding around the

parieto-occipital sulcus. Upper inset: The MdLF-II highlighted in blue. Lower inset: The TG and TAr areas highlighted in blue and red, respectively. d Same specimen, Hyper-selective dissection of the MdLF-III. The MdLF-I and MdLF-II have been removed and the fibers of the MdLF-III are revealed. The MdLF-III consists of fibers originating at the most anterior part of the TP and STS, which correspond to the areas TG and TAp, respectively. These fibers travel in the depth of the STS, pass under the AG and reach the posterior border of the occipital lobe/cuneus. Upper inset: The MdLF-III highlighted in yellow. Lower inset: an antero-inferior view of the TP of the same left hemisphere highlighting the areas TG, TAr and TAp in blue, red and yellow, respectively. AG angular gyrus, C cuneus, HG Heschl's gyrus, MdLF middle longitudinal fasciculus, OL occipital lobe, POA parieto-occipital arcus, PrC precuneus, PTA posterior transverse area, SMG supramarginal gyrus, SPL superior parietal lobule, STS superior temporal sulcus, TP temporal pole, TTS transverse temporal sulcus. Reprinted from Kalyvas et al[79] by permission of Springer Nature [3]

Interestingly enough, the fibers originating at the dorsolateral TP were seen to travel through the transverse gyri to reach the SPL and the POA. More specifically, MdLF fibers entering the Heschl's gyrus, i.e. the first of the transverse temporal gyri in an anteroposterior direction, were documented to follow a superior trajectory and to terminate at the supero-posterior part of the SPL, while fibers travelling through the posterior transverse area, were found to course obliquely to reach the more medially and posteriorly placed POA. In addition, fibers originating at the most anterior part of the TP and STS were identified to travel ventrally in the depth of the STS, following a horizontal trajectory and fanning-out at the level of the posterior STS to reach through the AG the posterior border of the occipital lobe. In 70% of the studied hemispheres (14/20) the MdLF reached the superior third of the posterior border of the occipital lobe while in 30% we also observed termination fibers at the middle third. Following the posterior retraction of the 3 segments of the MdLF, the fibers of UF, IFOF and ILF can be identified (Step 7) (Figure 3.18).

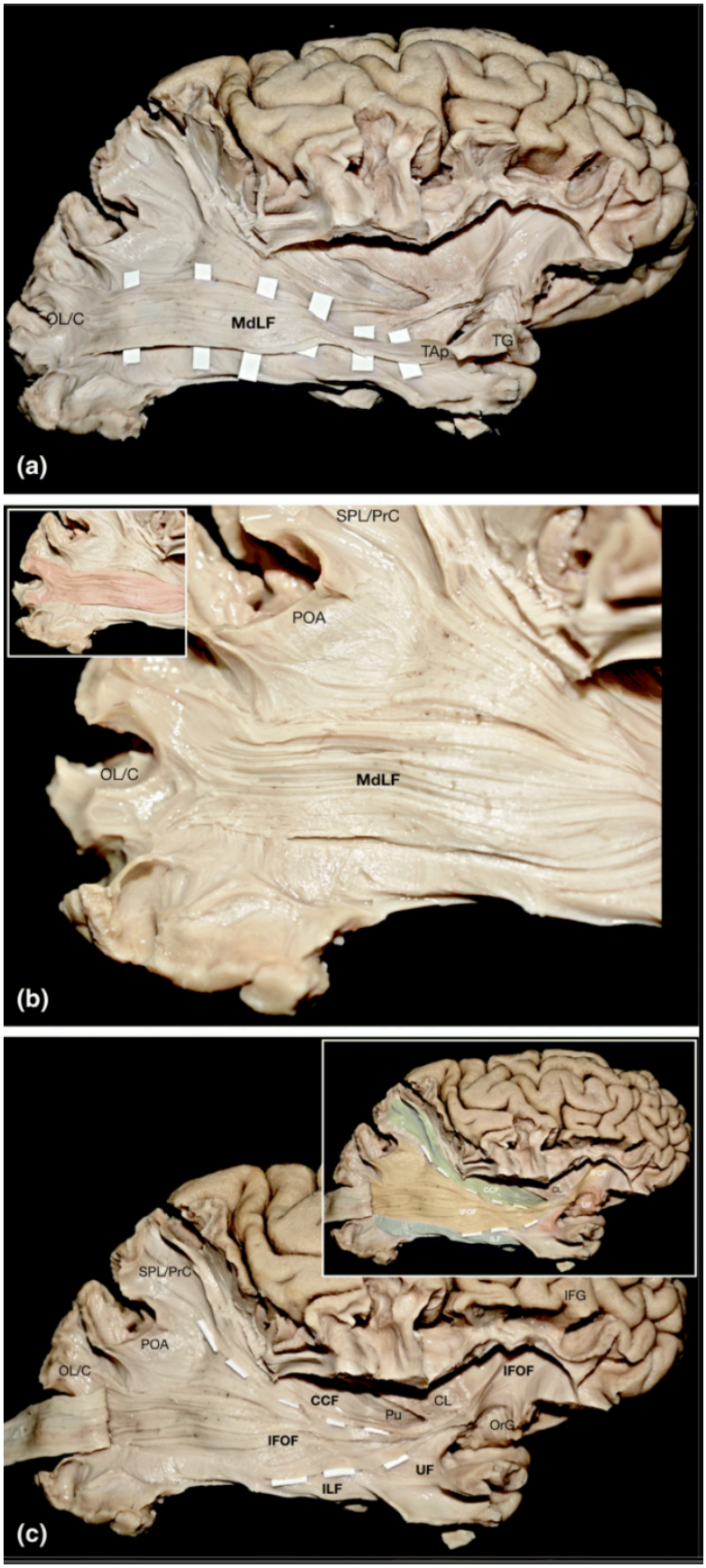


**Fig. 3.18.** MdLF Occipital terminations and relationship with deeper fiber tracts (Step 7). a Different specimen. Right lateral side. Hyper-selective dissection of the MdLF-III. b Focused view of the occipital area of the same specimen as in (a). Fibers of the MdLF-III are seen to terminate at the superior and middle third of the occipital lobe/cuneus. In 70% of the hemispheres studied (14/20), the MdLF was recorded to reach the superior third of the posterior border of the occipital lobe; while in the remaining 30%, termination fibers at the middle third were also detected. Inset: the MdLF-III highlighted in red. c Same specimen as in (a). Following the dissection and retraction of the MdLF-III (step 7) the fibers of UF, IFOF and ILF can be identified. The silhouette of the IFOF is depicted and demarcated from the CCF and UF with small white pads. The IFOF lies medial to the MdLF. The UF lies also medial to the MdLF at the anterior temporal lobe and terminates more anteriorly in the temporal pole as illustrated in the figure. In contrast to the MdLF, the fibers of the ILF are seen to originate from the ventral TP and to course in an inferior plane with respect to the MdLF, however sharing some cortical terminations. Inset: The MdLF, IFOF, UF, CCF and ILF highlighted in red, yellow, orange, green and blue, respectively. C cuneus, CCF claustro-cortical fibers, CL claustrum, IFG inferior frontal gyrus, IFOF inferior fronto-occipital fasciculus, ILF inferior longitudinal fasciculus, MdLF middle longitudinal fasciculus, OL occipital lobe, OrB orbital gyri, POA parieto-occipital arcus, PrC precuneus, Pu putamen, SPL superior parietal lobule, UF uncinate fasciculus. Reprinted from Kalyvas et al[79] by permission of Springer Nature [3]

*Trajectory and morphology of the MdLF*

The MdLF was invariably identified and recorded as a white matter bundle travelling under the U-fibers of the anterior STG/STS area and medial to both the U-fibers and the SLF/AF complex at the posterior temporal lobe and IPL. It was documented to connect the STG to the SPL and parieto-occipital area, by passing through the transverse gyri, and the STG to the posterior border of the occipital lobe through the AG. Regarding its configuration, the MdLF exhibits an anterior narrow part that progressively fans-out at the posterior temporal lobe to reach the different parietal and occipital areas (SPL/PrC, POA and the occipital lobe/cuneus). With respect to its trajectory, the MdLF was observed to follow an anterolateral to posteromedial direction, as it moves from a more superficial layer anteriorly (medial to the U fibers) to a deeper dissection plane posteriorly (medial to the SLF/AF and VOF complex). Interestingly, as the MdLF runs through the transverse gyri it demonstrates a characteristic "S-shaped" configuration with two slight curves; a lateral curve facing posteriorly and a medial curve facing anteriorly. The fibers that do not enter the transverse gyri exhibit a horizontal configuration with a slightly inferior and medial trajectory.

*Subcortical Correlative anatomy of the MdLF*

Before highlighting the spatial relationship of the MdLF with adjacent fiber pathways we have to stress that in almost all cases we were able to achieve a discrete cleavage plane of this tract. We could therefore properly dissect it away from neighboring white matter bundles, mark it with white stripes, follow and lift the fibers of the different subcomponents from their origin to their termination points (Figures 3.15,3.16 and 3.17).

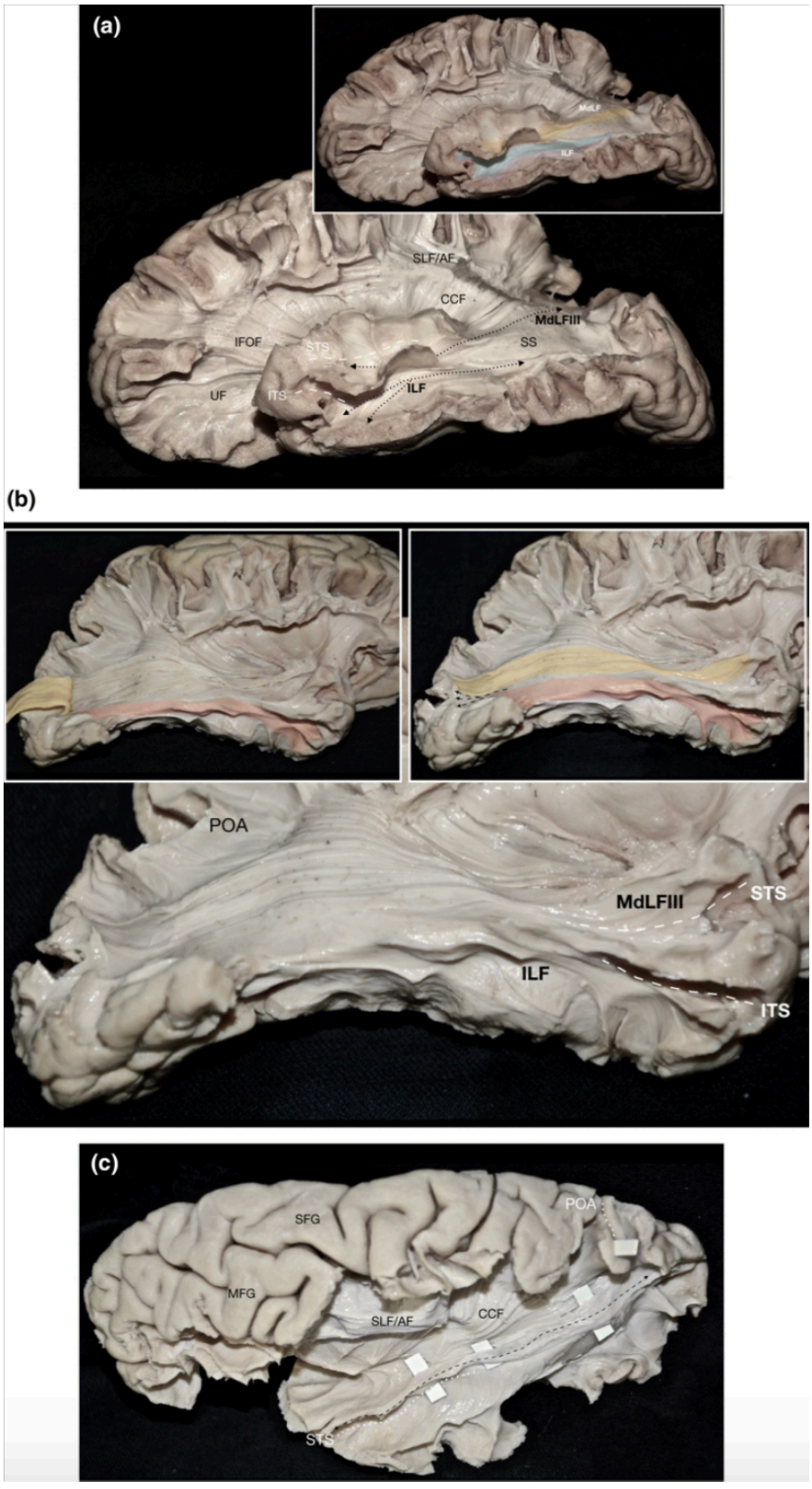


**Figure 3.19 Mdlf Results.** MdLF-III correlative anatomy with respect to ILF at the sulcal and deep subcortical levels. a Different specimen. Left hemisphere. Inferolateral view. The levels of the STS and ITS are outlined with dashed white lines. The MdLF-III is seen terminating anteriorly at the level of the STS and dorsal TP, while the ILF anterior terminations are being recorded at the level of ITS and ventral TP. Inset: The MdLF-III and ILF highlighted in yellow and blue, respectively. b Same specimen as in Figure 5. Right hemisphere. Inferolateral view. Again, MdLF-III and ILF anterior terminations at the level of the STS and ITS/ventral TP, respectively. ILF fibers are seen turning towards the medial TP at the most anterior aspect of the tract. Posteriorly both tracts merge with the sagittal stratum and share occipital cortical terminations. Insets: MdLF-III and ILF are highlighted in yellow and red, respectively. In the right inset, their shared occipital cortical terminations are outlined with black dashed arrowed lines. In the left inset, the MdLF-III has been retracted posteriorly. c Different Specimen. Left hemisphere. Superior view. The STS and POA are outlined with white dotted lines. MdLF-III is demarcated with small white pads and outlined with a black dashed arrowed line. The MdLF-III is seen as a distinct white matter tract, coursing at the level of STS towards the occipital lobe. Residual U-fibers of the STS delineate MdLF-III from other long white matter tracts in vicinity including ILF. d Same specimen as in Figure 3a. Left hemisphere. Lateral view. MdLF-III is dissected away from neighboring tracts and demarcated with small white pads. ILF is highlighted in blue. UF is outlined with black dashed arrowed line. The anterior terminations of the MdLF lie superior and posterior to the uncinate fasciculus fibers, while the ILF lying inferior to them. The ILF

fibers terminate distinctly more anteriorly in the temporal pole. IFOF is outlined with black dotted arrowed line. MdLF-I and -II have been retracted posteriorly and highlighted with yellow and red, respectively. e Same specimen as in Fig. 3a. Left Hemisphere. Inferolateral view. The distinctly different anterior terminations of MdLF-III and ILF are apparent. The space between them is outlined with black dotted arrowed line. Again, the ILF is seen turning towards the medial TP. Right inset: MdLF-III and ILF are highlighted in green and blue, respectively. Left inset: MdLF-I, -II (retracted posteriorly) and -III are highlighted in yellow, red and green, respectively, while the ILF is outlined with dashed arrowed lines. CCF claustro-cortical Fibers, CL = claustrum, IFOF inferior fronto-occipital fasciculus, ILF inferior longitudinal fasciculus, ITS inferior temporal sulcus, MdLF middle longitudinal fasciculus, MFG middle frontal gyrus, POA parieto-occipital Arcus, SFG superior frontal gyrus, SLF/AF superior longitudinal fasciculus/arcuate fasciculus complex, SS sagittal stratum, STS superior temporal sulcus, UF uncinate fasciculus Reprinted from Kalyvas et al[79] by permission of Springer Nature [3]

The specific plane of latero-medial dissection and the distinct axonal connectivity of the discrete segments of the MdLF differentiate it from all the other fiber tracts that travel in the vicinity such as the SLF/AF complex, ILF, IFOF, UF, claustrocortical and external capsule radiations.

MdLF and SLF/AF complex

We consistently identified the fibers of the MdLF to course just medial to the SLF/AF complex at the area of the parietal and occipital lobe. A tight anatomical proximity was observed between the fibers of the MdLF residing in the posterior transverse area and the most medial fibers of the "C" shaped AF at the level of the STG. We therefore focused our dissection at the temporo-parietal junction and consistently developed a cleavage plane between the arching fibers of the AF and the more medially located fibers of the MdLF, which were seen to course towards the SPL and POA (Figures 3.18,3.19).

MdLF and Dorsal External Capsule

Although the MdLF fibers that reside in Heschl's gyrus and the Dorsal External Capsule exhibit the same direction and trajectory there is nevertheless a clear cleavage plane between them. Indeed, the MdLF courses more superficially and posteriorly than the dorsal external capsule while their anterior terminations are completely different and distinct; the claustrum for the dorsal external capsule and the STG for the MdLF (Figure 3.15b)

MdLF and UF

Deep to the anterior part of the STG, fibers of the UF and MdLF were found to course in proximity. However, we observed the UF to lie medially to the MdLF at the anterior temporal lobe and to terminate more anteriorly in the temporal pole (Figures 3.15-3.19).

MdLF and IFOF

We consistently recorded the IFOF to course in a deeper dissection plane than the MdLF, as its fibers dive towards the limen insula to reach the frontal lobe, thus corresponding to the ventral external capsule, whereas the MdLF was seen to lie in a more superficial plane; medially to the U-fibers of the anterior STG-STS. Moreover, as the tracts travel posteriorly towards the occipital lobe, both the IFOF and MdLF merge with the sagittal stratum following however, a distinct course; the MdLF runs dorsolaterally while the IFOF exhibits a medial trajectory (Figures 3.15-3.19).

MdLF and ILF

The ILF connects the TP to the occipital region, with its main stem travelling deep in the fusiform gyrus. Starting from the TP and focusing on their anterior correlative topography, the MdLF originates from the dorsal TP while the ILF from the ventral TP (Fig. 3.18,3.19). More specifically, the most inferior fibers of the MdLF are apparent at the level of the STS (Fig. 7c) while the stem of the ILF is located below the level of the ITS with its most superior fibers at the level of the middle temporal gyrus but always terminating more anteriorly and caudally in the TP, when compared to the MdFL fibers (Fig. 3.19). At a deeper subcortical level, we recorded the anterior terminations of the MdLF to lie superior and posterior to the Uncinate Fasciculus fibers while the ILF lying inferior to them (Fig. 3.19). Again, the ILF fibers terminate distinctly more anteriorly in the temporal pole (Fig. 3.19). Importantly, the ILF fibers turn towards the medial TP at the most anterior aspect of the tract (Fig. 3.18,3.19). Tilting our dissection posteriorly, we consistently observed the fibers of the ILF to course and terminate in an inferior plane with respect to the MdLF (Fig. 3.18,3.19). However, as they

approach the posterior most aspect of the occipital lobe and during their course in the sagittal stratum, the most superior ILF fibers seem to share occipital cortical terminations with the most inferior of the MdLF fibers in most of the cases (Fig. 3.19b).

**Segmentation and connectivity pattern**

After dissecting, detaching and retracting posteriorly the fibers of the MdLF, we consistently identified and recorded a specific connectivity and segmentation pattern. More specifically, fibers that originate from the dorsolateral TP were seen to enter the transverse gyri and to reach the SPL/PrC and POA, while the fibers originating more anterior and inferior (anteriormost part of STS and TP) were never encountered to pass through the transverse gyri. Instead, they course in a more medial and inferior trajectory, exhibiting a horizontal configuration and finally reaching the occipital lobe (Fig. 3.15). Three segments and connectivity patterns were invariably recorded. In line with previous white matter anatomy studies where the subcomponents of a full bundle have been described [i.e., SLF], we used a similar nomenclature and we defined the three MdLF segments as MdLF-I, MdLF-III and MdLF-III.

<u>MdLF-I: Dorsolateral TP & STG -Heschl's Gyrus-SPL/Precuneus</u>

The MdLF fibers that travel through the anterior transverse gyrus (Heschl's Gyrus), exhibit an "S-shaped" configuration and terminate at the postero-superior SPL. These fibers reside more anteriorly and superiorly than the MdLF fibers entering the Posterior Transverse Area and also exhibit a superior trajectory towards the SPL. This segment travels parallel and posterolateral in relation to the claustrocortical fibers of the dorsal external capsule (Fig. 3.15b).

<u>MdLF-II: Dorsolateral TP & STG- Posterior transverse area- SMG - POA</u>

The MdLF fibers that originate at the dorsolateral TP and travel through the Posterior Transverse Area were seen to course obliquely and deep to the SMG. More specifically, they

were always seen to terminate in a “U-shaped” configuration as a subcortical loop of fibers folding around the parieto-occipital sulcus, namely the parieto-occipital arcus (POA). The MdLF-II lies more posteriorly, inferiorly and medially when compared to the MdLF-I and in an oblique and posteriorly directed course.

MdLF-III: most anterior part of TP/STS & STG -AG – occipital lobe/cuneus

The MdLF fibers that stem from the most anterior part of the temporal pole and STS were consistently recorded to course in a relatively deep and inferior trajectory at the level of the STS. This segment exhibits a horizontal configuration and fans-out at the level of the posterior STS to reach the posterior border of the occipital lobe and cuneus by passing deep to the AG. It joins the sagittal stratum as its most dorsolateral part. In 70% of the hemispheres this segment was seen to terminate at the superior third of the posterior lip of the occipital lobe, while in 30% we also observed termination fibers in the middle third. Reprinted from Kalyvas et al[79] by permission of Springer Nature [3]

## **3.5** The IFOF

*Microanatomical fiber dissections*

We started our microdissections at the superior temporal sulcus (STS) and gyrus (STG), including the transverse gyri, we moved our plane posteriorly and superiorly towards the parieto-occipital area, eventually extending our way to the frontal area of the hemisphere. Following the removal of cortical grey matter, the arcuate or U-fibers of the lateral aspect of the hemisphere are evident. These fibers connect adjacent gyri and form the most superficial layer of white matter. Removing the U-fibers of the inferior central lobe, inferior parietal lobule (IPL) and temporo-parieto-occipital (TPO) junction and frontal area discloses the superior longitudinal fasciculus (SLF)/arcuate fasciculus (AF) complex, which essentially connects the IFG and middle frontal gyrus (MFG) with the IPL and temporal lobe Dissecting the U-fibers of the STG/STS and the SLF/AF complex, unveils the MdLF. The insula and the most anterior part of the inferior frontal gyrus (IFG) were also included in the dissection to reveal the dorsal external capsule, the UF and IFOF. More specifically, the U-fibers of the insula are dissected away in order to delineate the claustrocortical fibers of the dorsal external capsule. Fibers stemming from the SLF were seen travelling through the IPS and finally terminating at the AG. Dissecting away the U-fibers of the IPS, reveals fibers of the MdLF reaching the postero-superior part of the SPL/Precuneus and the parieto-occipital arcus (POA). Removing the U-fibers of the TPO junction, unveils MdLF fibers continuing further posteriorly to enter the occipital lobe. In this dissection step we recorded a discrete group of fibers, which were seen to run under the U-fibers of the occipital lobe and exhibit a vertical trajectory, corresponding to the Vertical Occipital Fasciculus (VOF). Following the complete exposure of the MdLF in the lateral cerebral aspect, we meticulously dissected, detached and retracted its fibers, starting from the TP and anterior STG. Following the posterior retraction of the 3 segments of the MdLF, the posterior fibers IFOF can be identified (Fig.3.20).[79]

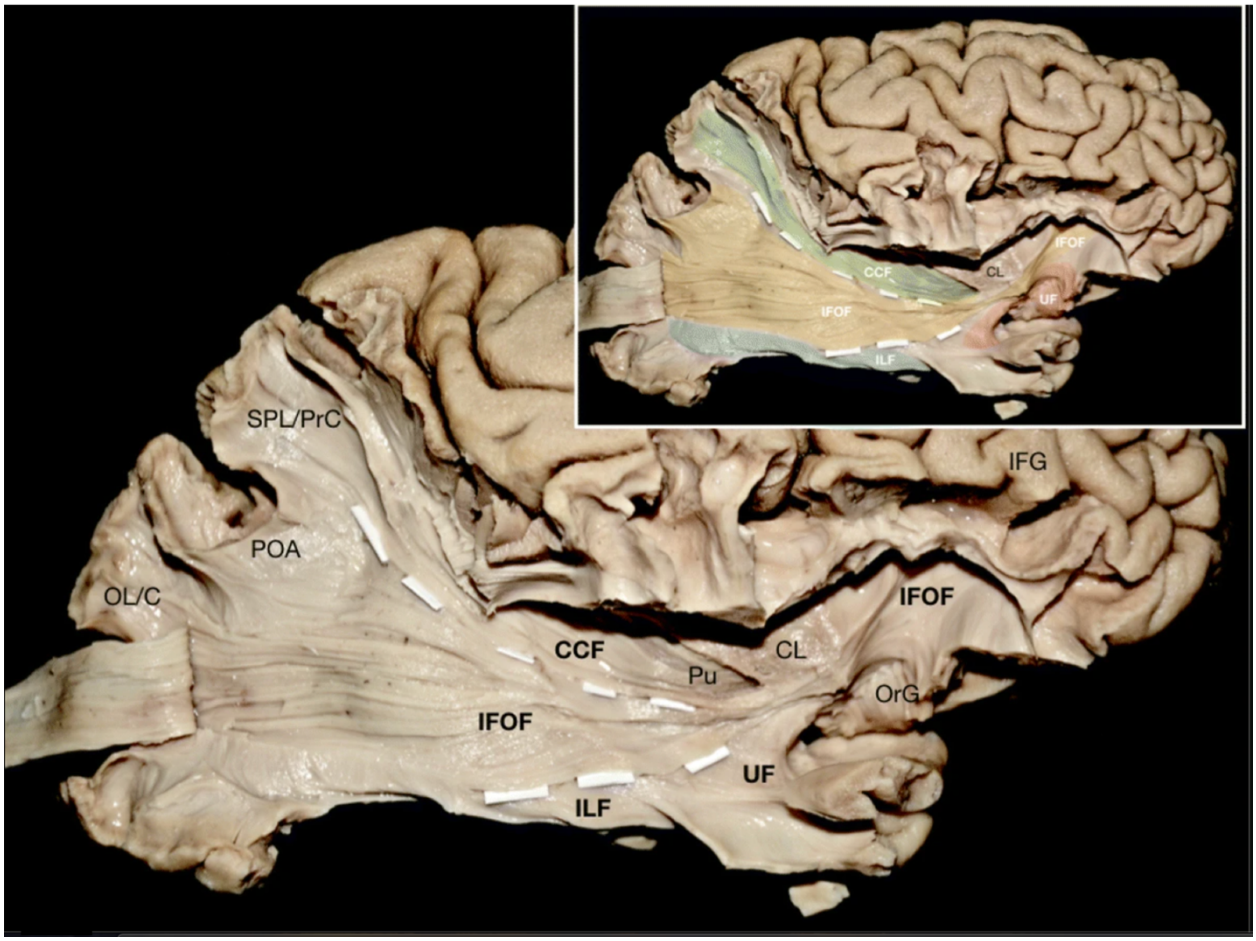


**Figure 3.20** Following the dissection and retraction of the MdLF-III (step 7) the fibers of UF, IFOF and ILF can be identified. The silhouette of the IFOF is depicted and demarcated from the CCF and UF with small white pads. The IFOF lies medial to the MdLF. The UF lies also medial to the MdLF at the anterior temporal lobe and terminates more anteriorly in the temporal pole as illustrated in the figure. In contrast to the MdLF, the fibers of the ILF are seen to originate from the ventral TP and to course in an inferior plane with respect to the MdLF, however sharing some cortical terminations. Inset: The MdLF, IFOF, UF, CCF and ILF highlighted in red, yellow, orange, green and blue, respectively. C cuneus, CCF claustro-cortical fibers, CL claustrum, IFG inferior frontal gyrus, IFOF inferior fronto-occipital fasciculus, ILF inferior longitudinal fasciculus, MdLF middle longitudinal fasciculus, OL occipital lobe, OrB orbital gyri, POA parieto-occipital arcus, PrC precuneus, Pu putamen, SPL superior parietal lobule, UF uncinate fasciculus Reprinted from Kalyvas et al[79] by permission of Springer Nature [3]

Following dissection of the frontoparietal area and the central core we removed the U-fibers connecting the insula with the inferior frontal gyrus reveling the anterior fibers of the IFOF and uncinate fasciculus under the level of the inferior frontal gyrus. The IFOF was consistently found at the level of the crossing between external capsule and claustrum. In all

specimens studied we found the IFOF to reach the superior part of the SPL/Precuneus while it was clearly demarcated and distinguished from the UF, MdLF and ILF (Fig 3.21).

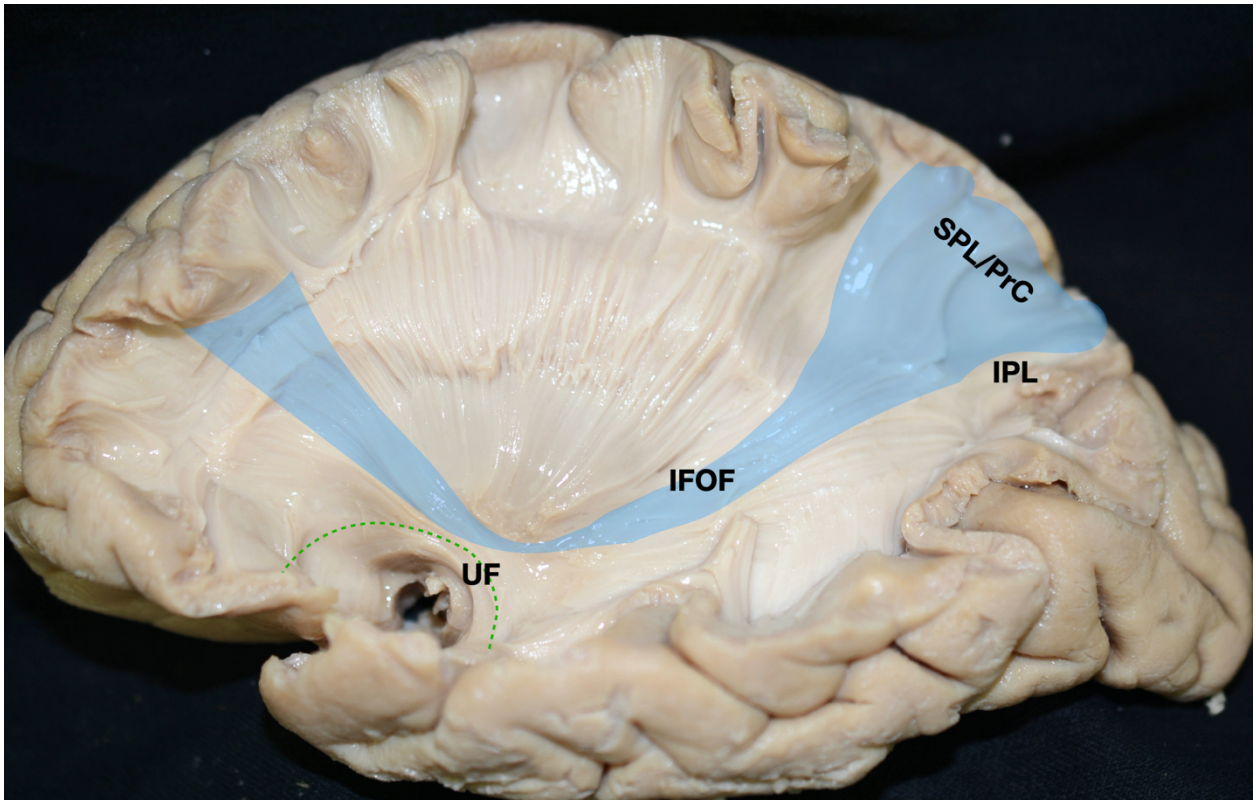


**Figure 3.21** Cortical terminations of IFOF to the precuneus.

*Connectivity of the IFOF*

We documented the IFOF to connect with different cortical regions of the frontal, parietal, occipital and temporal lobes. We consistently found the posterior dorsal fibers of the IFOF to reach the SPL/precuneus after traveling through the sagittal stratum and lateral surface of the atrium.

*Subcortical Correlative anatomy of the IFOF*

IFOF and SLF/AF complex

We consistently identified the fibers of the IFOF to course medial and inferior to the SLF/AF complex at the area of the frontal, parietal and occipital lobe. We therefore focused our dissection at the temporo-parietal junction and consistently developed a cleavage plane between the arching fibers of the AF and the more medially located fibers of the IFOF, which were seen to course towards the SPL/ precuneus.

IFOF and MdLF

We consistently recorded the IFOF to course in a deeper dissection plane than the MdLF, as its fibers dive towards the limen insula to reach the frontal lobe, thus corresponding to the ventral external capsule, whereas the MdLF was seen to lie in a more superficial plane; medially to the U-fibers of the anterior STG-STS. Moreover, as the tracts travel posteriorly towards the occipital lobe, both the IFOF and MdLF merge with the sagittal stratum following however a distinct course; the MdLF runs dorso-laterally while the IFOF exhibits a medial trajectory.

IFOF and Dorsal External Capsule

The IFOF fibers exhibit the same direction and trajectory with fibers of the Dorsal External Capsule. However, we were able to establish a clear cleavage plane between them. In fact, the IFOF courses more inferior than the dorsal external capsule while their anterior terminations are completely different and distinct; the claustrum for the dorsal external capsule and the frontal lobe for the IFOF.

IFOF and UF

We found the IFOF and the uncinate fasciculus in close proximity at the level of the ventral portion of the extreme capsule. We found the IFOF located posterior and dorsal to the

uncinate fasciculus. However, we observed the UF to terminate more inferiorly in the frontal lobe.

**3.6** Claustro-cortical fibers.

To study the claustro-cortical fibers of the precuneus, we started our microdissections at the superior temporal sulcus (STS) and gyrus (STG), including the transverse gyri, we moved our plane posteriorly and superiorly towards the parieto-occipital area, eventually extending our way anteriorly to the frontal area of the hemisphere and the insula. Following the removal of cortical grey matter, we revealed the arcuate or U-fibers of the lateral aspect of the hemisphere. Removing the U-fibers of the inferior central lobe, inferior parietal lobule (IPL) and temporo-parieto-occipital (TPO) junction and frontal area discloses the superior longitudinal fasciculus (SLF)/arcuate fasciculus (AF) complex, which essentially connects the IFG and middle frontal gyrus (MFG) with the IPL and temporal lobe. After meticulous dissection of the U-fibers of the STG/STS and the SLF/AF complex, we exposed the MdLF and some of the claustrocortical fibers. The insula and the most anterior part of the inferior frontal gyrus (IFG) were also included in the dissection to reveal the dorsal external capsule / claustrocortical fibers, the UF and IFOF. More specifically, the U-fibers of the insula are dissected away in order to delineate the claustrocortical fibers of the dorsal external capsule. Fibers stemming from the SLF were seen travelling through the IPS and finally terminating at the AG. (Fig. 3.20).[79]

*Connectivity of precuneal claustrocortical fibers*

We documented the claustrocortical fibers of the dorsal external capsule to connect the precuneus/ superior parietal lobule with the claustrum in all specimens.

*Subcortical Correlative anatomy of the precuneal claustrocortical fibers*

<u>Precuneal claustrocortical fibers and SLF/AF complex</u>

We consistently identified the fibers of the precuneal claustrocortical fibers to course medial to the SLF/AF complex at the temporo-parietal junction. We therefore focused our dissection at the temporo-parietal junction and consistently developed a cleavage plane between the arching fibers of the AF and the more medially located fibers of the IFOF, which were seen to

course towards the SPL/ precuneus. We consistently found the posterior dorsal fibers of the IFOF to reach the SPL/precuneus after traveling through the sagittal stratum and lateral surface of the atrium (Fig 3.22).

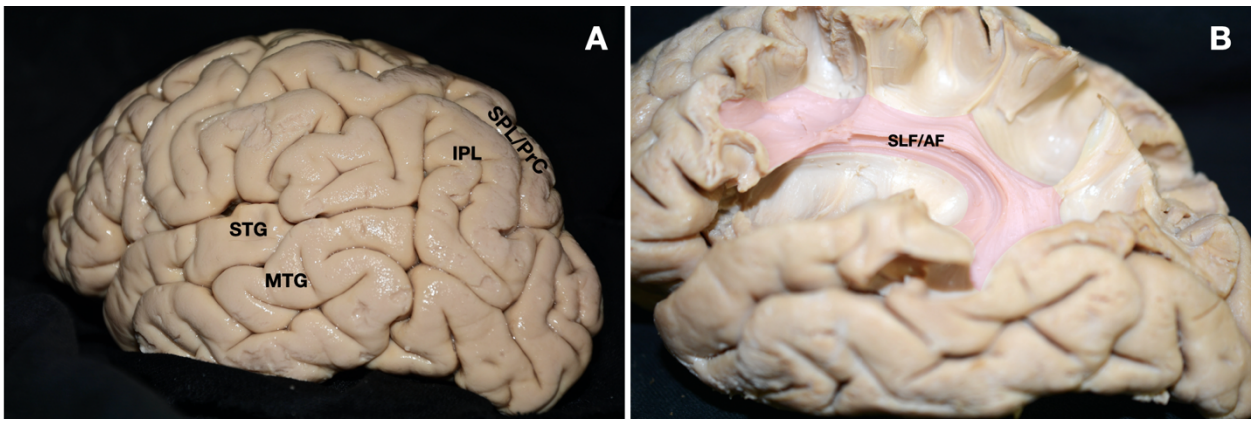


**Figure 3.22** Left hemisphere illustrating the SLF/AF complex The U-fibers of the inferior central lobe, IPL and TPO junction have been dissected and the SLF/AF complex, connecting the IFG, MFG and central lobe with the IPL and temporal lobe is illustrated. The inner fibers of the "C" shaped part of the SLF/AF complex terminating at the STG and STS should be removed with caution in order to preserve the underlying MdLF fibers. The Transverse Temporal Sulcus plane is depicted using a white bold dashed line, while the rest of the sulci with black dashed lines. Inset: the SLF/AF complex highlighted in red. AG = Angular Gyrus, CS = Central Sulcus, HG = Heschl's Gyrus, IFG = Inferior Frontal Gyrus, IFS = Inferior Frontal Sulcus, IN = Insula, IPS = Intraparietal Sulcus, ITG = Inferior Temporal Gyrus, ITS = Inferior Temporal Sulcus, MTG = Middle Temporal Gyrus, OL = Occipital Lobe, PCG = Postcentral Gyrus, PCS = Postcentral Sulcus, PrCS = Precentral Sulcus, PrG = Precentral Gyrus, PTA = Posterior Transverse Area, SLF/AF = Superior Longitudinal Fasciculus/Arcuate Fasciculus Complex, SMG = Supramarginal Gyrus, SoJ = Sulcus of Jensen, SPL = Superior Parietal Lobule, STG = Superior Temporal Gyrus, STS = Superior Temporal Sulcus, SyF = Sylvian Fissure, TP = Temporal Pole, TTS = Transverse Temporal Sulcus

Claustrocortical fibers and MdLF

We consistently recorded the IFOF to course in a deeper dissection plane than the MdLF, as its fibers dive towards the limen insula to reach the frontal lobe, thus corresponding to the ventral external capsule, whereas the MdLF was seen to lie in a more superficial plane; medially to the U-fibers of the anterior STG-STS. Moreover, as the tracts travel posteriorly towards the occipital lobe, both the IFOF and MdLF merge with the sagittal stratum following however, a distinct course; the MdLF runs dorso-laterally while the IFOF exhibits a medial trajectory.

Claustrocortical fibers and IFOF

The IFOF fibers exhibit the same direction and trajectory with fibers of the Dorsal External Capsule. However, we were able to establish a clear cleavage plane between them. In fact, the IFOF courses more inferior than the dorsal external capsule while their anterior terminations are completely different and distinct; the claustrum for the dorsal external capsule and the frontal lobe for the IFOF (Fig 3.23).

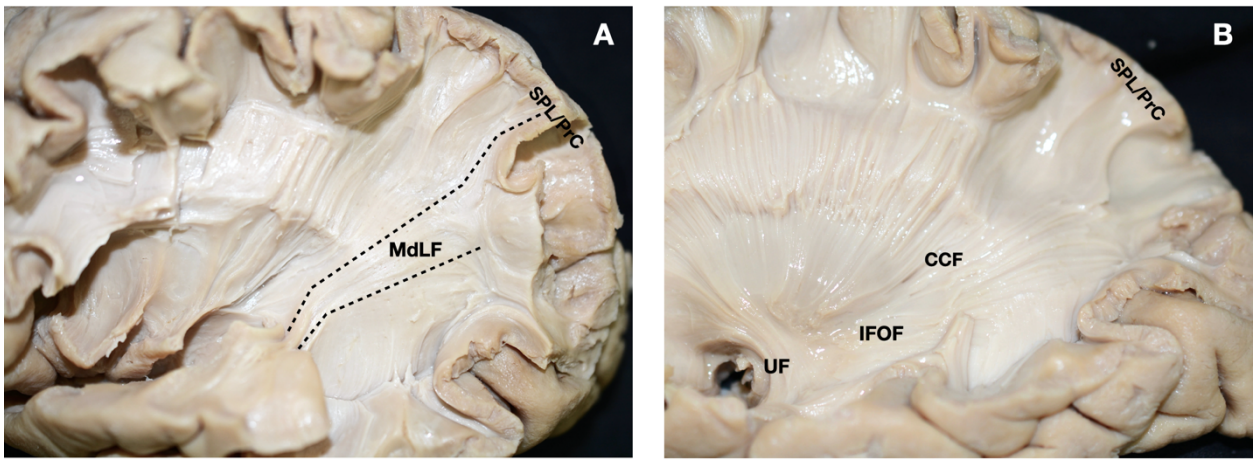


**Fig 3.23.** We consistently recorded the IFOF to course in a deeper dissection plane than the MdLF, as its fibers dive towards the limen insula to reach the frontal lobe, thus corresponding to the ventral external capsule, whereas the MdLF was seen to lie in a more superficial plane; medially to the U-fibers of the anterior STG-STS. Moreover, as the tracts travel posteriorly towards the occipital lobe, both the IFOF and MdLF merge with the sagittal stratum following however, a distinct course; the MdLF runs dorso-laterally while the IFOF exhibits a medial trajectory.

## 3.6 The CBV

*Microanatomical Fiber Dissection*

Upon removing the cortex and superficial U-fibers of the parieto-occipital sulcus (POS), calcarine fissure, cuneus, precuneus, posterior cingulate area, lingual, parahippocampal and fusiform gyri, we invariably expose a group of fibers seen to radiate from the area of the posterior precuneus (BA7 - anterior bank of the POS) to the basal temporo-occipital junction (BA37 - middle third of the fusiform gyrus). (Figures 3.24-3.27)

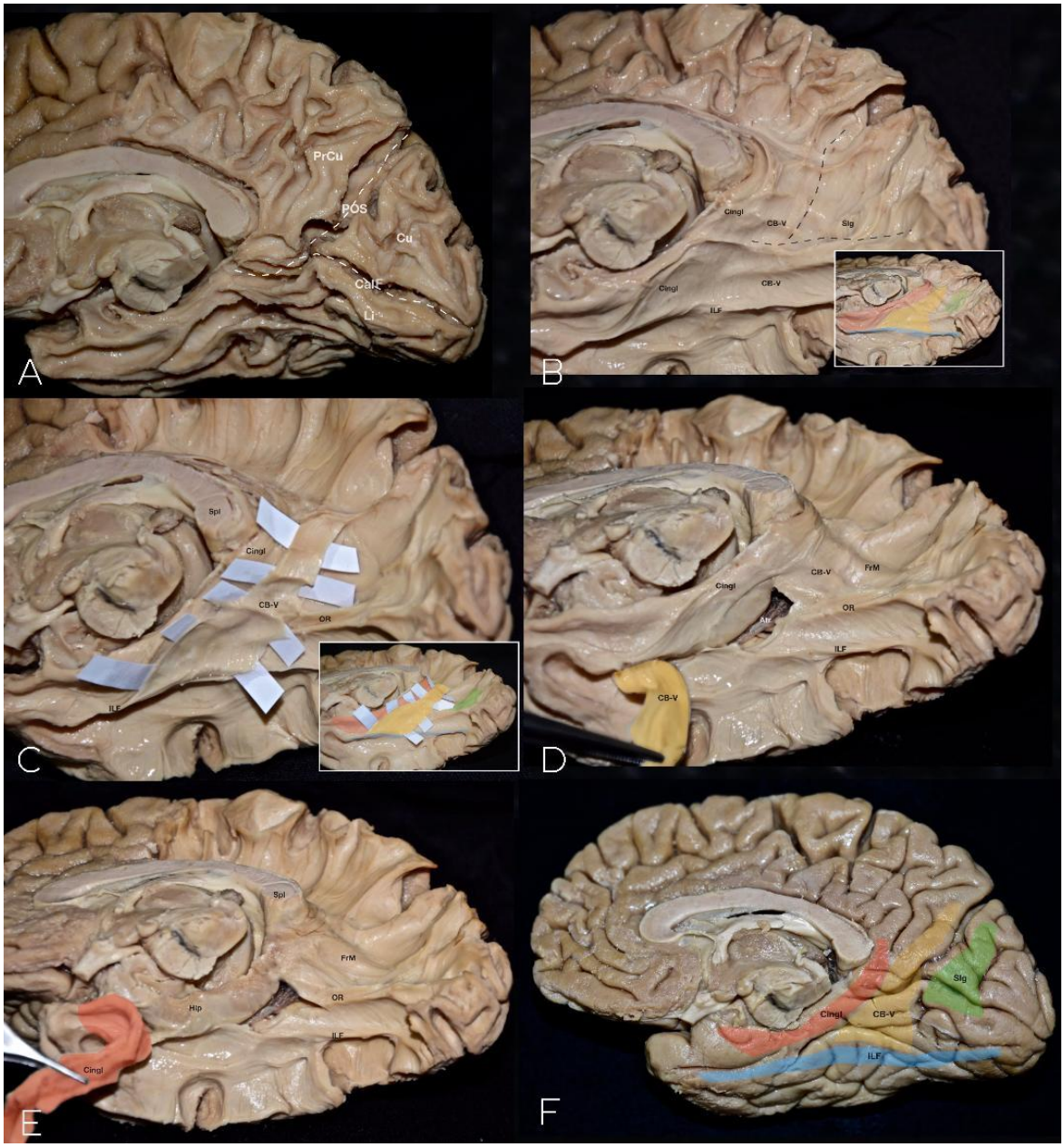


**Figure 3.24** Progressive dissection of a right hemisphere, medial views. A: Gray matter has been removed. The superficial U-fibers are apparent. The contour of the main sulci is indicated by a dashed white line. B: Upon removing the superficial U-fibers, the inferior arm of the cingulum (CingI), cingulum bundle V (CB-V), inferior longitudinal fasciculus (ILF), and sledge runner fasciculus (Slg) are visible. These fasciculi are highlighted in red, yellow, blue, and green, respectively (inset, B). C: The fibers of the CB-V are followed along their trajectory, from the posterior precuneus to the area of the fusiform gyrus and medial temporal lobe. The CB-V fibers can be dissected without affecting the structural integrity of the CingI. These two fiber systems appear in a "kissing" configuration but without intermingling. The CingI, CB-V, Slg, and ILF are highlighted in red, yellow, green, and blue, respectively (inset, C). D: Fibers of the CB-V are followed toward the medial temporal lobe. The structural integrity of the CingI remains intact. E: The CingI is gradually dissected. Its inferior terminations follow a

trajectory that is medial in relation to that of the CB-V. F: The anatomical silhouettes of the CingI (red), CB-V (yellow), Slg (green), and ILF (blue) are superimposed on the medial surface anatomy. Atr = atrium; CalF = calcarine fissure; Cu = cuneus; FrM = forceps major; Hip = hippocampus; Li = lingual gyrus; OR = optic radiation; POS = parietooccipital sulcus; PrCu = precuneus; Spl = splenium of the corpus callosum.

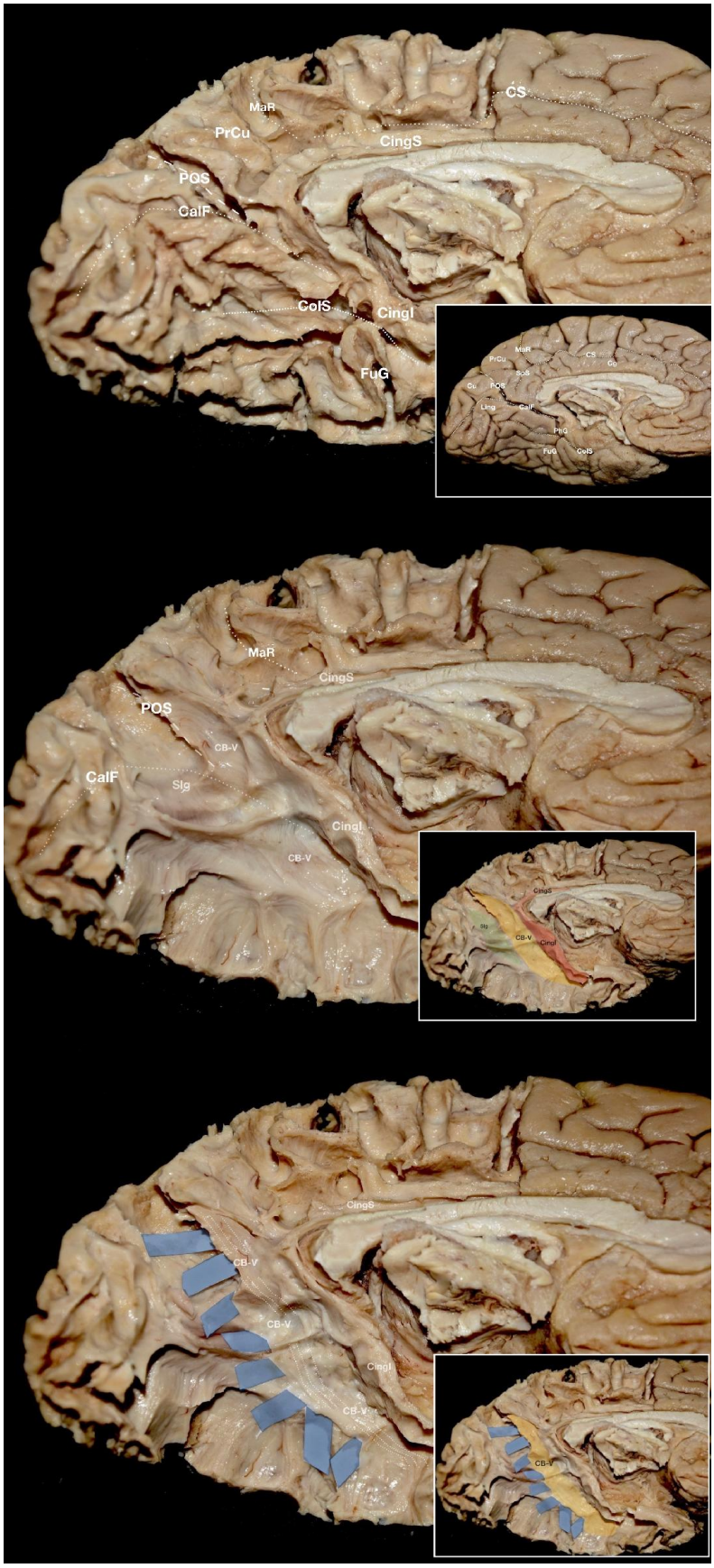
CS
MaR
PrCu
CingS
POS
CalF
ColS
CingI
FuG
MaR
CingS
POS
CB-V
CalF
Slg
CingI
CB-V
CingS
CB-V
CB-V
CingI
CB-V

**Figure 3.25** Progressive dissection of a left hemisphere. Medial views. A: Superficial U-fibers exposed. The contour of the main sulci is illustrated. Inset: The superficial landmarks including the sulci and gyri are marked. B: U-fibers removed, and the inferior arm of the cingulum, CB-V and Sledge runner fasciculus are depicted. The Sledge runner fasciculus resides caudally with its fibers running from the anterior cuneus towards the PPA and RSC. CB-V is located between the Sledge runner and Inferior arm of the cingulum. Its fibers travel anterior to the POS from the posterior precuneus to the middle third of the fusiform gyrus. Anterior to CB-V, the inferior arm of the cingulum projects and terminates to medial temporal structures. Inset: These tracts are highlighted in yellow (CB-V), red (inferior arm of the cingulum) and green (sledge runner fasciculus) color respectively. C: CB-V is gradually dissected, starting from the posterior precuneus to the fusiform gyrus. CB-V and inferior arm of the cingulum run as independent pathways. Inset: The CB-V is highlighted in yellow color. CalF= Calcarine fissure (distal part), CB-V= Cingulum Bundle V, Cg= Cingulate Gyrus, CingI= Inferior arm of the Cingulum, CingS= Superior Arm of the Cingulum, ColS= Collateral Sulcus, CS= Cingulate Sulcus, Cu= Cuneus, FuG= Fusiform Gyrus, Ling= Lingual Gyrus, MaR= Marginal Ramus of the Cingulate Sulcus, PhG= Parahippocampal Gyrus, POS= Parieto-occipital Sulcus, PrCu= Precuneus, Slg= Sledge runner Fasciculus, SpS= Subparietal Sulcus

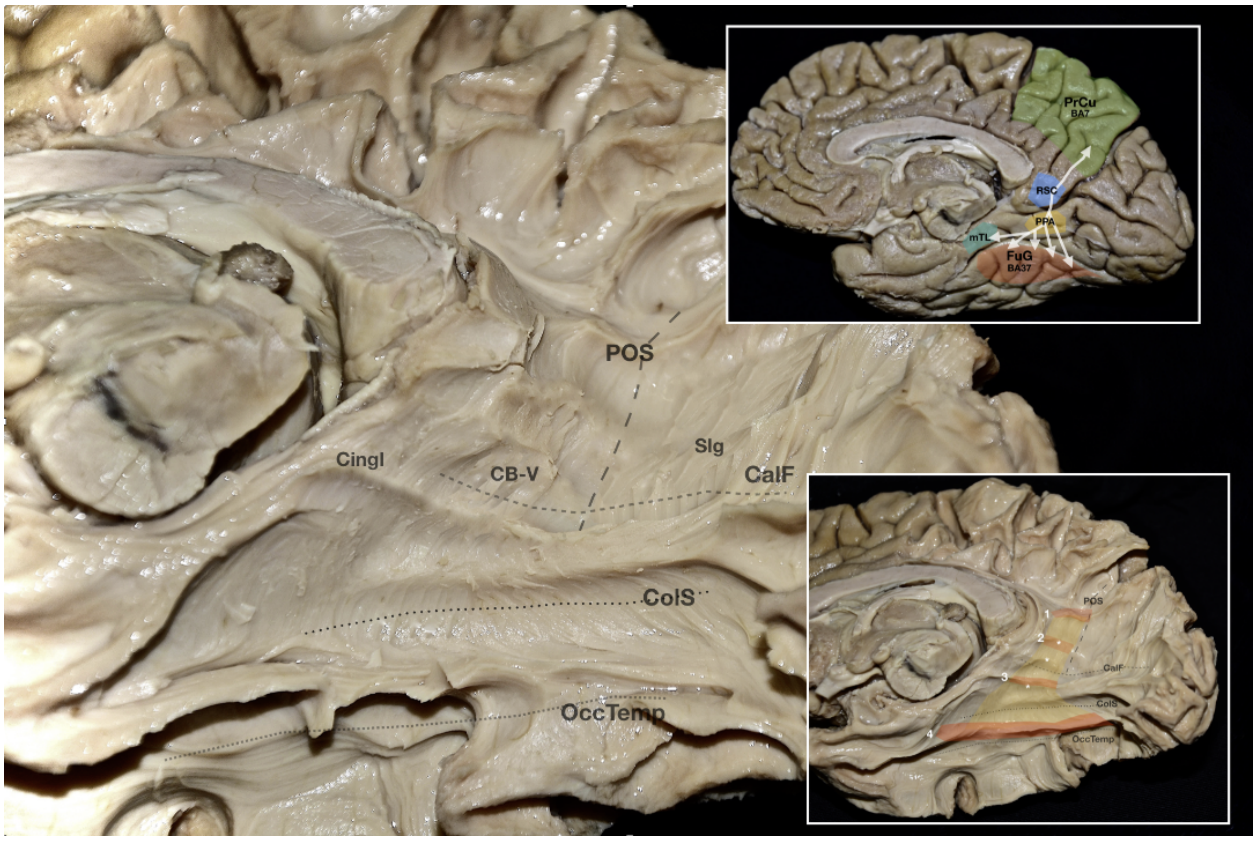

**Figure 3.26** - Infero-medial view of a right hemisphere. Morphology and connectivity of the CB-V illustrated. CB-V can be seen running at the level of the anterior bank of the POS. Its fibers spread towards the fusiform area and medial temporal lobe. Its narrowest part corresponds to the area of the posterior precuneus while the widest to the area of the fusiform gyrus. CB-V exhibits 3-4 medially projecting "knees". These "knees" usually appear near the level of the RSC and PPA. Four termination zones can be appreciated. The superior terminations of the CB-V project towards the posterior precuneus. Two termination zones are recorded at the level of the RCS and PPA. The inferior terminations of the CB-V radiate in a wide area corresponding to the middle and, sometimes, posterior aspect of the fusiform gyrus and part of the pyriform cortex. Upper Inset: The trajectory of the CB-V superimposed on the superficial anatomy. Terminations cover a wide area including the posterior precuneus(green), RSC (blue), PPA(yellow), Fusiform gyrus(Red) and medial temporal lobe (magenta). Lower Inset: The "knees" of the CB-V are marked with stars. The termination zones are highlighted with red color: 1= posterior precuneus, 2=Retrosplenial Cortex 3= Parahippocampal place area 4= fusiform gyrus and medial temporal lobe. CalF= Calcarine Fissure, CB-V= Cingulum Bundle V, CingI= Inferior arm of the cingulum, ColS= Collateral Sulcus, FuG= Fusiform Gyrus, mTL= Medial Temporal Lobe, OccTemp= Occipitotemporal Sulcus, POS= Parieto-occipital Sulcus, PPA= Parahippocampal place area, PrCu= Precuneus, RSC= Retrosplenial Cortex, Slg= Sledge runner Fasciculus

This distinct white matter bundle, previously described as CBV, follows the trajectory of the POS, bends around the splenium of the Corpus Callosum, then curves caudo-medially passing under the posterior half of the proximal calcarine fissure to reach the Posterior Parahippocampal Area and further dives under the collateral sulcus in a deeper plane to terminate to the middle third of the fusiform gyrus (BA 37-FFA)

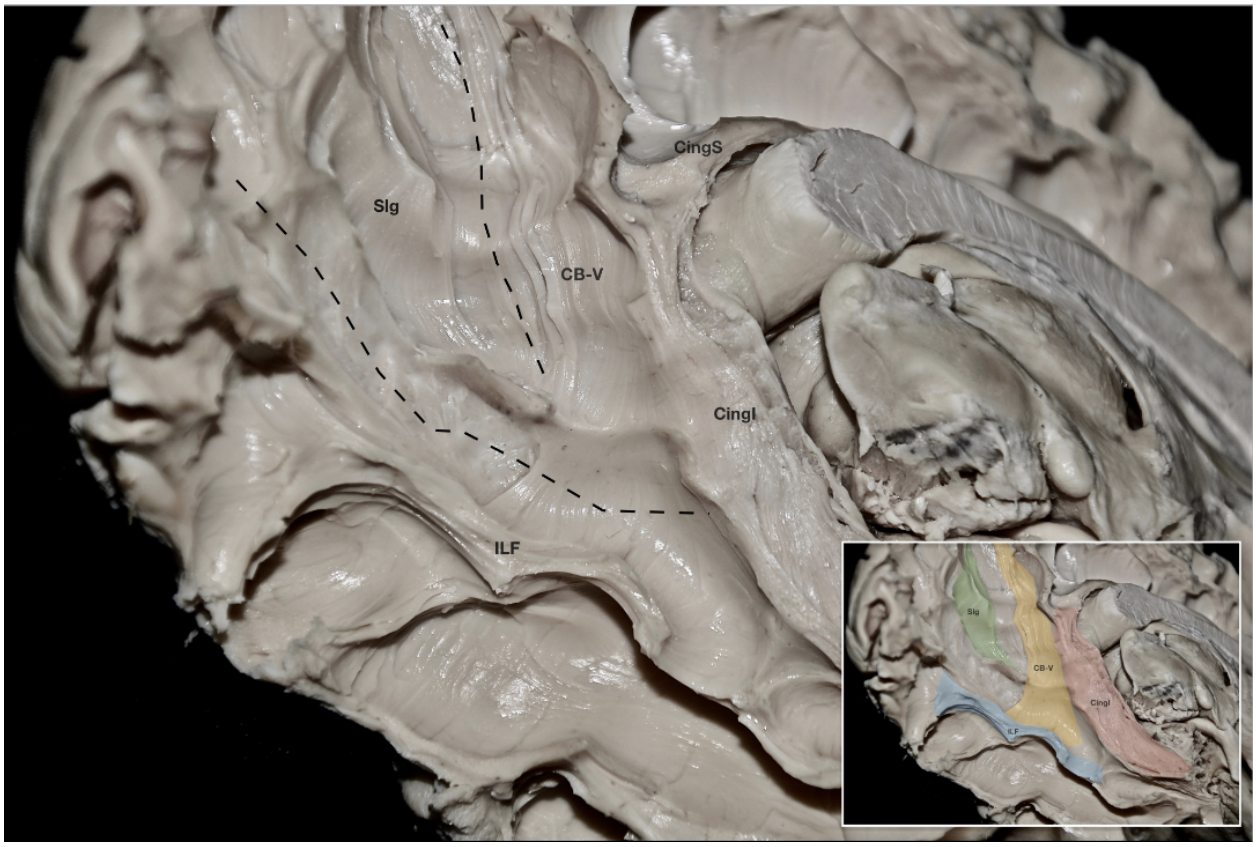


**Figure 3.27**- Left hemisphere. Infero-medial view. The spatial relationship of the inferior arm of the cingulum, ILF, CB-V and Sledge runner is illustrated. The Sledge runner fasciculus follows a short trajectory from the anterior cuneus towards the PPA and RSC and is located caudal to the CB-V. CB-V is seen to have a longer configuration, originating from the posterior precuneus and traveling mainly towards the fusiform gyrus. It exhibits a "funnel like" shape with its narrowest part seen in the area of posterior precuneus and its wider in the fusiform area. The stem of the ILF travels within the fusiform gyrus, keeping a perpendicular trajectory to that of CB-V and Slg. Interestingly, the inferior terminations of the CB-V penetrate the fibers of the ILF to terminate in the mid-fusiform gyrus. The inferior arm of the cingulum curves around the splenium of the corpus callosum to terminate to the medial temporal lobe. Inset: The correlative anatomy of the four fasciculi is illustrated. Red: Inferior arm of the cingulum. Yellow: CB-V. Green: Slg. Blue: ILF. CB-V= Cingulum Bundle V, CingI= Inferior arm of the Cingulum, CingS= Superior Arm of the Cingulum, ILF= Inferior Longitudinal Fasciculus, Slg= Sledge runner Fasciculus


**Figure 3.28** Right hemisphere. Infero-medial view CB-V and adjacent fasciculi illustrated in relation to the sulcal anatomy. The silhouette of the main sulci including the Collateral, Occipito-temporal and Parieto-occipital sulci is depicted. CB-V travels anterior to the POS while Slg resides posteriorly. ILF is confined within the fusiform gyrus. The inferiormost fibers of the CB-V travel below the depth of the collateral sulcus terminating in the area of the mid-fusiform gyrus. Inset: The Inferior arm of the cingulum, CB-V, Slg and ILF area highlighted with red, yellow, green and blue color respectively. The silhouette of the main sulci is also marked for orientation purposes. CB-V = Cingulum Bundle V, CingI = Inferior arm of the Cingulum, ColS= Collateral Sulcus, OccTemp= Occipitotemporal Sulcus, OR = Optic Radiation, POS= Parieto-occipital sulcus, Slg = Sledge runner Fasciculus, Spl = Splenium of the Corpus Callosum.

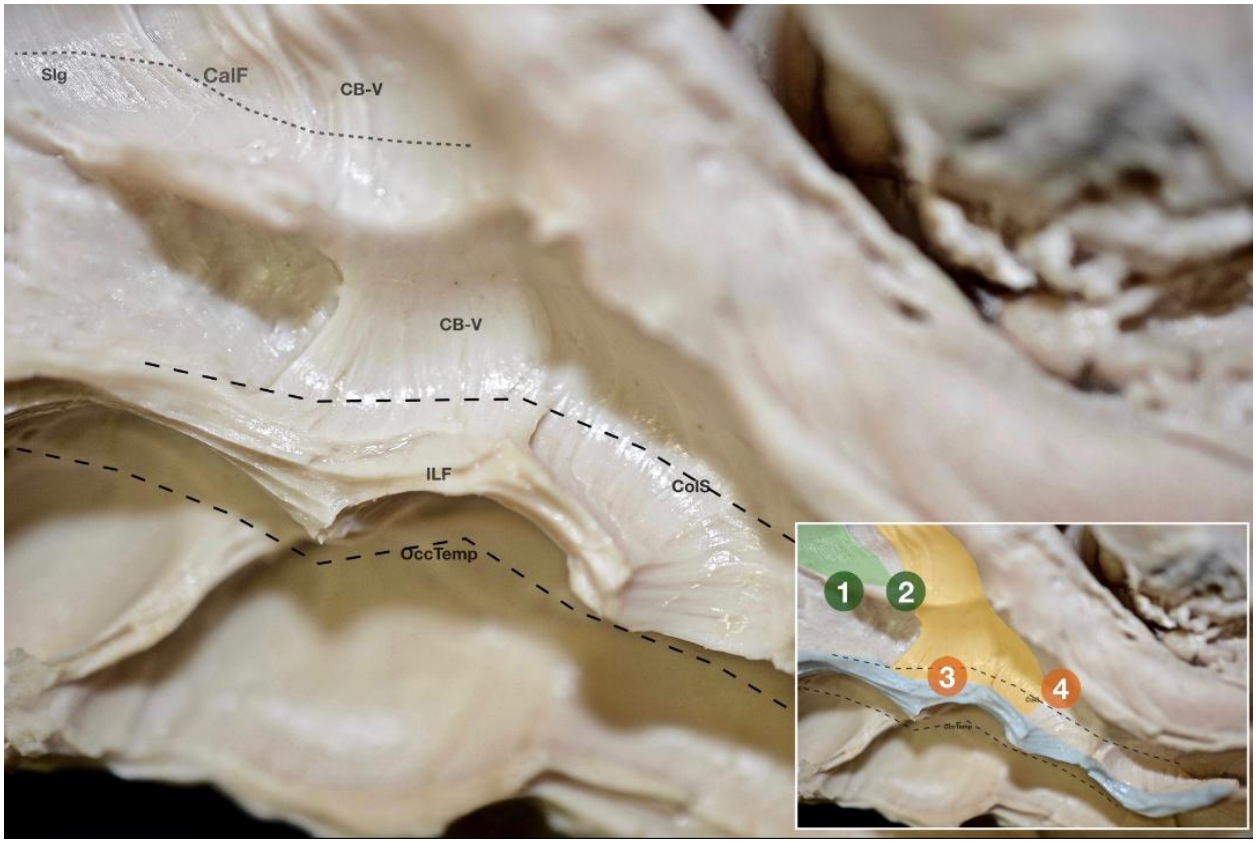


**Figure 3.29** - Close - up of a left hemisphere. Infero-medial view. Inferior terminations of the CB-V and Sledge runner fasciculus illustrated. The Slg terminates inferiorly in the retrosplenial cortex and parahippocampal place area, while CB-V follows a longer trajectory reaching the level of the fusiform gyrus. Inset: The inferiormost terminations of the Sledge runner and CB-V are highlighted in green and yellow color respectively. The Sledge runner terminates in the area of the retrosplenial cortex (1) and parahippocampal place area (2), while the CB-V reaches the middle part of the fusiform gyrus, which corresponds to the fusiform face area (3), and the medial temporal structures (4). ILF is highlighted in blue color. CalF= Calcarine Fissure, CB-V= Cingulum Bundle V, ColS= Collateral Sulcus, ILF= Inferior Longitudinal Fasciculus, OccTemp= Occipitotemporal Sulcus, Slg= Sledge runner fasciculus

In 80% of cases, (12/15 hemispheres), fibers of the CB-V were also recorded to terminate at the medial temporal lobe and more specifically at the lateral piriform area (BA35). This fiber tract follows a dorso-medial to ventrolateral trajectory and usually exhibits three medially projecting knees, specifically at the level of the Forceps Major, Retrosplenial Cortex and parahippocampal gyrus. It displays a triangular silhouette with the narrowest part seen in the area of the posterior precuneus and the widest part in the area of the fusiform gyrus.

*Subcortical correlative anatomy of the CBV*

Inferior arm of the Cingulum and CBV.

Fibers of the inferior arm of the cingulum originate from frontal cortices and bend around the splenium of the corpus callosum in an almost parallel trajectory to the mid-sagittal plane, whereas CBV fibers originate at the precuneus and run in an oblique dorsolateral to ventromedial direction, crossing the parasagittal plane. Although these two bundles exhibit what is widely known as a "kissing pattern" of fiber distribution, indeed the white matter dissection technique has allowed us to specifically differentiate the fibers of the CBV, which are encountered more lateral and caudal in relation to the fibers of the inferior arm of the cingulum.

Sledge Runner Fasciculus and CBV.

We observed the fibers of the cingulum lying adjacent to the fibers of the SR. This relation was particularly tight with regard to the most anteroinferior part of the SR, which runs deep to the isthmus of the cingulate gyrus and posterior part of the parahippocampal gyrus. The Sledge Runner Fasciculus (SRF) is an adjacent fiber tract which also travels in the depth of the POS, at the same plane and in a close spatial relationship with the CBV. (Figures 3.23-3.29) However, in contrast to CBV, which stems from the anterior bank of the POS (caudal precuneus), the SRF originates at the posterior bank of the POS (rostral cuneus) and travels in an oblique rostro-ventral direction following a shorter trajectory and terminating at the RSC, PPA and anterior lingula. CBV and SRF fibers are seen to cross the deep segment of the POS and most probably share common terminations in the PPA area.

Forceps Major and CBV

The forceps major, also known as posterior forceps, consists of fibers originating from the splenium of the corpus callosum that travel towards the occipital cortex. When compared to

the CBV, the fibers of this bundle are seen to reside in a deeper plane and follow a perpendicular trajectory thus creating a superior knee in the dorsal half of the CBV.

ILF

ILF fibers run in the axial plane in the depth of the fusiform gyrus. CBV fibers originate from the precuneus and terminate at the mid-portion of the fusiform gyrus, abutting the fibers of the middle third of the ILF in a perpendicular fashion. The CBV fibers that continue towards the medial temporal pole, travel in a direction parallel to that of the ILF.

*Connectivity pattern*

In all cases, we found CB-V fibers terminating in the area of caudal precuneus (BA7), PPA and Mid-Fusiform gyrus (BA 20&37). Fibers of the CB-V were also recorded to terminate in the Retrosplenial Area (BA29&30) in 93% of cases (14/15). In 80% (12/15) of specimens, we additionally encountered fibers of the CB-V in the lateral piriform cortex (BA35). Material reused from Skandalakis GP et al.[179] by permission of JNS Publishing Group. [7]

# Discussion

To our knowledge this is the first thorough anatomical laboratory investigation on the architecture of the human precuneus. The SRF is a novel fiber tract that was believed to interconnect the precuneus with the lingual gyrus.[9,64]. The SRF was first described in a post-mortem dissection study" in which the authors identified a novel fiber bundle that wasn't previously described and named it "sledge runner fasciculus" after its peculiar shape. In this study the authors explored the white matter architecture of the occipital lobe in three (3) cadaveric hemispheres through the fiber dissection (Klingler's) technique and compared their results to the anatomic atlas written by H. Sachs "The hemispheric white matter of the human brain. Part I: The occipital lobe" (Sachs 1892). During their dissections they found a very close concordance between the histological preparations of Sachs and the Klingler's technique that they used, with the only difference being the identification of an unrecognized fiber pathway located in a plane deep to the calcarine fissure. However, Vergani and colleagues did not proceed to a more detailed description of this tract in terms of morphology, topography and connectivity since it was out of the scope of their manuscript.

In this context, the present study attempts to address this gap and enhance anatomical knowledge regarding the sledge runner fasciculus (SRF) through cadaveric white matter dissection which is considered the gold standard method for investigating novel fiber tracts and is used to validate evidence coming from DTI studies. More specifically, twenty (20) normal adult cadaveric hemispheres were dissected using the Klingler's technique and the microscope with the aim to describe in detail the topography, morphology and connectivity of this elegant fiber tract, establish the degree of correspondence between microanatomic dissection. We therefore consistently identified the SRF as a distinct white matter pathway lying under the U fibers of the medial occipital lobe, exhibiting an oblique dorsomedial to ventrolateral direction and connecting the areas of the anterior cuneus, anterior lingula, isthmus of the cingulum and posterior parahippocampal gyrus. It originates as a relatively narrow tract, at the area of the cuneus, and during its course, it fans out and progressively widens as it descends towards the parahippocampal region, displaying two medial curves at

the level of the forceps major and inferior part of the ventricular atrium respectively. With regard to its topography, the SRF was seen to cross the plane of the calcarine fissure and that of the common trunk formed by the calcarine fissure and parieto-occipital sulcus, thus connecting the cuneus to the lingula and posterior parahippocampal region, while it was observed to course deep to the proximal 1/3 of the parieto-occipital sulcus, connecting the cuneus to the isthmus of the cingulum. It was consistently found not to cross the plane of the sub-parietal sulcus or to enter the white matter of the precuneal lobule. The fibers of the SRF lie in the same plane and just anterior to the fibers of the stratum calcarinum, a vertically oriented white matter tract that connects the upper and lower lips of the calcarine cortex that has been previously described in the anatomic atlas of H. Sachs. The two tracts display a clear boundary in 60% of studied specimens, while in the remaining 40% they were observed to progressively intermingle in their ventral projection, exhibiting however a different trajectory, which aids in their proper identification and differentiation. Due to this elegant morphology, these fiber pathways should be carefully identified and dissected since anatomic misinterpretation can very easily occur. Topographically and in deeper dissection plane, the dorsal part of the SRF was found to correspond to the forceps major while its ventral part to the medial wall of the ventricular atrium.

The first description of the MdLF in humans can be traced back to the recent past when Makris and colleagues provided novel radiological evidence on its existence and structure. The authors, by implementing a focused DTI protocol, supported the hypothesis that the MdLF represents a long cortico-cortical tract between the STG and AG [113]. Subsequent anatomical and anatomo-tractographic studies however underpinned a wider and at times different connectivity pattern, by including various post-rolandic areas such as the SMG, SPL, PrC, occipital lobe, cuneus and have inevitably introduced ambiguity and controversy regarding the tract's inherent architecture. [32,114-116,118,126,197,210]. In this vein, although the main body of DTI data converge on the robust connectivity between the STG and AG [113-116,126,197], the two available anatomic reports suggest otherwise[118,210]. On a closer look, Maldonado and colleagues claim that the thus far prominent MdLF terminations to the AG and SMG were not identified while Wang and colleagues have demonstrated very few fibers terminating to the IPL. Further, Maldonado describes the MdLF largely as a temporo-

occipital tract with no parietal connections while Wang on the contrary emphasizes on the tract's dissemination to the SPL and PrC [118,210].

Hence, in order to clarify the MdLF connectivity pattern, we meticulously investigated all the previously described putative connections of the STG and TP through a focused anatomo-imaging protocol. Indeed, we identified and recorded a tight anatomical relationship with all the aforementioned areas. However, although we have consistently demonstrated the MdLF to pass deep to the IPL (AG and SMG), we did not isolate any significant cortical terminations to the SMG and AG, therefore agreeing with previous anatomical and anatomo-tractographic studies [118,210]. The theory that the SMG-AG complex is as a principal MdLF termination area, advocated by the majority of DTI studies, is in our view susceptible to the inherent limitations of this technique, which are mainly attributed to the crossing, kissing and bending effects of adjacent white matter fibers and which consequently decrease the anatomical accuracy of this method [47,75,97,138,208]. In this regard, the presence of a sizable SLF/AF complex located in a superficial plane to the MdLF in the area of the IPL [64,89] and exhibiting abundant fibers radiating towards the IPS and AG [128] lends support to the notion that the hypothetical MdLF fibers terminating to the AG and identified as such by DTI studies are in essence SLF/AF fibers (Fig. 3). On the contrary, the potential MdLF connections to the SPL, PrC, occipital lobe and cuneus can be readily and consistently identified thus proving that this bundle is both a temporo-parietal and temporo-occipital white matter pathway. Importantly, the qualitative comparison of our dissection and tractography results provides evidence of similar findings concerning the anatomical trajectory of the entire MdLF and its topography in relation to adjacent white matter tracts (i.e. ILF, IFOF, UF, SLF).

Finally, a lack of agreement on whether the MdLF reaches the TP or not can be traced through out the relevant literature. Although the majority of the available DTI evidence points positively towards this direction [114-116,126,197] the study by Conner and colleagues places the MdLF further posteriorly along the temporal lobe [32]. Ambiguity remains even in the two published anatomical reports, with Maldonado and colleagues not reaching a safe conclusion on this issue while Wang and colleagues on the contrary advocate that only the deep and long subcomponent of the MdLF, which terminates at the occipital lobe, reaches the temporal

pole [118,210]. In this study, we have vividly demonstrated and consistently recorded all three segments of the MdLF to terminate in different areas of the TP. Recently, Ding and colleagues parcellated the human temporo-polar Cortex into specific sub-regions by using cytoarchitectonic and chemoarchitectonic methods as well as pathological markers [41]. According to the authors, the area TAr is located at the dorsolateral TP, anterior to the typical TA area or parabelt auditory cortex, the area TAp is located at the dorsal bank of the anterior superior temporal sulcus, and the area TG is a dysgranular region of the most anterior part of the TP, occupying to some extend the dorsal aspect of the TP Our results therefore suggest that the anterior terminations of the MdLF-I and II reside at the TAr area while these of the MdLF-III correspond to the areas TG and TAp. [41]

**Functional Considerations and segmentation pattern of the MdLF**

Early theories have hypothesized that the MdLF is a component of the language pathway [112,113]. This hypothesis was largely based on its connectivity pattern which involved language specific areas such as the STG and IPL; More specifically, on the basis of contemporary speech processing models [61,71], it has been advocated that the STG-AG MdLF connection is implicated in translating phonemes into articulatory forms while the STG-SMG connection subserves phonetic processing [116]. Regarding the non-dominant hemisphere, the MdLF has been associated with visuospatial processing due to its parietal connections [57,58,108]. Beyond language and visuospatial functions, the MdLF has been also linked to the integration of higher order auditory and audiovisual functions [115,116,210] with very recent findings strongly implicating this tract in speech perception and auditory processing ability in noise [197]

In line with our results, evidence from previous anatomical [118] and anatomo-tractographic studies [210] have supported the lack of a rich connectivity between the STG and the IPL (Geschwind's area) through the MdLF. In addition, direct cortical stimulation of the dominant MdLF in 8 patients during awake craniotomies revealed no language interference during picture-naming tasks while the detailed postoperative language assessment following surgical resection of brain regions including the MdLF showed no permanent speech related deficits [36].

However, the intraoperative stimulation and the surgical resections included only the anterior part of the MdLF and therefore no insights were gathered with respect to the function of the posterior part of the tract. Furthermore, a statistically significant leftward lateralization of the MdLF was not disclosed, in terms of descriptive DTI measures such as volume and FA, by previous [113-115,210] and the present study. Conversely, it has been well documented that tracts crucial for language, such as the AF [124] and SLF [110], exhibit considerable asymmetry in terms of volume and FA, according to language lateralization [25]. All the above tend to shift the paradigm of the MdLF away from language functions.

In our study, a tight anatomical relationship between the MdLF and the transverse gyri i.e. the primary and secondary auditory cortices, has been invariably recorded both in white matter dissections and in vivo tractography (Fig. 3). We have thus demonstrated the MdLF-I to course always through the anterior transverse gyrus (Heschl's Gyrus) (Fig. 5b) and the MdLF-II to travel just under the cortex of the posterior transverse gyri/posterior transverse area (Fig. 5c). Further, the observation that the MdLF proves to be the most prominent white matter pathway of the transverse gyri provides a sound structural basis for its alleged functional implication in auditory processing [72,73,101,103]. In that respect, although assumptions on the role of the MdLF in higher auditory processing have been previously made [20,210], none of the published studies has provided anatomical evidence on the structural correlation of the MdLF and its segments with the auditory cortex. The potential auditory role of the MdLF is additionally supported by novel functional data regarding specific subregions of the temporal pole to which the tract is seen to terminate. More specifically, we have demonstrated that the MdLF terminates at the dorsolateral TP and the most anterior part of the STS and TP, areas which correspond to the TAr, TAp and TG subregions respectively [41] (Fig. 5). According to functional studies in non-human primates, the area TAr (Fig. 5) i.e. the equivalent of the dorsolateral TP, has been implicated in high order auditory processing [66,147,164] with remarkable neural activities being detected following specific vocal calls [146]. Moreover, the area TAp, which equals the upper bank and fundus of the superior temporal sulcus, was documented to respond both to auditory and visual stimuli in non-human primates, and has thus been considered as a polysensory association cortex [175,176].

Functional literature focusing on auditory pathways and perception of sounds supports the hypothesis that non-primary auditory cortex located posterior to the Heschl's gyrus is involved in the spatial processing of sounds [19,92,184,185,213,234] while areas in or anterior to Heschl's gyrus subserve the processing of phonetic stimuli [10,136] and pitch characteristics [212]. Further, similar to the well-established dorsal and ventral visual streams, the existence of respective parallel auditory pathways is also advocated by field researchers [107,154,155,192]. More specifically, Ahveninen and colleagues, using functional MRI (fMRI) and magnetoencephalography (MEG) in humans, demonstrated that the "what" auditory pathway, which is responsible for processing auditory object identity characteristics, stems from the anterior auditory cortex (anterolateral Heschl's gyrus, anterior STG and posterior Planum Polare) while the "where" auditory pathway, which is responsible for processing the location characteristics of sound, stems from the posterior auditory cortex (posterior Planum Temporale and STG). Most importantly, they prove that the ''where'' pathway is activated significantly earlier than the ''what'' pathway therefore aiding in auditory object appreciation through a top-down spatial information transmission [1]. In other words, the activation of the "where" pathway precedes in order to shift and maintain the attention towards the identity characteristics of the pertinent auditory object [74].

Hence, in an effort to couple function to anatomy, it could well be argued that the MdLF-II, which is anatomically proved to connect the TAr area to the posterior auditory cortex and posterior parietal cortex, may resemble the posterior or "where" pathway, whereas the MdLF-I, which connects the parietal cortex to the anterior auditory cortex and TAr, could represent the anterior or "what" auditory pathway. Hypothetically, the MdLF-I and MdLF-II as parts of the parallel "what" and "where" pathways, could reciprocally convey information in order to assist in the perception of sounds, possibly through changes in attentional biases. From a hodotopical standpoint, their common termination areas in the TAr [41] and the supero-posterior parietal cortex, could possibly function as hubs for the relay of information through a feed-forward and feed-back interaction. The MdLF-III in turn, which was found to connect the Polysensory area named as TAp [41,175,176] to the AG and occipital lobe/cuneus, could potentially play a role in the integration of auditory and visual information [116].

Finally, studies in patients with Semantic Dementia [34,59,94,131,133,135] and herpes simplex virus encephalitis (HSVE) [80,93,135] as well as data from positron emission tomography (PET) [38,204] and repetitive transcranial magnetic stimulation (rTMS) [95,145] in normal participants point towards a potential role of the TP and anterior temporal lobe in semantic processing and auditory comprehension. More specifically, findings stemming from functional imaging implicate the anterior STG, near the anterior-lateral aspect of Heschl's gyrus, in sublexical processing and auditory word-form recognition [39,40]. In the same vein, intraoperative brain mapping in 90 patients suggests that stimulation of the left STG leads to impairment of auditory single-word comprehension [166]. Keeping with the putative role of MdLF in auditory processing and the fact that it represents an important subcortical connection of the STG, we could further postulate that it might serve as an anatomo-functional interface between auditory representations and semantic/lexical access.

The idea of segmentation of major association tracts such as the Superior Longitudinal Fasciculus and Cingulum has been enthusiastically gaining ground in the field of human brain connectivity as it refines brain circuitry in a more accurate manner. Indeed, a few studies focusing on the anatomy of different components of the SLF, ILF, Arcuate Fasciculus, as well as the cingulum, have been recently published.[84,141,143,218] According to this approach, these fiber pathways can be studied as individual anatomo-functional entities as they exhibit distinctive connectivity in terms of axonal termination patterns, while their structure and function can be conceptualized as the cluster effect of smaller tributaries that converge and contribute to the formation of a main subcortical "river".

In this context, Wu and colleagues, in an anatomo-tractographic study proposed a nuanced segmentation of the cingulum bundle based on the different connectivity of each component. The authors use the term CB-V to describe the segment of the cingulum that connects the precuneus with temporo-basal and temporo-mesial structures. Further, in a study by Jones and colleagues the same bundle -described as the "parahippocampal cingulum"- was recorded to interconnect the posterior precuneus, posterior cingulate cortex and medial

temporal lobe.[78] However, to our knowledge current literature is quite limited on this medially projecting parieto-temporal pathway and therefore its very existence, topography, morphology and intricate anatomical characteristics remain vague to date. With this in mind, we strived to provide original, human, ex vivo, direct structural evidence on the existence of CBV as a discrete component of the cingulum bundle and further on the direct axonal connectivity between the precuneal territory and mesio-temporal regions.

Our results invariably demonstrate that the CB-V exhibits extensive cortical projections and termination points to the caudal precuneus. Findings in healthy individuals suggest that the precuneus is the core structure of the default mode network.[56,200] The idea of the Default Mode Network (DMN) has derived from the classical studies of Shulman and Raichle. [30,62,153] The authors using data stemming from functional imaging (fMRI and PET) observed a group of cortical areas in the human brain, including the posterior cingulate cortex (PCC), medial prefrontal cortex (mPFC) and precuneus, that were consistently found to exhibit reduced activity during non-self-oriented and goal directed tasks. In light of this observation, the term "Default Mode" was coined by Raichle.[151] The very same areas show significant co-activation during resting-state conditions and theoretically support a default-mode of brain function activated during day-dreaming, self-oriented and theory-of-mind related tasks. This task-negative network allegedly participates in high order amodal functions such as self-awareness, mind-wandering and future planning.[62,202]

Moreover, the precuneal lobule is consistently found to activate in a broad range of high-order functions such as navigation, memory retrieval, attention, intelligence comparison, visuo-spatial imagery, representational similarity analysis (RSA) and transitive reasoning.[2,121,139,165,215] In the same vein, data stemming from a recent repetitive transcranial magnetic stimulation (rTMS) study documented the precuneus to be involved in the process of updating place representations during self-motion.[130] Additionally, the CBV is recorded to project to the cortex of the PPA, which is consistently seen to participate in the visuo-spatial circuitry involving location representation, context retrieval as well as perception and utilization of spatial landmarks.[46]

Another key hub area participating in the "navigation pathway" is the retrosplenial cortex also known as retrosplenial complex area (RSC). This region encodes visual information and supports navigation, orientation and spatial memory.[46] According to our results, the CBV exhibits its higher fiber density on this brain region. Similarly, and slightly anteriorly the parahippocampal gyrus was also found to be one of the areas that CB-V fibers constantly radiate. This specific region is implicated in high-level visuospatial perception and memory processing and, as recently demonstrated, the underlying structural architecture of these two aforementioned discrete functions is parceled along the longitudinal axis.[8] More specifically, visuospatial perception is localized at the posterior half of the parahippocampal gyrus whereas the anterior half is involved in contextual memory processing**.** CB-V also exhibits profound cortical projections to the fusiform gyrus and particularly to the Fusiform Face Area (FFA). FFA has been extensively implicated in face recognition, facial expression perception and visual word recognition but it has also been documented to participate in a handful of other visual and memory cognitive processes such as visual mental imagery and visual memory. [67]

We have therefore provided direct structural evidence on the invariable existence, topography, morphology and axonal connectivity of a thus far vague and ambiguous white matter pathway previously coined in the neuroscientific literature as the CBV. This separate bundle of fibers was recorded to participate in the connectivity of high order cerebral areas such as the caudal precuneus, PPA, RSC and FFA.

**Implications in Approaches to the Atrium of the Lateral Ventricle**

CB-V underlies a wide cerebral area which extends from the precuneus to the fusiform gyrus. This region is exposed and manipulated in an effort to elegantly approach and resect lesions residing in or around the atrium of the lateral ventricle. Trigonal/Peritrigonal lesions, have been traditionally accessed through a variety of surgical approaches including the posterior transcallosal corridor or the transcortical operative variants through the inferior parietal lobule or posterior temporal lobe. However, the neurological sequelae linked with these surgical trajectories-including disconnection syndromes, damage to the optic radiations,

dyslexia, agraphia, apraxia, motor disturbances and high incidence of epileptic seizures- have paved the way towards more sophisticated routes in the era of modern Microneurosurgery.

In this context, Yasargil was the first to describe the parieto-occipital interhemispheric trans-precuneus approach for the treatment of Peritrigonal lesions.[195] This surgical avenue was further elaborated by Goel in 1995 who proposed the contralateral interhemispheric transfalcine transprecuneus approach (CITP) to avoid the ill effects of excessive brain retraction.[12,219] Although elegant, these surgical pathways have to inevitably manipulate, retract or even transgress the cortex and white matter of the precuneus and neighboring structures. As shown in the current study, the CB-V radiates to this very same area, lying just laterally to the superficial u-fibers of the posterior precuneus and connecting this cortical hub to the PPA, FFA, Retrosplenial Cortex and Lateral Piriform Cortex therefore participating in a multimodal association network believed to integrate visuospatial, facial, self-relevant and other type of cues with mnemonic functions. Interrupting this network could potentially result in disconnection syndromes involving spatial and episodic memory, awareness as well as the ability to recognize faces.

The supracerebellar transtentorial transcollateral sulcus (STTS) approach described by Kawashima and colleagues is an alternative sophisticated corridor for accessing atrial and peri-atrial lesions.[230] Through a wide transsulcal opening of at least 3cm of the collateral sulcus, the surgeon can allegedly access trigonal/peritrigonal lesions without damaging the optic radiations. However, doubts have been raised with regard to the visual-related morbidity of this approach since the route provided by the collateral sulcus may involve damaging the anterior bundle of the optic radiations.[85] Additionally and in a hodotopical point of view, by interrupting the inferior part of the CB-V within the fusiform gyrus may impede the flow of information arising from BA37 (FFA) relevant to face and word recognition to the precuneal hub.

Limited data exists with regard to memory and supramodal integration deficits following CITP/ STTS approaches.[195] This could be possibly attributed to the fact that a thorough pre-

operative and post-operative neuropsychological battery is required to assess deficits in high-order functions subserved by fine tracts such as the CB-V, something that is not routinely applied in the daily management of such patients. However, in the modern era of extensive multidisciplinary research into the brain connectome, the Neuro-oncology surgeon should be an integral part of scientific groups exploring cerebral structure to function relationships not only by providing in-vivo data though brain mapping techniques but also by investigating the cortico-subcortical architecture through anatomical fiber dissections and DTI protocols.

**Study strengths and limitations**

The revival and utilization of the white matter fiber dissection technique in an effort to unveil the structural architecture of brain connectivity has been mainly fueled by the propagation of MRI based diffusion tensor imaging tractography, since indirect tractographic results have to be fully validated against a robust and direct anatomical method. Undoubtedly, both tensor and non-tensor sophisticated techniques such as HARDI, CSD based and global tractography have significantly improved connectome reconstructions and have led to a more accurate in vivo mapping of the cerebral subcortical architecture. Nevertheless, even the most new and advanced neuroimaging methods generate considerable numbers of false positive tracts, mainly due to noisy (spurious) peaks or from ambiguous fanning and bending fiber populations.[109,156,170,178] This effect is further accentuated when long distance connections are explored, as the reconstruction error accumulates with each tracking step.[109,178,191] It has been therefore emphasized by current literature that the fundamental problem tractography faces is that it infers connectivity from local orientation fields and even in ideal experimental conditions the anatomical accuracy of an indirect method like DWI is suboptimal. [109,156,170,178,191] For these reasons the application of a direct anatomical method like the white matter dissection technique in validating tractographic results and most importantly in ruling out invalid and erroneous tracts is mandatory.

The fiber dissection method (freeze –thaw process) has been microscopically proven to maintain the anatomical integrity of the white matter fibers thus providing structural

evidence of high accuracy.[228] In a further step, the development of the "cortex sparing" white matter dissection approach has allowed for a more detailed and comprehensive investigation of the three dimensional cerebral connectivity and termination pattern of fiber pathways.[123] As such, this technique is currently regarded as the "gold standard' procedure for validating tractographic data and therefore we have been intentionally using it as our basic method to explore the subcortical architecture of complex brain territories and novel or under-recognized fiber tracts.[83,86,102]

This technique, apart from being an in vitro, time consuming, operator dependent and very expensive process it also provides data of lower spatial resolution in comparison to optical coherence tomography.[209] Lastly, in our experience the sensitivity of this method can be relatively reduced when investigating fiber tracts that cross in a perpendicular trajectory, since the proper dissection of the one involves disfigurement of the other.

Studying the subcortical architecture and connectivity through the fiber dissection technique is not just a simple laboratory academic exercise that improves a static view of brain anatomy and sharpens neurosurgical hand skills. Instead, this endeavor provides the neurosurgeon with a more accurate understanding of the brain structure to function relationships and subsequently informs surgical practice not only in the context of modern brain mapping techniques, which aim to optimize the patients' onco-functional balance, but also in the process of pre-operative patient informed consent and approach related decision making.

In a step further, modern neurosurgery is and should remain an integral part of a wider multidisciplinary approach aiming to gain a better insight on cerebral anatomo-functional connectivity, not only by providing awake online data about cognitive behaviors but also by investigating the cortico-subcortical architecture through anatomical fiber dissections and DTI protocols.

## CONCLUSIONS

The surface anatomy of the precuneus exhibits considerable variations due to the intricate patterns the SpS and the POS. Laboratory white matter dissections were employed with the aim to study and record the structural architecture of the SRF, SLF-1, CB-V and MdLF. Our results demonstrate that the SRF is not involved in the axonal connectivity of the precuneus. Instead, we found the SRF connecting the cortical areas of the anterior cuneus, anterior lingula, isthmus of the cingulum and posterior parahippocampal gyrus. Although the SLF-I has been investigated through a number of sophisticated DTI protocols and anatomical studies, ambiguity remains not only regarding its exact structural architecture but also as to whether it represents a discrete anatomical entity or instead an intrinsic part of the cingulum. Through a focused fiber micro-dissection technique, we were able to record the SLF-I as a distinct fiber pathway of the medial cerebral aspect in all cases and elucidate its precise morphological characteristics. Moreover, we provide data supporting the existence of the Cingulum Bundle-V as a discrete subcomponent of the cingulum pathway. We further provide solid structural background on the direct axonal connectivity of the precuneus and medial temporal lobe, cerebral territories that are heavily implicated in the neural circuit of core cognitive functions such as face and word recognition, facial expression perception, spatial navigation and updating, visuo-spatial perception memory and imagery. This constant anatomo-functional "dialogue" between these regions through discrete white matter pathways, provides useful insights on the adjustment and integration of the neural inputs and correlates of complex social cognition. Our results draw on the robust anterior terminations of MdLF to specific subregions of the TP, the intrinsic anatomical relationship of the tract to the auditory cortex and the lack of significant connections with the IPL (SMG and AG). Conversely, in light of the theory of parallel "where" and "what" auditory pathways, the strong relationship of the MdLF with the auditory cortex and the functional role of the cortical areas that it interconnects tend to shift the paradigm towards auditory function. Allegedly, the MdLF-I and MdLF-II as parts of the parallel "what" and "where" pathways, respectively, may play a role in the perception of sounds whereas the MdLF-III could underpin the integration of auditory and visual information. Since recent data support the notion that the TP and anterior STG should be treated as "hubs" for semantic processing and

auditory word-form recognition, the working hypothesis viewing the MdLF as an anatomo-functional interface between auditory representations and semantic/lexical access gains further ground. Lastly, awareness is also raised with regard to the involvement of the CBV in microneurosurgical corridors employed to access lesions residing in or around the atrium of the lateral ventricle.

# References


1. Ahveninen J, Jaaskelainen IP, Raij T, Bonmassar G, Devore S, Hamalainen M, et al: Task-modulated "what" and "where" pathways in human auditory cortex. **Proc Natl Acad Sci U S A 103:**14608-14613, 2006
2. Alfred KL, Connolly AC, Kraemer DJM: Putting the pieces together: Generating a novel representational space through deductive reasoning. **Neuroimage 183:**99-111, 2018
3. Alves RV, Ribas GC, Parraga RG, de Oliveira E: The occipital lobe convexity sulci and gyri. **J Neurosurg 116:**1014-1023, 2012
4. Anatomica N: 1968 Excerpta Medica Foundation. **Amsterdam, New York, London, Paris, Milan, Tokyo, Buenos Aires**
5. Andersen RA, Bracewell RM, Barash S, Gnadt JW, Fogassi L: Eye position effects on visual, memory, and saccade-related activity in areas LIP and 7a of macaque. **Journal of Neuroscience 10:**1176-1196, 1990
6. Bailey P, Bonin GV, McCulloch WS: The isocortex of the chimpanzee. 1950
7. Basser PJ, Mattiello J, LeBihan D: MR diffusion tensor spectroscopy and imaging. **Biophysical journal 66:**259-267, 1994
8. Baumann O, Mattingley JB: Functional Organization of the Parahippocampal Cortex: Dissociable Roles for Context Representations and the Perception of Visual Scenes. **J Neurosci 36:**2536-2542, 2016
9. Baydin S, Gungor A, Tanriover N, Baran O, Middlebrooks EH, Rhoton Jr AL: Fiber tracts of the medial and inferior surfaces of the cerebrum. **World neurosurgery 98:**34-49, 2017
10. Binder JR, Frost JA, Hammeke TA, Bellgowan PS, Springer JA, Kaufman JN, et al: Human temporal lobe activation by speech and nonspeech sounds. **Cerebral cortex 10:**512-528, 2000
11. Blum JS, Chow KL, Pribram KH: A behavioral analysis of the organization of the parieto-temporo-preoccipital cortex. **Journal of Comparative Neurology (and Psychology)**, 1950
12. Bohnstedt BN, Kulwin CG, Shah MV, Cohen-Gadol AA: Posterior interhemispheric transfalcine transprecuneus approach for microsurgical resection of periatrial lesions: indications, technique, and outcomes. **J Neurosurg 123:**1045-1054, 2015
13. Boling W, Olivier A, Bittar RG, Reutens D: Localization of hand motor activation in Broca's pli de passage moyen. **Journal of neurosurgery 91:**903-910, 1999
14. Bozkurt B, Yagmurlu K, Middlebrooks EH, Karadag A, Ovalioglu TC, Jagadeesan B, et al: Microsurgical and tractographic anatomy of the supplementary motor area complex in humans. **World neurosurgery 95:**99-107, 2016
15. Bremmer F, Schlack A, Duhamel J-R, Graf W, Fink GR: Space coding in primate posterior parietal cortex. **Neuroimage 14:**S46-S51, 2001

16. Broca P: Remarques sur le siège de la faculté du langage articulé, suivies d'une observation d'aphémie (perte de la parole). **Bulletin et Memoires de la Societe anatomique de Paris 6:**330-357, 1861
17. Brodal A: Neurological Anatomy in Relation to Clinical Medicine 3rd edn Oxford University Press. **New York**, 1981
18. Brodmann K: **Vergleichende Lokalisationslehre der Grosshirnrinde in ihren Prinzipien dargestellt auf Grund des Zellenbaues**: Barth, 1909
19. Brunetti M, Belardinelli P, Caulo M, Del Gratta C, Della Penna S, Ferretti A, et al: Human brain activation during passive listening to sounds from different locations: an fMRI and MEG study. **Human brain mapping 26:**251-261, 2005
20. Burks JD, Boettcher LB, Conner AK, Glenn CA, Bonney PA, Baker CM, et al: White matter connections of the inferior parietal lobule: A study of surgical anatomy. **Brain Behav 7:**e00640, 2017
21. Burles F, Slone E, Iaria G: Dorso-medial and ventro-lateral functional specialization of the human retrosplenial complex in spatial updating and orienting. **Brain Struct Funct 222:**1481-1493, 2017
22. Caminiti R: From vision to movement: combinatorial computations in the dorsal stream. **Vision and movement mechanisms in the cerebral cortex Strasbourg: Human Frontier Science Program:**42-49, 1996
23. Caminiti R, Genovesio A, Marconi B, Mayer AB, Onorati P, Ferraina S, et al: Early coding of reaching: frontal and parietal association connections of parieto-occipital cortex. **European Journal of Neuroscience 11:**3339-3345, 1999
24. Campbell AW: **Histological studies on the localisation of cerebral function**: University Press, 1905
25. Catani M, Allin MP, Husain M, Pugliese L, Mesulam MM, Murray RM, et al: Symmetries in human brain language pathways correlate with verbal recall. **Proc Natl Acad Sci U S A 104:**17163-17168, 2007
26. Catani M, Catani M: From hodology to function. **Brain 130:**602-605, 2007
27. Catani M, De Schotten MT: A diffusion tensor imaging tractography atlas for virtual in vivo dissections. **cortex 44:**1105-1132, 2008
28. Catani M, Howard RJ, Pajevic S, Jones DK: Virtual in vivo interactive dissection of white matter fasciculi in the human brain. **Neuroimage 17:**77-94, 2002
29. Cavada C, Goldman-Rakic PS: Posterior parietal cortex in rhesus monkey: II. Evidence for segregated corticocortical networks linking sensory and limbic areas with the frontal lobe. **Journal of Comparative Neurology 287:**422-445, 1989
30. Cavanna AE, Trimble MR: The precuneus: a review of its functional anatomy and behavioural correlates. **Brain 129:**564-583, 2006
31. Cavanna AE, Trimble MR: The precuneus: a review of its functional anatomy and behavioural correlates. **Brain 129:**564-583, 2006
32. Conner AK, Briggs RG, Rahimi M, Sali G, Baker CM, Burks JD, et al: A Connectomic Atlas of the Human Cerebrum-Chapter 12: Tractographic Description of the Middle Longitudinal Fasciculus. **Oper Neurosurg (Hagerstown) 15:**S429-S435, 2018
33. Critchley M: The parietal lobes. 1953

34. Davies R, Graham KS, Xuereb JH, Williams GB, Hodges JR: The human perirhinal cortex and semantic memory. **European Journal of Neuroscience 20:**2441-2446, 2004
35. De Benedictis A, Duffau H: Brain hodotopy: from esoteric concept to practical surgical applications. **Neurosurgery 68:**1703-1723, 2011
36. De Witt Hamer PC, Moritz-Gasser S, Gatignol P, Duffau H: Is the human left middle longitudinal fascicle essential for language? A brain electrostimulation study. **Human brain mapping 32:**962-973, 2011
37. Dejerine J, Dejerine-Klumpke A: **Anatomie des centres nerveux: Méthodes générales d'étude-embryologie-histogénèse et histologie. Anatomie du cerveau**: Rueff, 1895, Vol 1
38. Devlin JT, Russell RP, Davis MH, Price CJ, Wilson J, Moss HE, et al: Susceptibility-induced loss of signal: comparing PET and fMRI on a semantic task. **Neuroimage 11:**589-600, 2000
39. DeWitt I, Rauschecker JP: Convergent evidence for the causal involvement of anterior superior temporal gyrus in auditory single-word comprehension. **Cortex 77:**164-166, 2016
40. DeWitt I, Rauschecker JP: Wernicke's area revisited: parallel streams and word processing. **Brain and language 127:**181-191, 2013
41. Ding SL, Van Hoesen GW, Cassell MD, Poremba A: Parcellation of human temporal polar cortex: a combined analysis of multiple cytoarchitectonic, chemoarchitectonic, and pathological markers. **J Comp Neurol 514:**595-623, 2009
42. Duffau H: **Brain mapping: from neural basis of cognition to surgical applications**: Springer Science & Business Media, 2011
43. Duffau H: Hodotopy, neuroplasticity and diffuse gliomas. **Neurochirurgie 63:**259-265, 2017
44. Duffau H, Duffau H: Awake surgery for non-language mapping. **Neurosurgery**, 2010
45. Duvernoy H: The Human Brain Springer-Verlag. **New York**, 1991
46. Epstein RA, Patai EZ, Julian JB, Spiers HJ: The cognitive map in humans: spatial navigation and beyond. **Nat Neurosci 20:**1504-1513, 2017
47. Fernandez-Miranda JC, Pathak S, Engh J, Jarbo K, Verstynen T, Yeh FC, et al: High-definition fiber tractography of the human brain: neuroanatomical validation and neurosurgical applications. **Neurosurgery 71:**430-453, 2012
48. Fernández-Miranda JC, Rhoton AL, Kakizawa Y, Choi C, Álvarez-Linera J: The claustrum and its projection system in the human brain: a microsurgical and tractographic anatomical study. **Journal of neurosurgery 108:**764-774, 2008
49. Fernández-Miranda JC, Rhoton Jr AL, Álvarez-Linera J, Kakizawa Y, Choi C, de Oliveira EP: Three-dimensional microsurgical and tractographic anatomy of the white matter of the human brain. **Neurosurgery 62:**SHC989-SHC1028, 2008
50. Ferraina S, Johnson P, Garasto M, Battaglia-Mayer A, Ercolani L, Bianchi L, et al: Combination of hand and gaze signals during reaching: activity in parietal area 7m of the monkey. **Journal of neurophysiology 77:**1034-1038, 1997
51. Filley CM: The behavioral neurology of cerebral white matter. **Neurology 50:**1535-1540, 1998

52. Filley CM: White matter and behavioral neurology. **Ann N Y Acad Sci 1064:**162-183, 2005
53. Finger S: **Origins of neuroscience: a history of explorations into brain function**: Oxford University Press, USA, 2001
54. Foville AL: **Traité complet de l'anatomie, de la physiologie et de la pathologie du système nerveux cérébro-spinal**: Fortin, Masson et cie, 1844, Vol 2
55. Frackowiak RS: **Human brain function**: Elsevier, 2004
56. Fransson P, Marrelec G: The precuneus/posterior cingulate cortex plays a pivotal role in the default mode network: Evidence from a partial correlation network analysis. **Neuroimage 42:**1178-1184, 2008
57. Galati G, Committeri G, Sanes JN, Pizzamiglio L: Spatial coding of visual and somatic sensory information in body-centred coordinates. **Eur J Neurosci 14:**737-746, 2001
58. Galletti C, Fattori P: Posterior parietal networks encoding visual space. 2002
59. Galton CJ, Patterson K, Graham K, Lambon-Ralph MA, Williams G, Antoun N, et al: Differing patterns of temporal atrophy in Alzheimer's disease and semantic dementia. **Neurology 57:**216-225, 2001
60. Goldman-Rakic PS: Topography of cognition: parallel distributed networks in primate association cortex. **Annual review of neuroscience**, 1988
61. Gow Jr DW, Segawa JA, Ahlfors SP, Lin F-H: Lexical influences on speech perception: a Granger causality analysis of MEG and EEG source estimates. **Neuroimage 43:**614-623, 2008
62. Greicius MD, Krasnow B, Reiss AL, Menon V: Functional connectivity in the resting brain: a network analysis of the default mode hypothesis. **Proc Natl Acad Sci U S A 100:**253-258, 2003
63. Güngör A, Baydin S, Middlebrooks EH, Tanriover N, Isler C, Rhoton AL: The white matter tracts of the cerebrum in ventricular surgery and hydrocephalus. **Journal of neurosurgery 126:**945-971, 2017
64. Gungor A, Baydin S, Middlebrooks EH, Tanriover N, Isler C, Rhoton AL, Jr.: The white matter tracts of the cerebrum in ventricular surgery and hydrocephalus. **J Neurosurg 126:**945-971, 2017
65. Gürer B, Bozkurt M, Neves G, Cikla U, Hananya T, Antar V, et al: The subparietal and parietooccipital sulci: an anatomical study. **Clinical Anatomy 26:**667-674, 2013
66. Hackett TA, Stepniewska I, Kaas JH: Prefrontal connections of the parabelt auditory cortex in macaque monkeys. **Brain Res 817:**45-58, 1999
67. Harvey DY, Burgund ED: Neural adaptation across viewpoint and exemplar in fusiform cortex. **Brain Cogn 80:**33-44, 2012
68. Hau J, Sarubbo S, Perchey G, Crivello F, Zago L, Mellet E, et al: Cortical terminations of the inferior fronto-occipital and uncinate fasciculi: anatomical stem-based virtual dissection. **Frontiers in neuroanatomy 10:**58, 2016
69. Hebscher M, Levine B, Gilboa A: The precuneus and hippocampus contribute to individual differences in the unfolding of spatial representations during episodic autobiographical memory. **Neuropsychologia 110:**123-133, 2018
70. Heimer L: **The human brain and spinal cord: functional neuroanatomy and dissection guide**: Springer Science & Business Media, 2012

71. Hickok G, Poeppel D: The cortical organization of speech processing. **Nat Rev Neurosci 8:**393-402, 2007
72. Howard MA, 3rd, Volkov IO, Abbas PJ, Damasio H, Ollendieck MC, Granner MA: A chronic microelectrode investigation of the tonotopic organization of human auditory cortex. **Brain Res 724:**260-264, 1996
73. Howard MA, Volkov IO, Mirsky R, Garell PC, Noh MD, Granner M, et al: Auditory cortex on the human posterior superior temporal gyrus. **J Comp Neurol 416:**79-92, 2000
74. Jääskeläinen IP, Ahveninen J, Bonmassar G, Dale AM, Ilmoniemi RJ, Levänen S, et al: Human posterior auditory cortex gates novel sounds to consciousness. **Proceedings of the National Academy of Sciences 101:**6809-6814, 2004
75. Johansen-Berg H, Rushworth MF: Using diffusion imaging to study human connectional anatomy. **Annu Rev Neurosci 32:**75-94, 2009
76. Johnson P: S., Ferraina, L. Bianchi, and R. Caminiti (1996) Cortical networks for visual reaching: Physiological and anatomical organization of frontal and parietal lobe arm regions. **Cerebral Cortex 6:**102-119
77. Johnson PB, Ferraina S, Caminiti R: Cortical networks for visual reaching. **Experimental Brain Research 97:**361-365, 1993
78. Jones DK, Christiansen KF, Chapman RJ, Aggleton JP: Distinct subdivisions of the cingulum bundle revealed by diffusion MRI fibre tracking: implications for neuropsychological investigations. **Neuropsychologia 51:**67-78, 2013
79. Kalyvas A, Koutsarnakis C, Komaitis S, Karavasilis E, Christidi F, Skandalakis GP, et al: Mapping the human middle longitudinal fasciculus through a focused anatomo-imaging study: shifting the paradigm of its segmentation and connectivity pattern. **Brain Structure and Function 225:**85-119, 2020
80. Kapur N, Barker S, Burrows E, Ellison D, Brice J, Illis L, et al: Herpes simplex encephalitis: long term magnetic resonance imaging and neuropsychological profile. **Journal of Neurology, Neurosurgery & Psychiatry 57:**1334-1342, 1994
81. Klingler J: **Erleichterung der makrokopischen Präparation des Gehirns durch den Gefrierprozess**: Orell Füssli, 1935
82. Klingler J, Ludwig E: **Atlas cerebri humani**: Karger Publishers, 1956
83. Komaitis S, Kalyvas AV, Skandalakis GP, Drosos E, Lani E, Liouta E, et al: The frontal longitudinal system as revealed through the fiber microdissection technique: structural evidence underpinning the direct connectivity of the prefrontal-premotor circuitry. **J Neurosurg:**1-13, 2019
84. Komaitis S, Skandalakis GP, Kalyvas AV, Drosos E, Lani E, Emelifeonwu J, et al: Dorsal component of the superior longitudinal fasciculus revisited: novel insights from a focused fiber dissection study. **J Neurosurg:**1-14, 2019
85. Koutsarnakis C, Kalyvas AV, Komaitis S, Liakos F, Skandalakis GP, Anagnostopoulos C, et al: Defining the relationship of the optic radiation to the roof and floor of the ventricular atrium: a focused microanatomical study. **J Neurosurg:**1-12, 2018
86. Koutsarnakis C, Kalyvas AV, Skandalakis GP, Karavasilis E, Christidi F, Komaitis S, et al: Sledge runner fasciculus: anatomic architecture and tractographic morphology. **Brain Struct Funct 224:**1051-1066, 2019

87. Koutsarnakis C, Kalyvas AV, Skandalakis GP, Karavasilis E, Christidi F, Komaitis S, et al: Sledge runner fasciculus: anatomic architecture and tractographic morphology. **Brain Struct Funct**, 2019
88. Koutsarnakis C, Liakos F, Kalyvas AV, Sakas DE, Stranjalis G: A laboratory manual for stepwise cerebral white matter fiber dissection. **World neurosurgery 84:**483-493, 2015
89. Koutsarnakis C, Liakos F, Kalyvas AV, Sakas DE, Stranjalis G: A Laboratory Manual for Stepwise Cerebral White Matter Fiber Dissection. **World Neurosurg 84:**483-493, 2015
90. Koutsarnakis C, Liakos F, Kalyvas AV, Skandalakis GP, Komaitis S, Christidi F, et al: The Superior Frontal Transsulcal Approach to the Anterior Ventricular System: Exploring the Sulcal and Subcortical Anatomy Using Anatomic Dissections and Diffusion Tensor Imaging Tractography. **World Neurosurg 106:**339-354, 2017
91. Koutsarnakis C, Liakos F, Liouta E, Themistoklis K, Sakas D, Stranjalis G: The cerebral isthmus: fiber tract anatomy, functional significance, and surgical considerations. **J Neurosurg 124:**450-462, 2016
92. Krumbholz K, Schönwiesner M, von Cramon DY, Rübsamen R, Shah NJ, Zilles K, et al: Representation of interaural temporal information from left and right auditory space in the human planum temporale and inferior parietal lobe. **Cerebral Cortex 15:**317-324, 2004
93. Lambon Ralph MA, Lowe C, Rogers TT: Neural basis of category-specific semantic deficits for living things: evidence from semantic dementia, HSVE and a neural network model. **Brain 130:**1127-1137, 2007
94. Lambon Ralph MA, Patterson K: Generalization and differentiation in semantic memory: insights from semantic dementia. **Annals of the New York Academy of Sciences 1124:**61-76, 2008
95. Lambon Ralph MA, Pobric G, Jefferies E: Conceptual knowledge is underpinned by the temporal pole bilaterally: convergent evidence from rTMS. **Cerebral Cortex 19:**832-838, 2008
96. Le Bihan D, Mangin JF, Poupon C, Clark CA, Pappata S, Molko N, et al: Diffusion tensor imaging: concepts and applications. **Journal of Magnetic Resonance Imaging: An Official Journal of the International Society for Magnetic Resonance in Medicine 13:**534-546, 2001
97. Le Bihan D, Poupon C, Amadon A, Lethimonnier F: Artifacts and pitfalls in diffusion MRI. **J Magn Reson Imaging 24:**478-488, 2006
98. Leichnetz G, Goldberg M: Higher centers concerned with eye movement and visual attention: cerebral cortex and thalamus. **Reviews of oculomotor research 2:**365, 1988
99. Leichnetz G, Gonzalo-Ruiz A: Prearcuate cortex in the Cebus monkey has cortical and subcortical connections like the macaque frontal eye field and projects to fastigial-recipient oculomotor-related brainstem nuclei. **Brain research bulletin 41:**1-29, 1996
100. Leichnetz GR: Connections of the medial posterior parietal cortex (area 7m) in the monkey. **The Anatomical Record: An Official Publication of the American Association of Anatomists 263:**215-236, 2001
101. Lewald J, Getzmann S: When and where of auditory spatial processing in cortex: a novel approach using electrotomography. **PLoS One 6:**e25146, 2011

102. Liakos F, Koutsarnakis C: The role of white matter dissection technique in modern neuroimaging: can neuroradiologists benefit from its use? **Surg Radiol Anat 38:**275-276, 2016
103. Liegeois-Chauvel C, Musolino A, Chauvel P: Localization of the primary auditory area in man. **Brain 114 ( Pt 1A):**139-151, 1991
104. Liouta E, Stranjalis G, Kalyvas AV, Koutsarnakis C, Pantinaki S, Liakos F, et al: Parietal association deficits in patients harboring parietal lobe gliomas: a prospective study. **Journal of neurosurgery 130:**773-779, 2018
105. Liu Z, Zhang J, Zhang K, Zhang J, Li X, Cheng W, et al: Distinguishable brain networks relate disease susceptibility to symptom expression in schizophrenia. **Hum Brain Mapp 39:**3503-3515, 2018
106. Logothetis NK, Pauls J, Augath M, Trinath T, Oeltermann A: Neurophysiological investigation of the basis of the fMRI signal. **Nature 412:**150, 2001
107. Lomber SG, Malhotra S: Double dissociation of'what'and'where'processing in auditory cortex. **Nature neuroscience 11:**609, 2008
108. Macaluso E, Driver J, Frith CD: Multimodal spatial representations engaged in human parietal cortex during both saccadic and manual spatial orienting. **Current Biology 13:**990-999, 2003
109. Maier-Hein KH, Neher PF, Houde JC, Cote MA, Garyfallidis E, Zhong J, et al: The challenge of mapping the human connectome based on diffusion tractography. **Nat Commun 8:**1349, 2017
110. Makris N, Kennedy DN, McInerney S, Sorensen AG, Wang R, Caviness Jr VS, et al: Segmentation of subcomponents within the superior longitudinal fascicle in humans: a quantitative, in vivo, DT-MRI study. **Cerebral cortex 15:**854-869, 2004
111. Makris N, Meyer JW, Bates JF, Yeterian EH, Kennedy DN, Caviness VS: MRI-Based topographic parcellation of human cerebral white matter and nuclei II. Rationale and applications with systematics of cerebral connectivity. **Neuroimage 9:**18-45, 1999
112. Makris N, Pandya DN: The extreme capsule in humans and rethinking of the language circuitry. **Brain Struct Funct 213:**343-358, 2009
113. Makris N, Papadimitriou GM, Kaiser JR, Sorg S, Kennedy DN, Pandya DN: Delineation of the middle longitudinal fascicle in humans: a quantitative, in vivo, DT-MRI study. **Cereb Cortex 19:**777-785, 2009
114. Makris N, Preti MG, Asami T, Pelavin P, Campbell B, Papadimitriou GM, et al: Human middle longitudinal fascicle: variations in patterns of anatomical connections. **Brain Struct Funct 218:**951-968, 2013
115. Makris N, Preti MG, Wassermann D, Rathi Y, Papadimitriou GM, Yergatian C, et al: Human middle longitudinal fascicle: segregation and behavioral-clinical implications of two distinct fiber connections linking temporal pole and superior temporal gyrus with the angular gyrus or superior parietal lobule using multi-tensor tractography. **Brain Imaging Behav 7:**335-352, 2013
116. Makris N, Zhu A, Papadimitriou GM, Mouradian P, Ng I, Scaccianoce E, et al: Mapping temporo-parietal and temporo-occipital cortico-cortical connections of the human middle longitudinal fascicle in subject-specific, probabilistic, and stereotaxic Talairach spaces. **Brain Imaging Behav 11:**1258-1277, 2017

117. Maldjian JA, Laurienti PJ, Kraft RA, Burdette JH: An automated method for neuroanatomic and cytoarchitectonic atlas-based interrogation of fMRI data sets. **Neuroimage 19:**1233-1239, 2003
118. Maldonado IL, de Champfleur NM, Velut S, Destrieux C, Zemmoura I, Duffau H: Evidence of a middle longitudinal fasciculus in the human brain from fiber dissection. **J Anat 223:**38-45, 2013
119. Mancini M, Mastropasqua C, Bonni S, Ponzo V, Cercignani M, Conforto S, et al: Theta Burst Stimulation of the Precuneus Modulates Resting State Connectivity in the Left Temporal Pole. **Brain Topogr 30:**312-319, 2017
120. Mandonnet E, Sarubbo S, Petit L: The Nomenclature of Human White Matter Association Pathways: Proposal for a Systematic Taxonomic Anatomical Classification. **Front Neuroanat 12:**94, 2018
121. Marchette SA, Vass LK, Ryan J, Epstein RA: Anchoring the neural compass: coding of local spatial reference frames in human medial parietal lobe. **Nat Neurosci 17:**1598-1606, 2014
122. Martino J, Brogna C, Robles SG, Vergani F, Duffau H: Anatomic dissection of the inferior fronto-occipital fasciculus revisited in the lights of brain stimulation data. **cortex 46:**691-699, 2010
123. Martino J, De Witt Hamer PC, Vergani F, Brogna C, de Lucas EM, Vazquez-Barquero A, et al: Cortex-sparing fiber dissection: an improved method for the study of white matter anatomy in the human brain. **J Anat 219:**531-541, 2011
124. Matsumoto R, Okada T, Mikuni N, Mitsueda-Ono T, Taki J, Sawamoto N, et al: Hemispheric asymmetry of the arcuate fasciculus: a preliminary diffusion tensor tractography study in patients with unilateral language dominance defined by Wada test. **J Neurol 255:**1703-1711, 2008
125. Mazziotta J, Toga A, Evans A, Fox P, Lancaster J, Zilles K, et al: A probabilistic atlas and reference system for the human brain: International Consortium for Brain Mapping (ICBM). **Philosophical Transactions of the Royal Society of London. Series B: Biological Sciences 356:**1293-1322, 2001
126. Menjot de Champfleur N, Lima Maldonado I, Moritz-Gasser S, Machi P, Le Bars E, Bonafe A, et al: Middle longitudinal fasciculus delineation within language pathways: a diffusion tensor imaging study in human. **Eur J Radiol 82:**151-157, 2013
127. Mesulam M-M, Van Hoesen GW, Pandya DN, Geschwind N: Limbic and sensory connections of the inferior parietal lobule (area PG) in the rhesus monkey: a study with a new method for horseradish peroxidase histochemistry. **Brain research 136:**393-414, 1977
128. Monroy-Sosa A, Jennings J, Chakravarthi S, Fukui MB, Celix J, Kojis N, et al: Microsurgical Anatomy of the Vertical Rami of the Superior Longitudinal Fasciculus: An Intraparietal Sulcus Dissection Study. **Oper Neurosurg (Hagerstown) 16:**226-238, 2019
129. Mori S, Zhang J: Principles of diffusion tensor imaging and its applications to basic neuroscience research. **Neuron 51:**527-539, 2006
130. Muller NG, Riemer M, Brandt L, Wolbers T: Repetitive transcranial magnetic stimulation reveals a causal role of the human precuneus in spatial updating. **Sci Rep 8:**10171, 2018

131. Mummery CJ, Patterson K, Price CJ, Ashburner J, Frackowiak RS, Hodges JR: A voxel-based morphometry study of semantic dementia: relationship between temporal lobe atrophy and semantic memory. **Annals of neurology 47:**36-45, 2000
132. Naidich TP, Valavanis AG, Kubik S: Anatomic relationships along the low-middle convexity: Part I-Normal specimens and magnetic resonance imaging. **Neurosurgery 36:**517-532, 1995
133. Nestor PJ, Fryer TD, Hodges JR: Declarative memory impairments in Alzheimer's disease and semantic dementia. **Neuroimage 30:**1010-1020, 2006
134. Nieuwenhuys R, Donkelaar H, Nicholson C: The central nervous system of vertebrates. 1998. **PRO EDIT GmbH, Heidelberg**, 2002
135. Noppeney U, Patterson K, Tyler LK, Moss H, Stamatakis EA, Bright P, et al: Temporal lobe lesions and semantic impairment: a comparison of herpes simplex virus encephalitis and semantic dementia. **Brain 130:**1138-1147, 2007
136. Obleser J, Boecker H, Drzezga A, Haslinger B, Hennenlotter A, Roettinger M, et al: Vowel sound extraction in anterior superior temporal cortex. **Human brain mapping 27:**562-571, 2006
137. Ono M, Kubik S, Abernathey CD: **Atlas of the cerebral sulci**: Thieme Medical Publishers, 1990
138. Oouchi H, Yamada K, Sakai K, Kizu O, Kubota T, Ito H, et al: Diffusion anisotropy measurement of brain white matter is affected by voxel size: underestimation occurs in areas with crossing fibers. **AJNR Am J Neuroradiol 28:**1102-1106, 2007
139. Paladini RE, Muri RM, Meichtry J, Nef T, Mast FW, Mosimann UP, et al: The Influence of Alertness on the Spatial Deployment of Visual Attention is Mediated by the Excitability of the Posterior Parietal Cortices. **Cereb Cortex 27:**233-243, 2017
140. Pandya DN, Seltzer B: Intrinsic connections and architectonics of posterior parietal cortex in the rhesus monkey. **Journal of Comparative Neurology 204:**196-210, 1982
141. Panesar SS, Belo JTA, Yeh FC, Fernandez-Miranda JC: Structure, asymmetry, and connectivity of the human temporo-parietal aslant and vertical occipital fasciculi. **Brain Struct Funct 224:**907-923, 2019
142. Panesar SS, Yeh F-C, Deibert CP, Fernandes-Cabral D, Rowthu V, Celtikci P, et al: A diffusion spectrum imaging-based tractographic study into the anatomical subdivision and cortical connectivity of the ventral external capsule: uncinate and inferior fronto-occipital fascicles. **Neuroradiology 59:**971-987, 2017
143. Panesar SS, Yeh FC, Jacquesson T, Hula W, Fernandez-Miranda JC: A Quantitative Tractography Study Into the Connectivity, Segmentation and Laterality of the Human Inferior Longitudinal Fasciculus. **Front Neuroanat 12:**47, 2018
144. Petrides M, Pandya DN: Projections to the frontal cortex from the posterior parietal region in the rhesus monkey. **Journal of Comparative neurology 228:**105-116, 1984
145. Pobric G, Jefferies E, Ralph MAL: Anterior temporal lobes mediate semantic representation: mimicking semantic dementia by using rTMS in normal participants. **Proceedings of the National Academy of Sciences 104:**20137-20141, 2007
146. Poremba A, Malloy M, Saunders RC, Carson RE, Herscovitch P, Mishkin M: Species-specific calls evoke asymmetric activity in the monkey's temporal poles. **Nature 427:**448-451, 2004

147. Poremba A, Saunders RC, Crane AM, Cook M, Sokoloff L, Mishkin M: Functional mapping of the primate auditory system. **Science 299:**568-572, 2003
148. Pribram HB, Barry J: Further behavioral analysis of parietotemporo-preoccipital cortex. **Journal of Neurophysiology 19:**99-106, 1956
149. Price CJ: The anatomy of language: contributions from functional neuroimaging. **The Journal of Anatomy 197:**335-359, 2000
150. Quiñones-Hinojosa A, Ojemann SG, Sanai N, Dillon WP, Berger MS: Preoperative correlation of intraoperative cortical mapping with magnetic resonance imaging landmarks to predict localization of the Broca area. **Journal of neurosurgery 99:**311-318, 2003
151. Raichle ME: The brain's default mode network. **Annu Rev Neurosci 38:**433-447, 2015
152. Raichle ME: A brief history of human brain mapping. **Trends in neurosciences 32:**118-126, 2009
153. Raichle ME, MacLeod AM, Snyder AZ, Powers WJ, Gusnard DA, Shulman GL: A default mode of brain function. **Proc Natl Acad Sci U S A 98:**676-682, 2001
154. Rauschecker JP, Scott SK: Maps and streams in the auditory cortex: nonhuman primates illuminate human speech processing. **Nat Neurosci 12:**718-724, 2009
155. Rauschecker JP, Tian B: Mechanisms and streams for processing of "what" and "where" in auditory cortex. **Proc Natl Acad Sci U S A 97:**11800-11806, 2000
156. Reveley C, Seth AK, Pierpaoli C, Silva AC, Yu D, Saunders RC, et al: Superficial white matter fiber systems impede detection of long-range cortical connections in diffusion MR tractography. **Proc Natl Acad Sci U S A 112:**E2820-2828, 2015
157. Rhoton Jr AL: The cerebrum. **Neurosurgery 51:**S1-1-S1-52, 2002
158. Rhoton Jr AL: **Rhoton's cranial anatomy and surgical approaches**: Oxford University Press, 2019
159. Ribas G: Surgical anatomy of microneurosurgical sulcal key-points.{thesis}. **Faculdade de Medicina, Universidade de São Paulo, São Paulo (in Portuguese)**, 2005
160. Ribas GC: The cerebral sulci and gyri. **Neurosurgical focus 28:**E2, 2010
161. Ribas GC, Ribas EC, Rodrigues CJ: The anterior sylvian point and the suprasylvian operculum. **Neurosurgical focus 18:**1-6, 2005
162. Ribas GC, Yasuda A, Ribas EC, Nishikuni K, Rodrigues Jr AJ: Surgical anatomy of microneurosurgical sulcal key points. **Operative Neurosurgery 59:**ONS-177-ONS-211, 2006
163. Rilling JK, Glasser MF, Preuss TM, Ma X, Zhao T, Hu X, et al: The evolution of the arcuate fasciculus revealed with comparative DTI. **Nat Neurosci 11:**426-428, 2008
164. Romanski LM, Bates JF, Goldman-Rakic PS: Auditory belt and parabelt projections to the prefrontal cortex in the rhesus monkey. **J Comp Neurol 403:**141-157, 1999
165. Rosen ML, Stern CE, Devaney KJ, Somers DC: Cortical and Subcortical Contributions to Long-Term Memory-Guided Visuospatial Attention. **Cereb Cortex 28:**2935-2947, 2018
166. Roux F-E, Minkin K, Durand J-B, Sacko O, Réhault E, Tanova R, et al: Electrostimulation mapping of comprehension of auditory and visual words. **Cortex 71:**398-408, 2015
167. Salamon G, Salamon-Murayama N, Mongkolwat P, Russell EJ: Magnetic resonance imaging study of the parietal lobe: anatomic and radiologic correlations. **Advances in neurology 93:**23-42, 2003

168. Sarkisov S, Filimonoff I, Preobrashenskaya N: Cytoarchitecture of the human cortex cerebri. **Moscow: Medgiz**, 1949
169. Sarubbo S, De Benedictis A, Merler S, Mandonnet E, Balbi S, Granieri E, et al: Towards a functional atlas of human white matter. **Hum Brain Mapp 36:**3117-3136, 2015
170. Schilling K, Gao Y, Janve V, Stepniewska I, Landman BA, Anderson AW: Confirmation of a gyral bias in diffusion MRI fiber tractography. **Hum Brain Mapp 39:**1449-1466, 2018
171. Schmahmann JD, Pandya DN: Anatomical investigation of projections from thalamus to posterior parietal cortex in the rhesus monkey: A WGA-HRP and fluorescent tracer study. **Journal of Comparative Neurology 295:**299-326, 1990
172. Schmahmann JD, Pandya DN: Cerebral white matter--historical evolution of facts and notions concerning the organization of the fiber pathways of the brain. **J Hist Neurosci 16:**237-267, 2007
173. Schmahmann JD, Pandya DN, Wang R, Dai G, D'arceuil HE, de Crespigny AJ, et al: Association fibre pathways of the brain: parallel observations from diffusion spectrum imaging and autoradiography. **Brain 130:**630-653, 2007
174. Selemon LD, Goldman-Rakic PS: Common cortical and subcortical targets of the dorsolateral prefrontal and posterior parietal cortices in the rhesus monkey: evidence for a distributed neural network subserving spatially guided behavior. **Journal of Neuroscience 8:**4049-4068, 1988
175. Seltzer B, Pandya DN: Afferent cortical connections and architectonics of the superior temporal sulcus and surrounding cortex in the rhesus monkey. **Brain Res 149:**1-24, 1978
176. Seltzer B, Pandya DN: Post-rolandic cortical projections of the superior temporal sulcus in the rhesus monkey. **J Comp Neurol 312:**625-640, 1991
177. Sheldon S, Farb N, Palombo DJ, Levine B: Intrinsic medial temporal lobe connectivity relates to individual differences in episodic autobiographical remembering. **Cortex 74:**206-216, 2016
178. Sinke MRT, Otte WM, Christiaens D, Schmitt O, Leemans A, van der Toorn A, et al: Diffusion MRI-based cortical connectome reconstruction: dependency on tractography procedures and neuroanatomical characteristics. **Brain Struct Funct 223:**2269-2285, 2018
179. Skandalakis GP, Komaitis S, Kalyvas A, Lani E, Kontrafouri C, Drosos E, et al: Dissecting the default mode network: direct structural evidence on the morphology and axonal connectivity of the fifth component of the cingulum bundle. **Journal of Neurosurgery 1:**1-12, 2020
180. Smith GE: A new topographical survey of the human cerebral cortex, being an account of the distribution of the anatomically distinct cortical areas and their relationship to the cerebral sulci. **Journal of anatomy and physiology 41:**237, 1907
181. Sporns O, Tononi G, Kötter R: The human connectome: a structural description of the human brain. **PLoS computational biology 1:**e42, 2005
182. Sun J, Liu Z, Rolls ET, Chen Q, Yao Y, Yang W, et al: Verbal Creativity Correlates with the Temporal Variability of Brain Networks During the Resting State. **Cereb Cortex 29:**1047-1058, 2019
183. Talairach J, Tournoux P: Co-planar stereotaxic atlas of the human brain. 1988. **Theime, Stuttgart, Ger 270:**90128-90125, 1988

184. Tata MS, Ward LM: Early phase of spatial mismatch negativity is localized to a posterior "where" auditory pathway. **Experimental Brain Research 167:**481-486, 2005
185. Tata MS, Ward LM: Spatial attention modulates activity in a posterior "where" auditory pathway. **Neuropsychologia 43:**509-516, 2005
186. Taveras JM, Wood EH: Diagnostic neuroradiology. **Academic Medicine 39:**1135, 1964
187. Testut L, Jacob O: Topographic anatomy textbook, in: Barcelona: Salvat, 1932
188. Testut L, Latarjet A: Human anatomy textbook, in **Myology**: Doin Paris, 1921
189. Thier P, Andersen R: Electrophysiological evidence for a second medial «parietal eye field», in **Abstr. Soc Neurosci**, 1993, Vol 19, p 27
190. Thier P, Andersen RA: Electrical microstimulation distinguishes distinct saccade-related areas in the posterior parietal cortex. **Journal of Neurophysiology 80:**1713-1735, 1998
191. Thomas C, Ye FQ, Irfanoglu MO, Modi P, Saleem KS, Leopold DA, et al: Anatomical accuracy of brain connections derived from diffusion MRI tractography is inherently limited. **Proc Natl Acad Sci U S A 111:**16574-16579, 2014
192. Tian B, Reser D, Durham A, Kustov A, Rauschecker JP: Functional specialization in rhesus monkey auditory cortex. **Science 292:**290-293, 2001
193. Tian J-R, Lynch JC: Corticocortical input to the smooth and saccadic eye movement subregions of the frontal eye field in Cebus monkeys. **Journal of Neurophysiology 76:**2754-2771, 1996
194. Tian J-R, Lynch JC: Functionally defined smooth and saccadic eye movement subregions in the frontal eye field of Cebus monkeys. **Journal of Neurophysiology 76:**2740-2753, 1996
195. Tokunaga K, Tamiya T, Date I: Transient memory disturbance after removal of an intraventricular trigonal meningioma by a parieto-occipital interhemispheric precuneus approach: Case report. **Surg Neurol 65:**167-169, 2006
196. Tosoni A, Pitzalis S, Committeri G, Fattori P, Galletti C, Galati G: Resting-state connectivity and functional specialization in human medial parieto-occipital cortex. **Brain Struct Funct 220:**3307-3321, 2015
197. Tremblay P, Perron M, Deschamps I, Kennedy-Higgins D, Houde JC, Dick AS, et al: The role of the arcuate and middle longitudinal fasciculi in speech perception in noise in adulthood. **Hum Brain Mapp 40:**226-241, 2019
198. Türe U, Yaşargil DC, Al-Mefty O, Yaşargil MG: Topographic anatomy of the insular region. **Journal of neurosurgery 90:**720-733, 1999
199. Türe U, Yaşargil MG, Friedman AH, Al-Mefty O: Fiber dissection technique: lateral aspect of the brain. **Neurosurgery 47:**417-427, 2000
200. Utevsky AV, Smith DV, Huettel SA: Precuneus is a functional core of the default-mode network. **Journal of Neuroscience 34:**932-940, 2014
201. Van Hoesen GW, Morecraft RJ, Vogt BA: Connections of the monkey cingulate cortex, in **Neurobiology of cingulate cortex and limbic thalamus**: Springer, 1993, pp 249-284
202. Vatansever D, Menon DK, Manktelow AE, Sahakian BJ, Stamatakis EA: Default mode network connectivity during task execution. **Neuroimage 122:**96-104, 2015
203. Vergani F, Mahmood S, Morris CM, Mitchell P, Forkel SJ: Intralobar fibres of the occipital lobe: a post mortem dissection study. **Cortex 56:**145-156, 2014

204. Visser M, Jefferies E, Lambon Ralph M: Semantic processing in the anterior temporal lobes: a meta-analysis of the functional neuroimaging literature. **Journal of cognitive neuroscience 22:**1083-1094, 2010
205. Von Bonin G, Bailey P: The neocortex of Macaca mulatta.(Illinois Monogr. med. Sci., 5, No. 4.). 1947
206. Von Economo C: **Cellular structure of the human cerebral cortex**: Karger Medical and Scientific Publishers, 2009
207. von Economo C, Koskinas GN: **Die Cytoarchitektonik der Hirnrinde des erwachsenen Menschen: Textband u. Atlas**: Springer, 1925
208. Vos SB, Jones DK, Viergever MA, Leemans A: Partial volume effect as a hidden covariate in DTI analyses. **Neuroimage 55:**1566-1576, 2011
209. Wang H, Black AJ, Zhu J, Stigen TW, Al-Qaisi MK, Netoff TI, et al: Reconstructing micrometer-scale fiber pathways in the brain: multi-contrast optical coherence tomography based tractography. **Neuroimage 58:**984-992, 2011
210. Wang Y, Fernandez-Miranda JC, Verstynen T, Pathak S, Schneider W, Yeh FC: Rethinking the role of the middle longitudinal fascicle in language and auditory pathways. **Cereb Cortex 23:**2347-2356, 2013
211. Wang Z, Williams VJ, Stephens KA, Kim CM, Bai L, Zhang M, et al: The effect of white matter signal abnormalities on default mode network connectivity in mild cognitive impairment. **Hum Brain Mapp**, 2019
212. Warren JD, Griffiths TD: Distinct mechanisms for processing spatial sequences and pitch sequences in the human auditory brain. **Journal of Neuroscience 23:**5799-5804, 2003
213. Warren JD, Zielinski BA, Green GG, Rauschecker JP, Griffiths TD: Perception of sound-source motion by the human brain. **Neuron 34:**139-148, 2002
214. Wen HT, Rhoton Jr AL, de Oliveira E, Cardoso AC, Tedeschi H, Baccanelli M, et al: Microsurgical anatomy of the temporal lobe: part 1: mesial temporal lobe anatomy and its vascular relationships as applied to amygdalohippocampectomy. **Neurosurgery 45:**549-592, 1999
215. Wen X, Cant JS, Xiang Y, Huang R, Mo L: The Neural Correlates of Intelligence Comparison. **Cereb Cortex 29:**253-264, 2019
216. Williams P, Warwick R: Gray's Anatomy ed 36 Philadelphia. **B. Saunders Co:**1135, 1980
217. Wise SP, Boussaoud D, Johnson PB, Caminiti R: Premotor and parietal cortex: corticocortical connectivity and combinatorial computations. **Annual review of neuroscience 20:**25-42, 1997
218. Wu Y, Sun D, Wang Y, Wang Y, Ou S: Segmentation of the Cingulum Bundle in the Human Brain: A New Perspective Based on DSI Tractography and Fiber Dissection Study. **Front Neuroanat 10:**84, 2016
219. Xie T, Sun C, Zhang X, Zhu W, Zhang J, Gu Y, et al: The contralateral transfalcine transprecuneus approach to the atrium of the lateral ventricle: operative technique and surgical results. **Neurosurgery 11 Suppl 2:**110-117; discussion 117-118, 2015
220. Yang Z, Qiu J, Wang P, Liu R, Zuo XN: Brain structure-function associations identified in large-scale neuroimaging data. **Brain Struct Funct 221:**4459-4474, 2016
221. Yasargil M: Microneurosurgery. Vol IVA, in: Stuttgart, Germany: Georg Thieme, 1994

222. Yaşargil M, Smith R, Young P, Teddy P: Microneurosurgery: Microsurgical anatomy of the Basal Cisterns and Vessels of the Brain. **Stuttgart: Theime 1**, 1984
223. Yasargil M, Teddy P, Roth P: Selective amygdalo-hippocampectomy operative anatomy and surgical technique, in **Advances and technical standards in neurosurgery**: Springer, 1985, pp 93-123
224. Yasargil MG, Krisht AF, Türe U, Al-Mefty O, Yasargil DC: Microsurgery of Insular Gliomas: Part I—Surgical Anatomy of the Sylvian Cistern. **Contemporary Neurosurgery 39:**1-8, 2017
225. Yeterian EH, Pandya DN: Corticothalamic connections of paralimbic regions in the rhesus monkey. **Journal of Comparative Neurology 269:**130-146, 1988
226. Yeterian EH, Pandya DN: Corticothalamic connections of the posterior parietal cortex in the rhesus monkey. **Journal of Comparative Neurology 237:**408-426, 1985
227. Yeterian EH, Pandya DN: Striatal connections of the parietal association cortices in rhesus monkeys. **Journal of Comparative Neurology 332:**175-197, 1993
228. Zemmoura I, Blanchard E, Raynal PI, Rousselot-Denis C, Destrieux C, Velut S: How Klingler's dissection permits exploration of brain structural connectivity? An electron microscopy study of human white matter. **Brain Struct Funct 221:**2477-2486, 2016
229. Zhang J, Andreano JM, Dickerson BC, Touroutoglou A, Barrett LF: Stronger Functional Connectivity in the Default Mode and Salience Networks Is Associated With Youthful Memory in Superaging. **Cereb Cortex**, 2019
230. Zhao X, Borba Moreira L, Cavallo C, Belykh E, Gandhi S, Labib MA, et al: Quantitative Endoscopic Comparison of Contralateral Interhemispheric Transprecuneus and Supracerebellar Transtentorial Transcollateral Sulcus Approaches to the Atrium. **World Neurosurg 122:**e215-e225, 2019
231. Zhu Y, Tang Y, Zhang T, Li H, Tang Y, Li C, et al: Reduced functional connectivity between bilateral precuneus and contralateral parahippocampus in schizotypal personality disorder. **BMC Psychiatry 17:**48, 2017
232. Zilles K, Eickhoff S, Palomero-Gallagher N: The human parietal cortex: a novel approach to its architectonic mapping. **Advances in neurology 93:**1-21, 2003
233. Zilles K, Palomero-Gallagher N: Cyto-, myelo-, and receptor architectonics of the human parietal cortex. **Neuroimage 14:**S8-S20, 2001
234. Zimmer U, Macaluso E: High binaural coherence determines successful sound localization and increased activity in posterior auditory areas. **Neuron 47:**893-905, 2005

# Appendix I

**List of Articles of reused material with Permissions**

[1] Material reused from Ribas GC. The cerebral sulci and gyri. Neurosurgical focus. 2010 Feb 1;28(2): E2. by Non-exclusive permission granted from JNS publishing group

[2] Material reused from Cavanna AE & Trimble MR. The precuneus: a review of its functional anatomy and behavioural correlates, Brain, 2006, 129, 3, by permission of Oxford University Press

[3] Material reused from Komaitis S, Skandalakis GP, Kalyvas AV, Drosos E, Lani E, Emelifeonwu J, Liakos F, Piagkou M, Kalamatianos T, Stranjalis G, Koutsarnakis C. Dorsal component of the superior longitudinal fasciculus revisited: novel insights from a focused fiber dissection study. Journal of Neurosurgery. 2019 Mar 1;132(4):1265-78. by non-exclusive permission granted from JNS publishing group

[4] Reprinted by permission from Springer Nature Customer Service Centre GmbH, Brain structure and function, Mapping the human middle longitudinal fasciculus through a focused anatomo-imaging study: shifting the paradigm of its segmentation and connectivity pattern. Kalyvas A, Koutsarnakis C, Komaitis S, Karavasilis E, Christidi F, Skandalakis GP, Liouta E, Papakonstantinou O, Kelekis N, Duffau H. 2020 Jan 1;225(1):85-119. 2020

[5] Material reused from Komaitis S, Skandalakis GP, Kalyvas AV, Drosos E, Lani E, Emelifeonwu J, Liakos F, Piagkou M, Kalamatianos T, Stranjalis G, Koutsarnakis C. Dorsal component of the superior longitudinal fasciculus revisited: novel insights from a focused fiber dissection study. Journal of Neurosurgery. 2019 Mar 1;132(4):1265-78. by non-exclusive permission granted from JNS publishing group

[6] Reprinted by permission from Springer Nature Customer Service Centre GmbH, Brain structure and function, Sledge runner fasciculus: anatomic architecture and tractographic morphology. Koutsarnakis C, Kalyvas AV, Skandalakis GP, Karavasilis E, Christidi F, Komaitis S, Velonakis G, Liakos F, Emelifeonwu J, Giavri Z, Kalamatianos T. 2019 Apr 1;224(3):1051-66. 2020 Jan 1;225(1):85-119. (2019

[7] Material reused from Skandalakis GP, Komaitis S, Kalyvas A, Lani E, Kontrafouri C, Drosos E, Liakos F, Piagkou M, Placantonakis DG, Golfinos JG, Fountas KN. Dissecting the default mode network: direct structural evidence on the morphology and axonal connectivity of the fifth component of the cingulum bundle. Journal of Neurosurgery. 2020 Apr 24;1(aop):1-2. by non-exclusive permission granted from JNS publishing group